# A Multi-Year Observational Study of Atmospheric Transport Corridors and Processes in California

Final Report
*APPENDICES*

Contract No. A032-145

*Prepared for:*

California Air Resources Board
Research Division
2020 L Street
Sacramento, California 95814

*Prepared by:*

Department of Commerce
National Oceanic and Atmospheric Administration
Environmental Research Laboratories
Environmental Technology Laboratory
325 Broadway
Boulder, Colorado 80303

May 1994

# APPENDICES: FINAL REPORT

## TABLE OF CONTENTS

APPENDIX A: Contamination of Wind Profiler Data by Migrating Birds: Characteristics of Corrupted Data and Potential Solutions

APPENDIX B: Northern California 1991 Site Audit Rawinsonde/Profiler Comparisons

APPENDIX C: Comparison of Travis North and Travis South Profilers: A Collocation Experiment

APPENDIX D: Summary Wind Distributions for Upper-Level Ridge and Trough Cases

APPENDIX E: Summary Wind Distributions for Upper-Level Ridge Case: Comparison of Morning and Afternoon Distributions

APPENDIX F: Summary Wind Distributions for High-and Low-Ozone Episodes for the North Central Coast Air Basin

APPENDIX G: Draft NOAA Technical Report on Workstation Development in Support of the California Profiler Network

APPENDIX H: Hourly Interpolated Northern California Transport Wind Fields for 10 July 1991 (Julian Day 191): A Typical Ridge Case

APPENDIX I: Hourly Interpolated Northern California Transport Wind Fields for 20 July 1991 (Julian Day 201): A Typical Trough Case

APPENDIX J: Hourly Interpolated Southern California Transport Wind Fields for Low-Ozone Days

APPENDIX K: Interpolated Southern California Transport Wind Fields for High-Ozone Days

# APPENDIX A

DRAFT PAPER

Contamination of Wind Profiler Data by Migrating Birds:
Characteristics of Corrupted Data and Potential Solutions

Submitted to the ***Bulletin of the American Meteorological Association***

# Contamination of Wind Profiler Data by Migrating Birds: Characteristics of Corrupted Data and Potential Solutions

J. M. Wilczak,[*] R. G. Strauch,[*] F. M. Ralph,[*] B. L. Weber,[*] D. A. Merritt,[*] J. R. Jordan,[*] D. E. Wolfe,[*] L. K. Lewis,[*] D. B. Wuertz,[*] J. E. Gaynor,[*] S. A. McLaughlin,[+] R. R. Rogers,[#] A. C. Riddle[**], T. S. Dye.[++]

[*]Environmental Technology Laboratory, ERL/NOAA, Boulder, Colorado

[+]U.S. Army Research Laboratory, White Sands Missile Range, New Mexico

[#]Department of Atmospheric and Oceanic Sciences, McGill University, Montreal, Canada

[**]CIRES, University of Colorado, Boulder, Colorado

[++]Sonoma Technology, Inc., Santa Rosa, California

RECEIVED

**Abstract**

Winds measured with 915- and 404-MHz wind profilers are frequently found to have nonrandom errors as large as 15 m $s^{-1}$ when compared to simultaneously measured rawinsonde winds. Detailed studies of these errors, which occur only at night below about 4 km altitude and have a pronounced seasonal pattern, indicate that they are due to the wind profilers' detection of migrating songbirds (passerines). Characteristics of contaminated data at various stages of data processing, including raw time series, individual spectra, averaged spectra, 30- or 60-s moments, 3- or 6-min winds, and hourly averaged winds, are described. An automated technique for the rejection of contaminated data in historical data sets, based on thresholding high values of moment-level reflectivity and spectral width, is shown to be effective. Techniques designed for future wind profiler data acquisition systems are described that show promise of rejecting bird echoes, with the additional capability of being able to retrieve the true wind velocity in most instances. Finally, characteristics of bird migration revealed by wind profilers are described, including statistics of the spring (March-May) 1993 migration season determined from the 404-MHz Wind Profiler Demonstration Network (WPDN). During that time, contamination of moment data occurred on 43% of the nights monitored.

## 1. Introduction

It has been known since the early days of their development that radars are sensitive to the movements of biological point targets such as birds. Unambiguous proof of this came first by suspending birds on threads held in a radar beam (Edwards and Houghton 1959), and later through studies in which birds were released from airplanes, helicopters, and cages fixed to tethered balloons, with the subsequent movement of the point targets observed with tracking radars (Konrad et al. 1968; Vaughn 1974). A vigorous interest in this subject, driven primarily by military concerns and for air traffic control, led to the development of the field of radar ornithology. More recently, a resurgent interest in radar ornithology has been motivated by a perceived decrease in the numbers of songbirds in the United States, hypothesized to result from the deforestation of winter habitats in Central and South America, from temperate zone agricultural and forestry practices, or possibly from the widespread use of pesticides (Robbins et al. 1989; Gauthreaux 1992; Petit et al. 1993; Rodenhouse et al. 1993; DeSante et al. 1993; Gard et al. 1993). The book *Radar Ornithology* (Eastwood 1967) and a more recent review article by Vaughn (1985), provide a detailed history of the development of radar techniques used to study bird behavior.

Radar studies of birds have yielded a wealth of information on migratory behavior. Some of the salient aspects of passerine migration in regard to wind profiling radars are as follows. Migration nearly always takes place during nighttime hours only, with starting times best correlated with civil twilight (defined as the time when the sun is 6° below the horizon);

passerines fly in a dispersed manner rather than in a tight flock, with densities often reaching $10^{-6}$ birds $m^{-3}$; their average airspeed varies from approximately 8 to 15 m $s^{-1}$, dependent on bird species; they tend to fly at the level of most favorable winds (tailwinds or weakest headwinds); the maximum height of migration (based principally on observations in the midwestern U.S.) is approximately 2 km AGL, although migrations to 4 km or higher are not uncommon if the winds are favorable; the rate of migration exhibits transient peaks (especially in the autumn) related to the passage of synoptic frontal systems; migrating flocks generally avoid clouds; "reverse" migrations (i.e., a southward flight in spring or a northward flight in the fall) can occur for short periods of time; migration can be nearly continuous from March through November in the eastern and central U.S., with different species of birds flying at different times; the peak migrations in the central U.S. probably occur in May and again in September, with a summer minimum occurring during nesting season in late June and early July.

Recently, evidence has been obtained implicating migrating birds as the source of large errors in hourly radar wind profiler data. Profiler data showing clear characteristics of migrating bird contamination have been found at many locations in North America, including the Wind Profiler Demonstration Network (WPDN) profilers located in the midwestern U.S., and portable 915-MHz profilers sited in California, Nevada, Arizona, Texas, Alabama, North Carolina, New York, and Montreal, Canada (see Ralph et al. 1994; Ecklund et al. 1988 for details of the WPDN and portable 915-MHz profiling systems). Contaminated profiler data have been found at almost every temperate continental site that we have investigated, as

well as at sites over water near continents (e.g., the Gulf of Mexico). In contrast, no evidence of contamination has been found in profilers operating on ships on the open ocean, on small islands far from continents, or in profilers operating in the Arctic and Antarctic.

During the development of the portable 915-MHz wind profiler, field tests in Illinois indicated that contamination from migrating birds could sometimes occur (Ecklund et al. 1990). However, during the development, testing, and evaluation of larger, permanently located wind profiling radars, much of which occurred in eastern Colorado over the past 15 years, little evidence was found that migrating birds significantly affected hourly winds. Several reasons for this inconsistency are apparent. First, and most important, the large statistical intercomparisons made between wind profiler velocities and rawinsonde velocities were done using 0000 and 1200 GMT National Weather Service balloon launches taken at Denver (Weber and Wuertz 1990; Weber et al. 1990). These times correspond to 1700 and 0500 LST, which are daylight or twilight hours during the spring and fall. Since passerines migrate almost exclusively during darkness, the intercomparison times would have missed the periods of severe wind profiler contamination. Secondly, one of the wind profilers extensively used for early evaluation purposes was a large 915-MHz system (operated at Denver's Stapleton Airport) that has a considerably smaller beam width compared to most other wind profilers (see section 6). Since the probability of having a bird in a pulse volume is directly proportional to the size of that volume, greater bird densities are required to affect the Stapleton profiler compared to the other profilers. In fact, we have found relatively fewer cases of apparent contamination in the Stapleton profiler's hourly winds when compared to a

nearby 404-MHz wind profiler. Finally, our radar observations to date indicate that somewhat weaker migrations occur in eastern Colorado than in many other locations.

In the following sections, we first describe some of the basic terminology and operational aspects of wind profilers that will be useful in discussing bird contamination. Next, we document cases of erroneous hourly profiler winds in both 915- and 404-MHz wind profiler data, and then describe in detail the characteristics of contaminated data, in the time domain and in the frequency or spectral domain (individual spectra, averaged spectra, and moment estimates). Using data from the 404-MHz WPDN, we present several case studies of bird contamination, discuss some of the unique aspects of bird migration that we have observed using the network, and provide some preliminary statistics on bird contamination during the 1993 spring migration season. Next, we discuss the relative sensitivity of several different profilers to migrating birds. We then describe a data editing technique that sets thresholds on acceptable values of reflectivity and spectral width and demonstrate its effectiveness in rejecting contaminated moment-level data in past data sets. Finally, we discuss techniques, designed to be implemented in future wind profiler data acquisition systems, that show the promise of being able to reject bird echoes while simultaneously retrieving the true wind velocity at all heights.

## 2. Wind profiler description

Here we provide a very brief description of the terminology and techniques used in the processing of radar wind profiler data. For more details on Doppler radar, the reader is referred to Doviak and Zrnić (1984). Details for wind profiler data processing are given in Strauch et al. (1984).

Radar wind profilers provide profiles of the horizontal wind by measuring the Doppler shift due to advection of a turbulent medium, typically on three beam pointing positions, usually to the zenith and in two orthogonal azimuth directions at about 15° zenith angles. The measured Doppler shift is inherently a volume-averaged quantity, with the size of the radar resolution volume determined by the width of the radar beam, the duration of the transmitted pulse, and the bandwidth of the receiving system. A complex time series of the frequency-shifted reflected signal is obtained simultaneously for each range resolution cell along the antenna pointing direction, with the length of each time series (dwell time) typically on the order of 1 sec. The complex time series consists of in-phase (I) and quadrature (Q) samples of the radar receiver output that represent the composite amplitude and phase of all the scatterers in the radar resolution cell. Samples of I and Q obtained from successive radar pulses are averaged for about 10 milliseconds; this reduces the data rate in subsequent processing steps while retaining the necessary Nyquist sampling rate. A Fast Fourier Transform is then computed for each of these averaged time series, followed by magnitude

squaring to produce a Doppler velocity spectrum. These spectra are then averaged, typically over a 30-s interval for 915-MHz profilers and a 60-s interval for 404-MHz profilers.

Next, signal spectral moments are estimated from each averaged signal-plus-noise spectrum by isolating the signal portion of the spectrum (see Strauch et al. 1984) and calculating the zeroth, first, and second spectral moments. The zeroth moment (total area of the signal spectrum) represents the power of the returned signal; the first moment of the signal spectrum gives the frequency shift of the signal, equivalent to the advective velocity of the turbulent medium; the second moment of the spectrum, or velocity variance, provides a measure of the distribution of the turbulent velocities within the pulse volume. (WPDN profilers record the velocity variance, while portable 915-MHz profilers generally record spectral width, defined as the square root of the velocity variance.) Since most profilers cycle through two different resolution modes on each of three beams, a new radial measurement of a particular resolution is made approximately every 3 min for 915-MHz profilers, and every 6 min for the WPDN 404-MHz profilers. Finally, a consensus averaging (Strauch et al. 1984) or pattern recognition scheme (Weber and Wuertz 1991) is applied to a sequence of first moment profiles, thereby eliminating outlying data points, and the averaged first moments from each of the beams are then combined to form an average (typically 1 h) wind vector.

Because of the bandwidth of the radar receiver, high-reflectivity point targets can be smeared into as many as two additional range gates. In addition, portable 915-MHz wind profilers often use pulse compression to improve sensitivity. This is usually done with binary

phase coding using complementary pairs of pulses (Schmidt et al. 1979). The compromise made when using pulse compression is that moving targets with very large reflectivities (such as birds) can be smeared into even more range resolution cells.

## 3. Evidence of bird contamination in wind profiler data

### *a. Hourly winds*

Serious discrepancies recently have been found between wind profiler estimates of wind velocities and those measured simultaneously with balloon tracking systems. One such case was documented during the evening of 7 May 1993 at the White Sands, New Mexico, 404-MHz WPDN site. Here a three-way intercomparison was made between the 404-MHz profiler, a portable 924-MHz wind profiler (located within 100 m of the 404-MHz profiler), and special CLASS rawinsondes.

At 0635 UTC, a rawinsonde was launched from a location approximately 1 km north of the two profilers. The rawinsonde wind profile is shown in Fig. 1. The wind direction backs slowly with height from westerly to southwesterly, while the wind speed increases from 8 m $s^{-1}$ at the surface to about 15 m $s^{-1}$ at 3.7 km msl. In contrast, the profiler data for the hour ending at 0700 UTC measured velocities of approximately 9 m $s^{-1}$ from the south-southwest from the surface up to 3.5 km. The vector difference between the profiler and balloon winds (Fig. 2) shows differences of 7-14 m $s^{-1}$, consistent with the flight speeds of

nocturnal migratory birds. The direction of these difference winds (indicative of the air-relative direction of bird flight) changes from southeasterly at the surface to easterly aloft, apparently as the birds compensate for the shear of the winds to maintain a nearly constant ground-relative southwesterly direction at all altitudes of migration. Between 3.7 and 5.2 km, no consensus winds were found by the 404-MHz wind profiler. At 5.2 km, well above the height of the migrating birds, both profiler and balloon data were again available, with the velocity difference a more normal 2 m $s^{-1}$. Time series, spectra, and moment data from these profilers, discussed in sections 3b,c,d, indicated the presence of birds up to approximately 3.7 km msl during the intercomparison period.

Other direct comparisons of hourly profiler winds and balloon-measured winds showing large discrepancies have been obtained at several 915-MHz profiler sites in California, Texas, and Louisiana. Again, the profiler velocity errors were between 8 and 15 m $s^{-1}$ and occurred only during nighttime hours, with direction errors consistent with the seasonal migration direction of birds.

*b. Time series characteristics*

Knowing that hourly wind profiler velocities can have errors as large as 7-15 m $s^{-1}$, we next examine contaminated profiler data at various stages of processing before the hourly winds are computed. The first of these stages is the raw time series of I and Q. Point targets such as aircraft and birds are readily observed by an oscilloscope display of the I and Q

signals that follow each transmitted pulse (A-scope display). When viewing the A-scope in real time, it is obvious when the returned signals have the characteristics of point targets, as opposed to clear-air scattering. Whereas a clear-air return has a coherence time of about 0.1 s and appears nearly random on the A-scope, point targets remain coherent for many seconds and appear as a sinusoid with slowly varying frequency. Examination of an A-scope display at White Sands immediately prior to the profiler/balloon intercomparison discussed in section 3a showed a nearly continuous presence of point targets in the vertical radar beam, appearing in radar range gates up to ~4 km AGL. The sinusoidal signature is also apparent in the I and Q data of Fig. 3a, which has point target characteristics, as compared to Fig. 3b, which is from clear air. The data in Fig. 3b were taken at the White Sands site with the 924-MHz profiler immediately prior to the balloon-profiler intercomparison data shown in Fig. 2.

*c. Spectral characteristics*

Single spectra obtained during periods of bird contamination are frequently found to exhibit trimodal peaks if the dwell time is longer than the birds' wing beat period, if the bird density is low enough that a single bird is captured in the radar pulse volume, and if the velocity resolution of the radar is sufficiently high. One such example, from the vertical beam of a 915-MHz profiler operated in Montreal, Canada, is shown in Fig. 4. With the dwell time here set at 0.7 s, the trimodal characteristic is evident in the upper three range

gates. The lowest gate shows the true atmospheric peak. The amplitude of each spectrum is scaled independently so that the much weaker atmospheric peak remains visible.

We interpret the central peak in the trimodal signature as the mean Doppler frequency shift of the bird due to its mean motion (with the frequency scale converted to m $s^{-1}$), and the symmetrical peaks on either side representing a modulation frequency due to the flapping of the birds' wings. Since very little water is typically present in a passerine's wings, it is likely that the wing beat frequency we observe is due to the oscillation of the bird as a whole as it beats its wings, and not to the wings themselves. For the example shown in Fig. 4, the modulation Doppler shift of the side peaks is approximately 0.5 m $s^{-1}$, which corresponds to a modulation frequency of 3 Hz. This compares well with the known wing beat frequencies of birds that typically range from 2 to 5 Hz (Vaughn, 1974).

Averaged spectra from the 404-MHz WPDN profiler at Lamont, Oklahoma, are shown in Fig. 5. These spectra were taken between 0818 and 0848 UTC, 26 September 1993, and correspond to seven consecutive range gates between 2750 and 4250 m AGL. Each spectrum is an average of 39 individual spectra over a 1-min period, with 6 min separating each consecutive averaged spectrum. Because the signal power of a bird relative to the atmosphere is less dominant at 404 MHz than at 915 MHz (see section 6), all spectra here are plotted with the same vertical scale. The topmost three levels are at heights above the migrating birds and show very well-defined, narrow spectra. The next lower level shows two peaks, one the true atmospheric peak continuous with the peaks above, and one displaced toward

larger values of a northerly wind. This second peak, due to bird contamination, merges with the main atmospheric peak in the lowest five levels.

In 404-MHz data, the amplitudes of the bird spectral peaks are sometimes of the same magnitude as the true atmospheric signal. Thus, in some cases the peak of the spectrum and its associated frequency may represent some combination of bird and atmospheric velocities. In the lowest five levels (Fig. 5), the spectra are extremely broad, with the calculated spectral widths (shown as a solid line below each spectrum) almost a factor of 10 larger than the clear-air values shown in the upper three gates. The broadness of the spectral peaks in the averaged spectrum results from the birds' wing beats, from uneven flight speeds, from the birds traversing a finite beam width that effectively spreads their speed over a range of values, and finally in some cases from a merging of the bird velocity peak with the true atmospheric velocity peak.

In contrast to 404-MHz data, birds produce a much stronger signal relative to the atmospheric return in 915-MHz wind profiler data because of the shorter wavelength of these profilers (see section 6). Consequently, in 915-MHz data, when birds are present it is most likely that the measured velocity will represent only that of the birds. In fact, in 915-MHz data, the bird return is often so strong as to produce a mirror image peak, symmetric about zero velocity, which further confuses the spectra. This image spectral peak is caused by imperfect phase and/or amplitude balance in the I and Q signals.

*d. Moment characteristics*

An important tool for determining whether profiler data are contaminated with birds is a graphical display of time-height cross sections of signal power, velocity, and spectral width for each radial beam. Fig. 6 is an example, from a portable 915-MHz profiler, of these cross sections over a 24-h period that shows both normal atmospheric signal and bird contamination. The profiler data were collected near Oroville, California, in the central Sacramento Valley, on 22 August 1991.

The upper panel shows signal power or reflectivity, converted to a refractive index structure constant $C_n^2$ scale normally used as a measure of clear-air reflectivity. The data were taken on a south-southeast-oriented beam, which had an elevation angle of 75°; the data were taken every 3 min, with a 30-s averaging time. The times of civil twilight at sunset and sunrise are indicated (subtract 8 h for LST). First, we note that whereas the daytime values of $C_n^2$ are generally smoothly varying, nighttime values show great variability in both height and time. Second, maximum nighttime values of $C_n^2$ reach nearly $10^{-9}$, which are greater than the largest daytime values, observed in the convective boundary layer at 2300 UTC. If expressed in terms of reflectivity, the large nighttime $C_n^2$ values correspond to greater than 40 $dBZ_e$, even though the sky was cloud-free. Both of these observations are contrary to what is expected from clear-air scattering.

The middle panel shows the radial component of velocity on the same beam. During the nighttime hours, a northwesterly velocity developed between 2 and 4 km AGL, and also in a layer near 1 km AGL starting at 0830 UTC. In both cases, the northwesterly winds during the nighttime hours displayed a mottled characteristic, with considerably greater small-scale variability than velocities observed during most of the daytime hours. Special radiosondes were launched from the profiler site at 2-h intervals between 0700 and 1300 UTC. Radiosonde winds at 0700 UTC indicated profiler errors as large as 10 m $s^{-1}$ in the layer between 2.0 and 3.5 km. Starting at about 0900 UTC, the radiosonde data indicated that a northeasterly drainage flow developed off the slopes of the Sierra Nevadas, eventually becoming about 1 km deep. As this flow developed, the birds descended to the level of the drainage flow, with most of the contamination between 1100 and 1300 UTC occurring within this drainage flow.

Spectral width, shown in the lower panel, also has large values that begin shortly after sunset, again reaching maxima as large as those seen within the midafternoon convective boundary layer. Similar to radial velocity and reflectivity, the spectral width also shows a very large variability in height and time during the same periods in which the reflectivity is high. This again is contrary to usual nighttime clear-air scattering observations, in which Doppler spectra have narrow widths.

During the month of August 1991, the Oroville, California, 915-MHz hourly wind profiler velocities contained obvious bird contamination on 24 of 31 nights. On most nights,

the birds had to fly against moderate headwinds, and the most dense contamination would occur at the height at which the headwind was weakest. If the winds changed during the night due to formation of drainage or other topographically generated flows, or because of a change in the synoptic weather pattern, the birds would change their flight level to that with the optimum wind. If the headwind was greater than approximately 5-6 m $s^{-1}$, the birds would not migrate.

## 4. Case studies of autumn and spring bird migration observed in the 404-MHz Profiler Demonstration Network

An important aspect of the bird migration that we have observed in the WPDN is its wide geographical distribution. We demonstrate this, as well as provide examples of contaminated 404-MHz moment data, with two case studies of typical contamination. The first occurred in the autumn after the passage of a midlevel frontal system, and the second occurred within a springtime southerly low-level jet.

At 1200 UTC on 25 September 1993, a 700-mb trough was located over western Nebraska and Kansas, and was rapidly moving eastward. By 0000 UTC 26 September, the trough had reached central Illinois and the 700-mb analysis indicated 5 to 15 m $s^{-1}$ northwesterly flow over two-thirds of the WPDN, winds favorable for autumn bird migration (Fig. 7). As a typical example of the contamination that occurred at most profiler sites, we

consider data from the profiler located at Lamont, Oklahoma. Spectral data indicating bird contamination at Lamont for this same period were discussed in section 3c.

Moment data for the 404-MHz WPDN profilers are obtained every 6 min from each of the 3-beam pointing directions. Time-height cross sections of 6-min moment data (signal power, radial velocity, and velocity variance) at Lamont are shown in Figs. 8a,b,c for the north beam. Each of these contains the same aspects described previously for contaminated 915-MHz data: unusually large values of signal power and velocity variance; a high degree of variability in space and time in all three moments; and a sharp increase in the northerly flow occurring immediately after sunset and ending near sunrise. Hourly values of the radial velocity, displayed in Fig. 8d, also show the sharp transitions to and from northerly flow, indicating that the strong northerly winds have passed the consensus algorithm. Consensus values of signal power and velocity variance also were obviously contaminated.

Large values of signal power and velocity variance can also be associated with precipitation. However, precipitation does not typically have the intense small-scale variability shown here. As with clear air, the signal correlation time for precipitation is much shorter than for single bird echoes. Also, precipitation can be easily distinguished by its characteristically large fall speed, which is readily detected in the vertical radar beam as demonstrated by Ralph (1994) and Ralph et al. (1994); for the present case, large vertical velocities were not observed.

Having recognized the signature of bird contamination in the moment data is relatively easy to distinguish the contaminated and uncontaminated hourly vector winds (Fig. 9). Here we see that preceding sunset (at ~0200 UTC), the profiler winds at 700 mb were in agreement with the rawinsonde-based analysis shown in Fig. 7. Following sunset, the profiler winds abruptly increased and turned to become due northerly, at the same time that the radar signal power and velocity variance increased. Near sunrise, the profiler winds abruptly decreased by ~10-15 m $s^{-1}$, bringing them into agreement with the 1200 UTC 700-mb analysis, and at the same time the signal power and velocity variance in Fig. 8 returned to more normal, lower values. The strongest bird contamination occurred near the 700-mb level, although the surface and 850-mb winds at 0000 UTC at Lamont were equally favorable for migration. This may be because to the immediate north in Kansas the low-level winds were southerly or light and variable. Profiler data at Haviland, Kansas, indicate that the birds were avoiding the lower levels, taking advantage of the favorable northerly flow aloft. Once at the 700-mb level, the greatest concentration of birds apparently remained at that level as they migrated south.

Similar patterns of high signal power, large velocity variance, and inexplicably strong northerly winds were found in almost all of the WPDN profilers. A contour map of the maximum height of contaminated hourly winds is shown in Fig. 10. [Because of range gate smearing (see section 2) the maximum height may be overestimated by as much as 2 range gates, or 500 m.] Where the 700-mb winds of Fig. 7 are favorable, the bird interference occurs up to near 4 km AGL. Where the winds were not favorable (i.e., the easternmost

sites), there is little or no contamination. At all sites, the ground-relative direction of bird migration (taken as the profiler-measured direction at the height of most obvious contamination) shows an almost due-southward migration.

A representative example of springtime bird contamination of 404-MHz profiler data is that of 5 May 1993. At 0000 UTC, the 850-mb analysis shows that winds over the WPDN had a southerly component (Fig. 11). A time-height cross section of moment data between 0100 and 1300 UTC from the WPDN profiler at Fairbury, Nebraska (Fig. 12), shows characteristics similar to the autumn example: high values of signal power and velocity variance beginning shortly after sunset, with a simultaneous increase in apparent wind speed (this time with a southerly component). Near sunrise, the signal power and velocity variance returned to their lower, more normal values, and the wind speed decreased. The vector winds at Fairbury (Fig. 13) show a nocturnal maximum in the southerly winds, reaching speeds greater than 20 m $s^{-1}$. In contrast, the 0000 and 1200 UTC analyses indicate that winds in the vicinity of southeastern Nebraska were only 5-10 m $s^{-1}$. Although part of this increase observed by the profiler may be due to a true nocturnal southerly low-level jet, it is clear that birds are also contaminating the data. This can be seen most clearly in the 6-min north beam radial velocity data shown in Fig. 12b. When the birds become more sporadic as sunrise approaches, range gates with the strong southerly component (shown as purple) begin to appear as isolated events in a background of lighter winds (blues and greens), particularly between 0800 and 1000 UTC near 700 mb. These individual range gates also have high signal power and velocity variance.

The maximum height of bird-contaminated hourly profiler velocities at 0500 UTC on 5 May 1993 is shown in Fig. 14. Of all the profiler data available, only two sites, Aztec and White Sands, New Mexico, show no contamination of the hourly velocities. The maximum height of bird contamination across the network exceeds 3000 m AGL, and again occurs in the south-central region of the network. However, the maximum height at individual profiler sites is generally lower than in the autumn case study (Fig. 10). Also shown in Fig. 14 are the ground-relative directions measured by the profiler at the height of strongest contamination. Here the direction of migration appears more spatially variable than in the fall migration example (Fig. 10), with directions of migration ranging toward the northwest to almost due east. Comparing these directions with the 850-mb winds (Fig. 11) shows that the migration direction is in fact nearly the same as the local true wind direction. Examination of data from selected profiler sites for several additional spring days generally supports this conclusion, although this is not always the case, as found at White Sands on 7 May (Fig. 2).

Ornithologists have come to contradictory conclusions on whether birds migrate only with the wind, or if they compensate for wind drift to maintain a constant heading (Gauthreaux 1991). Gauthreaux and Able (1970) and Gauthreaux (1991) conclude that passerines migrate only with the wind except in very light wind conditions (less than 3 m $s^{-1}$), but that ducks, geese, and shorebirds compensate for wind drift. Most of our observations generally agree with the hypothesis that except in light wind conditions, migrants fly with the wind. This seems to be especially true for springtime migrations. To a large degree, it is because the migrants are very adept at finding a level where the winds are favorable. In the

autumn, we find more cases where migrations occur at relatively large angles to the wind (as in Figs. 9 and 10), and where migrants will even fly against headwinds as strong as 5 m $s^{-1}$ (as at Oroville, California). Although our observations are limited in that we do not know the species of birds detected by the profilers at any given time, it does appear that more migrants are willing to compensate for lateral drift and to fight headwinds in the autumn than in the spring.

Because in the spring birds take advantage of the southerly low-level jet that has a nocturnal maximum, and because it appears that springtime bird migration is more likely to follow the background wind direction, determining those periods when the profiler velocities are contaminated is generally more difficult in spring than in autumn. Determining periods of contaminated profiler winds is also made difficult by the fact that sometimes the signal power and velocity variance will increase at sunset and the 3- or 6-min winds will become more variable, but there is no evidence of a net bias occurring in the hourly wind speeds. We documented this on the evening of 5 May 1993 at White Sands; the signal power and velocity variance showed characteristics similar to that of dense bird contamination, and yet a rawinsonde-profiler comparison showed good agreement in the winds. We believe that on this night the contamination was caused by bats or nonmigrating nocturnal birds. We also note that there was migration at White Sands on 7 May but not on 5 May, although the 700- and 850-mb winds were almost identical on these two days. One difference, however, was that on 5 May the profiler detected very strong turbulence aloft, with fluctuations in the 6-min vertical velocity greater than 1 m $s^{-1}$ at these heights. This observation is consistent with the

hypothesis of Kerlinger and Moore (1989) that one reason why most birds migrate at night is because atmospheric turbulence is generally weaker than during the daytime.

## 5. Statistics of the spring 1993 migration observed in the Profiler Demonstration Network

A statistical study of contamination in the WPDN was undertaken for the months of March, April, and May 1993, by applying a similar type of analysis as that described in the case study of the previous section. In this analysis, however, only the 6-min moment data were evaluated for contamination. Also, rather than investigating every profiler site, a geographically distributed subset consisting of 17 profilers was included. At each of these sites, it was subjectively determined whether bird contamination was obviously present, obviously absent, or ill-defined. The determination was based on a strong nocturnal enhancement of velocity variance, a simultaneous increase in radial velocity compared to background profiler measurements that was in the general direction of seasonal migration, and whether or not precipitation was evident in the radial vertical velocity data. At each site, the beginning and end times, as well as the maximum height, of the contamination were recorded. Because of a lack of true winds for comparison, this analysis cannot unambiguously determine whether contamination of the hourly consensus winds occurred. However, identifying those periods when birds were present in the 6-min moment data clearly identifies those intervals in time and height where hourly winds could have been contaminated by migrating birds.

Figure 15 presents a time series of the percentage of the 17 profilers for which there was obvious evidence of bird interference. A gradual increase in the number of profiler stations showing interference occurred over the three-month period. Superimposed on this gradual increase is a significant variation with an approximately 4-5 day period. Inspection of weather maps suggests that this variation is associated with eastward moving weather systems that periodically change the dominant flow pattern over the network from southerly to northerly. We note that on some days nearly all of the profiler stations showed interference.

The dependence of the migration on time of day is brought out in Fig. 16, which is based on data from May. Results from April and March are very similar, but are not shown. This figure represents average conditions, and is created by determining the average length of time during which bird interference is present for each profiler. This is plotted as a function of latitude and shows a definite trend with longer intervals present in the south than in the north. In fact, there is a 1.5-h difference between the northernmost and southernmost profilers. This variation in latitude is consistent with the fact that the nights are shorter at higher latitudes during May, as is demonstrated by the average length of night calculated from sunrise and sunset, and from civil twilight (Fig. 16). The agreement between this pattern and that anticipated from ornithological studies, such as Gauthreaux (1971), which found that the starting time of migrants was typically 30-45 min after sunset and was best correlated with civil twilight, provides verification that the pattern used to identify bird interference in the spectral moment data is reliable.

Table 1 provides monthly statistics as well as the total for the three-month period, during which 1365 station days were examined. Over the three-month period, 43% of the station days showed clear evidence of bird interference; the monthly averages are 29% in March, 43% in April, and 64% in May. Monthly average maximum heights of interference range from approximately 2 to 3 km AGL. However, the maximum altitude for interference observed was 5.9 km AGL.

## 6. Relative sensitivity of different types of profilers

The sensitivity of a wind profiler to migrating birds depends on a number of profiler characteristics, including its beam width, range resolution, and wavelength. Here we examine the relative sensitivity of three different profilers to bird contamination.

In clear-air conditions, radar backscattering occurs due to index of refraction variations in the atmosphere (Bragg scattering). In this case, the radar is most sensitive to variations on the scale of one-half of the radar wavelength, and the clear-air radar reflectivity has a weak wavelength dependence ($\lambda^{-1/3}$). The radar wavelengths for 915- and 404-MHz wind profilers are 33 and 74 cm, respectively. In contrast, birds can be considered as approximate Rayleigh scatterers whose radar cross section is inversely proportional to the fourth power of the radar wavelength. In addition, birds are strong reflectors because of the high water content of their bodies. For 915-MHz profilers, the signal from a single small bird is 20 to 40 dB greater than that of nighttime clear air. For the 404-MHz profilers, this is reduced by a factor of

about 14.2 dB. Thus, for both frequencies of profilers, the birds present sufficiently large signals that the bird echo will most often dominate the clear-air echoes. However, for a 50-MHz wind profiler (6.02-m wavelength) the profiler will usually be more sensitive to clear air than to birds, and it is less likely that contamination will occur, except in situations where there is little or no clear-air reflectivity. Also, because the lowest height of observation for a 50-MHz profiler is typically about 2 km AGL, much of the region of bird contamination will not even be observed by this radar.

In addition to the wavelength sensitivity, there also exists a significant sensitivity to beam widths, range resolution, and spectral averaging times; i.e., to the size of the effective radar resolution volume. To illustrate this, we calculate the minimum bird density necessary to contaminate each individual 1-s spectrum and each averaged spectrum, for the 404-MHz WPDN profilers, and for the 915-MHz Denver Stapleton and the portable 915-MHz wind profilers.

Continuous contamination of each spectrum (single or averaged) simply requires that a bird be present in the effective pulse volume that corresponds to the length of the time series used to calculate each spectrum. We assume that because of a bird's high reflectivity, its presence in the main beam for any portion of the total observing time will contaminate the spectrum; that the birds are uniformly distributed; and that a single bird contaminates only a single range resolution cell. We then estimate the effective pulse volume as a rectangular volume with the one horizontal side being equal to the altitude (AGL) times the sine of the

one-way, 3-dB beam width (equivalent to a two-way, 6 dB width); the second horizontal side is increased due to the ground-relative speed of the bird and the spectral averaging time; and the vertical dimension is the range resolution ($c*\tau/2$ for a rectangular pulse using a matched filter, where $\tau$ is the pulse duration; this also corresponds to a 6 dB width of the range dimension):

$$D_{min} = 1 \text{ bird/effective pulse volume} \qquad (1)$$

$$\text{Effective pulse volume} = [\Delta x + (U_B \Delta t)]\, \Delta y\, \Delta z,$$

where

$\Delta x$, $\Delta y$ = pulse width = h sin (beam width)

h = height, AGL

$\Delta z$ = range resolution

$U_B$ = ground relative bird speed

$\Delta t$ = dwell time for a single spectrum, or length of average for an average spectrum.

Using the values of beam width, range resolution, and spectral averaging time from Table 2, we find the minimum bird densities required for contamination, listed in Table 3, calculated at heights of 1 and 3 km, and for bird ground speeds of 10 m $s^{-1}$ (calm ambient winds) and 30 m $s^{-1}$ (a 20 m $s^{-1}$ background wind and a bird air speed of 10 m $s^{-1}$). The smaller the value of $D_{min}$, the more sensitive the radar is to bird contamination. Since all

three types of profilers typically cycle through two different range resolution values, the higher resolution value, given in Table 2, has been used in this calculation. Side lobe contamination and pulse coding will act to decrease the bird density required for contamination, while clustering of birds will increase the required density, which may modify the absolute magnitudes given. However, of these, only the side lobe problem will affect the relative sensitivity of the three radar systems, making the numbers given in Table 3 for the 915-MHz portable profiler (with the worst side lobes) too large by perhaps a factor of 2 relative to the other two profiler systems.

As can be seen in Table 3, the bird densities required for contamination of averaged spectra are least for the 404-MHz WPDN profilers; that is, the 404-MHz profilers are the most sensitive to birds. In comparison, the 915-MHz Denver Stapleton profiler can be less sensitive by almost a factor of four, depending on the height and ground relative velocity of the birds. The portable 915 MHz profiler's sensitivity falls between that of the 404-MHz and 915-MHz Stapleton profiler. The values in Table 2 also make apparent several other important considerations. First, the minimum density required for contamination is approximately 9 times smaller at 3 km than at 1 km for single spectra, and a factor of 4-5 times smaller for averaged spectra; and second, $D_{min}$ is about three times smaller for birds flying with a strong favorable tail wind than for calm winds. Finally, we note that known densities of migratory passerines [typically $10^{-7}$ to $10^{-6}$ $m^{-3}$ (Vaughn, 1985)] are greater than the minimum values required for continuous spectral contamination, listed in Table 3.

It is also of interest to compare the densities required for average spectrum contamination to the higher densities required to contaminate each individual single spectrum. The ratio of $D_{min}$ single spectrum to average spectrum values provides a measure of the relative improvement that could be attained for the different profilers by using a median instead of an arithmetic average. Here the advantages of having narrow beam widths and a small range resolution are apparent, with the largest minimum densities (smallest sensitivity) associated with the 915-MHz Denver Stapleton profiler.

An independent measure of bird density at the White Sands, New Mexico, WPDN site on the evening of 7 May 1993 (corresponding to Figs. 2 and 3) was obtained with a high-resolution 10-cm-wavelength FM-CW radar that was collocated with the 404- and 924-MHz profilers. The range resolution of the FM-CW was only 4 m, and its scan interval was 4.5 s. With a 2.7° beam width, the horizontal dimension of the FM-CW resolution volume was approximately 100 m at 2 km AGL. Side lobes are not considered to be a major factor in these measurements, as the first and largest is approximately 30 dB down from the main lobe.

Radar cross section (RCS) is often used to describe the relative radar backscatter from point targets. According to Vaughn (1985), the RCS for birds is $10^{0}$-$10^{2}$ $cm^2$, while most insects observed with a 10-cm radar will have an RCS several orders of magnitude smaller.

Figure 17 displays ten consecutive radar profiles of radar cross section per resolution volume plotted on top of each other, showing the passage of at least two birds through the

radar beam. A single large point target such as a bird will "spread" into other gates due to filtering and other signal processing effects. This is evident in the wide width of the two large signals at approximately 1890 and 2075 m. The "total" RCS for each point target is found by integrating the radar return through all of the range gates into which it is spread. Integration is required because the radar was calibrated with a point test target of known input signal power that was related to the total returned power from multiple range gates. Vertical integration of the large targets at 1890 and 2075 m gives total RCS values of 3.7 and 4.5 $cm^2$, respectively, within the known range of RCS for birds. Using an RCS/resolution volume (RCS/RV) minimum value of 0.1 $cm^2$, bird density was calculated with the FM-CW data displayed as color time-height cross sections. Although a bird might contaminate several temporal scans and many gates per scan, it was counted only once. Using the profiler-observed bird ground speed of ~10 m $s^{-1}$, the bird density for the hour starting at 0355 UTC 7 May was $4.3 \times 10^{-8}$ birds $m^{-3}$. Using equation (1) gives $D_{min} = 3.6 \times 10^{-8}$ birds $m^{-3}$ at a height of 2 km AGL for the 404-MHz profiler, so that the FM-CW observed bird density was sufficient to continuously contaminate each 1-min averaged spectrum, consistent with the observed contamination of the profiler winds (see section 3a). We note that the calculated bird density was not sensitive to the minimum RCS/RV value chosen, varying only by a factor of 2 over two orders of magnitude change in RCS/RV. However, for RCS/RV values less than 0.001, the number density rapidly increased; we interpret this as the result of the inclusion of insects, which also appeared as point targets in the FM-CW data.

## 7. Thresholding of historical moment data

Following the determination that wind profiler data are frequently contaminated by migrating birds, we have developed an automated technique to remove contaminated data. Historically, it has been common to record only the moment data (signal power, radial velocity, and velocity variance or spectral width) from wind profilers, as is the case for the WPDN profilers. In some cases, experimenters using portable 915-MHz profilers have also routinely recorded averaged spectra. Consequently, any technique used to remove bird-contaminated data from historical data sets can rely only on the averaged spectra or the subsequently derived moments.

For periods during which averaged spectra are recorded, it is possible to edit point target peaks in the spectra, while often leaving the true atmospheric peaks so that wind velocities can still be found. For 915-MHz profiler data, an automated algorithm has been devised that recognizes spectral peaks due to point targets by keying on their high correlation in adjacent range gates due to vertical smearing of a single point target (as is evident in Fig. 4), and their high signal power. This algorithm has been tested on portable 915-MHz wind profiler data and has been found to function well for periods with low bird densities. However, this technique is less successful during periods with dense birds, or when the bird and atmosphere spectral peaks overlap (when the wind and migration directions are nearly perpendicular to a beam or when the bird peak is very wide).

A second technique for editing historical data that has proven to be effective, yet is simple in concept, is to apply threshold limits on the signal power (or a related quantity such as $C_n^2$) and spectral width moments. This technique is based on the observations presented earlier that during nighttime periods of bird migration the contaminated profiler data have substantially higher values of spectral width, and, at least at 915 MHz, considerably higher $C_n^2$ as well.

Threshold values that we have found to be indicative of bird contamination in portable 915-MHz profiler data are $C_n^2$ greater than $10^{-10.5}$ and spectral widths greater than 2.5 m $s^{-1}$. Thresholding is applied only during those hours when most songbirds migrate, between sunrise and sunset. If either the $C_n^2$ or spectral width threshold is reached, the data point is eliminated. Because a radar resolution volume does not have sharp boundaries but rather has a Gaussian weighting distribution, a bird immediately outside of the nominal pulse volume can still contribute to the returned signal, but may do so with considerably less power. Rejection of these events (with lower reflectivity and spectral width but the erroneous bird velocity) was achieved by also eliminating the neighboring data points immediately preceding, following, above, and below a data point that exceeded the threshold values. Because the filter used in the radar receiver only approximates a matched filter, a single bird is generally found to produce a tear-drop shape with an upward elongation. Because of this, it was found to be necessary to eliminate a second data point above any that met the threshold criteria. When using pulse coding, even further smearing in the vertical of the bird

echo is possible, and rejecting more than two points above a thresholded point may be desirable.

An example of thresholded radial velocities from the Oroville, California, wind profiler is shown in Fig. 18. As can be seen, the thresholding does a good job of rejecting nearly all of the contaminated northerly velocities, while retaining most of the uncontaminated data. Following this procedure, the moment data are further processed by a consensus algorithm, during which additional editing may occur, before being used to generate hourly winds.

Similar thresholding techniques have been applied to case studies of 404-MHz data. However, because of the weaker signal power from birds relative to the clear air at this frequency, the thresholding was applied to the velocity variance only. Preliminary results show that a velocity variance threshold of 1.8 $m^2 s^{-2}$ effectively eliminates contaminated 404-MHz data. To keep from eliminating data during periods of precipitation, which may also have large reflectivity and spectral width, a check of the vertical velocity may be implemented. Thresholding would be turned off if the downward vertical velocity exceeds 0.7 m $s^{-1}$ at 404-MHz, or 0.5 m $s^{-1}$ at 915-MHz, values that are based on the terminal velocities measured by profilers in snow under conditions where Rayleigh scattering from the snow would dominate typical clear-air scattering (Ralph 1994). Because birds usually do not migrate through precipitation, it is less likely that these data would be contaminated by birds.

## 8. A potential solution for future data sets

Although effective in rejecting data contaminated by birds, the thresholding method outlined in the preceding section has the major shortcoming of leaving no atmospheric data at those heights and times where birds have been detected. Clearly, a superior technique would be one in which the bird signal and atmospheric signal could be differentiated from each other and processed independently, so that there would be no gaps in the atmospheric data. Any method of this type requires that the differentiation occur before spectra are averaged, because by that step in the data processing scheme the atmospheric echo will often already have been contaminated. Consequently, a technique of this nature could be implemented in the data processing scheme used for future data sets, but cannot be applied to past data sets. We briefly discuss here one such method, and present examples of its effectiveness. A more detailed description of this technique can be found in Merritt (1994).

Radar return signals from atmospheric turbulence and point targets have fundamentally different characteristics, and these differences can be exploited to distinguish the two from each other. In particular, for atmospheric turbulence, I and Q are zero-mean Gaussian random variables, the amplitude of the phasor $\sqrt{(I^2 + Q^2)}$ has Rayleigh statistics, and the power $(I^2 + Q^2)$ is exponentially distributed. In contrast, point targets have sinusoidal I and Q; the phasor amplitude and power are constant over short time intervals, only changing slowly as the bird moves across the beam; and the power is non-exponentially distributed, with a relative peak in the power probability distribution function at high power levels (Fig. 19).

The technique used here takes advantage of the difference in power distributions for turbulence and point targets. The procedure is first to collect a number of single spectra at a given range resolution cell, and to order these spectra in time, as shown in Fig. 20. Next, at each frequency bin (which corresponds to a particular velocity), the values of power are sorted in ascending order. At this point, a test is made to determine whether there are segments of the power distribution that do not follow an exponential fit. This is accomplished by starting at the lowest power datum and comparing the next highest point, in a manner similar to the Hildebrand-Sekhon (1974) method used for detecting the noise floor of spectra. If values having a distribution other than exponential are found, they are discarded. The mean of the remaining values is then calculated, and the procedure is repeated at each frequency. The resulting averaged spectrum is then subjected to the usual processing algorithm and the three spectral moments are calculated.

An example showing the benefit of this processing scheme is shown in Fig. 21. Here, single spectra were taken with the White Sands 404-MHz WPDN profiler during a period of strong bird contamination immediately prior to the radiosonde intercomparison discussed in section 3a. The top left panel shows a vertical profile of single spectra at 24 gates on the north beam. The top right panel is formed by taking the arithmetic average of 34 consecutive single spectra, which is the averaging procedure currently used by most profiling radars. The bottom left panel shows the result of calculating the median of the single spectra, as opposed to taking an arithmetic average. Here, the atmospheric signal starts to become apparent, although significant contamination still remains. Finally, the bottom right panel shows the

result of first eliminating data based on the exponential power test, and then calculating the mean. Here, the narrow atmospheric peak is dominant, showing a smoothly varying trend with height.

This method has been further tested on a 915-MHz wind profiler located near NOAA's instrumented 300-m tower at the Boulder Atmospheric Observatory. Figure 22 shows a 40-min segment of data during a period of strong fall migration. The profiler was continuously cycled through two different processing algorithms: the data before 0600 UTC were taken with the standard algorithms, while the data after 0600 UTC were processed using the scheme described above. The middle panel, showing radial velocity on a south-pointing beam, shows a clear decrease in radial velocity when the new scheme was used. The change is even more dramatic in $C_n^2$, shown in the top panel. Finally, the lower panel shows the resulting 3-min wind barbs, formed using moments from each single spectrum (without any consensus averaging). Winds obtained with the new algorithm have much greater uniformity, and are also approximately 10 m $s^{-1}$ less than those obtained using the standard processing scheme. Simultaneous *in situ* winds measured at the 200-m level of the BAO tower are in excellent agreement in speed and direction with the data using the new processing scheme (Fig. 23). Further tests of this method are being made to determine its optimum operating parameters (e.g., the number of spectra averaged), and to determine the practical limits (in terms of bird densities) to its effectiveness.

## 9. Summary and outlook for wind profiling

It has been shown that 915- and 404-MHz wind profiler data are frequently contaminated by migrating birds. This contamination has been found in data taken between March and November, although it may occur even earlier and later in the year, depending on geographical location. The contamination has been observed to occur almost exclusively during hours of darkness, which is when the vast majority of songbirds migrate over land. Velocity errors due to this contamination range from 7 to 15 m $s^{-1}$, and have often been observed from the surface to more than 4 km AGL. Birds take advantage of the winds that favor their direction of migration, and thus tend to most severely contaminate springtime southerly low-level jets and the southerly flow ahead of springtime cold fronts; conversely, in the autumn months they tend to most severely contaminate cold northerly surges. An analysis of a small portion of the profiler data record suggests that the direction of migration is most often in the direction of the wind, with more deviations from the local wind direction (toward due south) occurring in the autumn than in the spring. The contamination often occurs simultaneously over widespread geographic areas, which may further compound the detrimental effect of these errors if wind profiler data are used to initialize numerical weather prediction models.

Bird contamination in historical data sets can be readily determined by examining time-height cross sections of reflectivity, velocity, and velocity variance or spectral width.

Automated thresholding techniques have been tested that effectively eliminate periods of contaminated data by keying on abnormally high values of reflectivity and spectral width.

For future use on wind profiling radars, a simple technique has been developed that can remove the bird echoes while simultaneously retrieving the true winds. Preliminary results from tests of this algorithm have been very positive, and it is currently being installed on a network of portable 915-MHz profilers for further evaluation. We recommend that similar data processing techniques be considered for current and future wind profiling radar systems. We note that the "bird signal" detected by this algorithm could be processed independently of the atmospheric signal, generating data that may be useful for ornithological studies.

Finally, we note that migrating birds also contaminate scanning radars such as the WSR-88D (NEXRAD), and that care must be used in interpreting WSR-88D data. In fact, much of the information known concerning birds' migratory behavior was determined in studies using scanning radars and, in particular, in studies using the WSR-57 radar (Gauthreaux 1970; Gauthreaux 1971; Gauthreaux 1991), the predecessor to today's NEXRAD system. Because of fundamental differences in the operation of scanning radars and wind profilers, the processing algorithm described here for wind profilers cannot be used to alleviate bird contamination in scanning weather radars. Currently, the WSR-88D radar is being used by ornithologists in bird migration studies (Gauthreaux, personal communication,

1993). Unfortunately for meteorologists, until the new processing algorithm is installed on radar wind profilers, they too will be of great use in the study of bird migration.

*Acknowledgments.* We wish to acknowledge Dominique Ruffieux, Paul Neiman, Sasha Harris-Cronin, Lingling Zhang, Doug van de Kamp, Ye Jing Ping, Richard Fritz, and Leon Benjamin for assistance in accessing and displaying profiler and tower data. This work was partially sponsored by the California Air Resources Board.

## References

DeSante, D. F., O. E. Williams, and K. M. Burton, 1993: The Monitoring Avian Productivity and Survivorship (MAPS) program: Overview and progress. *Status and Management of Neotropical Migratory Birds*, D. M. Finch and P. W. Stangel, Eds. General Tech. Rep. RM-229, USDA, Forest Service, Rocky Mountain Forest and Range Experiment Station, Fort Collins, CO 80526, 208-222.

Doviak, R. J., and D. S. Zrnić, 1984: *Doppler Radar and Weather Observations*. Academic Press, 458 pp.

Eastwood, E., 1967: *Radar Ornithology*. Methuen & Co., Ltd., London, England, 278 pp.

Ecklund, W. L., D. A. Carter, and B. B. Balsley, 1988: A UHF wind profiler for the boundary layer: Brief description and initial results. *J. Atmos. Oceanic Tech.*, **5**, 432-441.

Ecklund, W. L., D. A. Carter, B. B. Balsley, P. E. Currier, J. L. Green, B. L. Weber, and K. S. Gage, 1990: Recent field tests of a lower tropospheric wind profiler. *Radio Sci.*, **25**, 899-906.

Edwards, J., and E. W. Houghton, 1959: Radar echoing area polar diagrams of birds. *Nature*, **184**, p. 1059.

Gard, N. W., M. J. Hooper, and R. S. Bennett, 1993: Effects of pesticides and contaminants on neotropical migrants. *Status and Management of Neotropical Migratory Birds*, D. M. Finch and P. W. Stangel, Eds. General Tech. Rep. RM-229, USDA, Forest Service, Rocky Mountain Forest and Range Experiment Station, Fort Collins, CO 80526, 310-314.

Gauthreaux, S. A., Jr., 1970: Weather radar quantification of bird migration. *BioScience*, 17-20.

Gauthreaux, S. A., Jr., 1971: A radar and direct visual study of passerine spring migration in southern Louisiana. *The Auk*, **88**(2), 343-365.

Gauthreaux, S. A., Jr., 1991: The flight behavior of migrating birds in changing wind fields: Radar and visual analyses. *Amer. Zool.*, **31**, 187-204.

Gauthreaux, S. A., Jr., 1992: The use of weather radar to monitor long-term patterns of trans-Gulf migration in spring. *Ecology and Conservation of Neotropical Migrant Landbirds*, J. M. Hagan III and D. W. Johnston, Eds., Smithsonian Institution Press, 96-100.

Gauthreaux, S. A., Jr., and K. P. Able, 1970: Wind and the direction of nocturnal songbird migration. *Nature*, **228**(5270), 476-477.

Hildebrand, P. H., and R. S. Sekhon, 1974: Objective determination of the noise level in Doppler spectra. *J. Appl. Meteor.*, **13**, 808-811.

Kerlinger, P. and F. R. Moore, 1989: Atmospheric structure and avian migration. *Current Ornithology*, **6**, 109-142.

Konrad, T. E., J. J. Hicks, and E. Dobson, 1968: Radar characteristics of birds in flight. *Science*, **159**, 274-280.

Merritt, D. A., 1994: A statistical averaging method for wind profiler Doppler spectra (to be published).

Petit, D. R., J. F. Lynch, R. L. Hutto, J. G. Blake, and R. B. Waide, 1993: Management and conservation of migratory landbirds overwintering in the neotropics. *Status and Management of Neotropical Migratory Birds*, D. M. Finch and P. W. Stangel, Eds. General Tech. Rep. RM-229, USDA, Forest Service, Rocky Mountain Forest and Range Experiment Station, Fort Collins, CO 80526, 70-92.

Ralph, F. M., 1994: Using radar-measured radial vertical velocities in rain and snow to distinguish precipitation scattering from clear-air scattering. (Submitted to *J. Atmos. Oceanic Tech.*)

Ralph, F. M., P. J. Neiman, D. W. van de Kamp, and D. C. Law, 1994: Using spectral moment data from NOAA's 404-MHz radar wind profilers to observe precipitation in mesoscale weather systems. (Submitted to *Bull. Amer. Meteor. Soc.*)

Robbins, C. S., J. R. Sauer, R. S. Greenberg, and S. Droege, 1989: Population declines in North American birds that migrate to the neotropics. *Proc. of the Natl. Academy of Sciences*, **86**, 7658-7662.

Rodenhouse, N. L., L. B. Best, R. J. O'Connor, and E. K. Bollinger, 1993: Effects of temperate agriculture on neotropical migrant landbirds. *Status and Management of Neotropical Migratory Birds*, D. M. Finch and P. W. Stangel, Eds. General Tech. Rep. RM-229, USDA, Forest Service, Rocky Mountain Forest and Range Experiment Station, Fort Collins, CO 80526, 280-295.

Schmidt, G., R. Ruster, and P. Czechowsky, 1979: Complementary code and digital filtering for detection of weak VHF radar signals from the mesosphere. *IEEE Trans. Geosci. Electron.*, **GE-17**(4), 154-xxx.

Strauch, R. G., D. A. Merritt, K. P. Moran, K. B. Earnshaw, and D. van de Kamp, 1984: The Colorado wind profiling network. *J. Atmos. Oceanic Tech.*, **1**, 37-49.

Vaughn, C. R., 1974: Intraspecific wingbeat rate variability and species identification using tracking radar. *Proc., Conf. on Biological Aspects of the Bird/Aircraft Collision Problem*, S. A. Gauthreaux, Jr., Ed. Clemson Univ., 443-476.

Vaughn, C. R., 1985: Birds and insects as radar targets: A review. *Proceedings of the IEEE*, 73(2), 205-227.

Weber, B. L., and D. B. Wuertz, 1990: Comparison of rawinsonde and wind profiler radar measurements. *J. Atmos. Oceanic Tech.*, **7**, 157-174.

Weber, B. L., and D. B. Wuertz, 1991: Quality control algorithm for profiler measurements of winds and temperatures. NOAA Tech Memo. ERL WPL-212, 32 pp. [Available from the National Technical Information Service, 5285 Port Royal Road, Springfield, VA 22161.]

Weber, B. L., D. B. Wuertz, R. G. Strauch, D. A. Merritt, K. P. Moran, D. C. Law, D. van de Kamp, R. B. Chadwick, M. H. Ackley, M. F. Barth, N. L. Abshire, P. A. Miller, and T. W. Schlatter, 1990: Preliminary evaluation of the first NOAA Demonstration Network Wind Profiler. *J. Atmos. Oceanic Tech.*, **7**, 909-918.

Figure Captions

Fig. 1. Rawinsonde wind speed and direction profiles at White Sands, New Mexico, at 0635 UTC, 7 May 1993.

Fig. 2. Profiles of vector difference wind speed and direction between the rawinsonde data of Fig. 1 and 924- and 404-MHz radar wind profiler hourly wind profiles. Solid symbols are wind speed; open symbols are direction; squares are 924-MHz profiler-rawinsonde; circles are 404-MHz profiler-rawinsonde.

Fig. 3. Time series of I (solid line) and Q (dashed line) during a period of contaminated signal (a) and normal atmospheric return (b).

Fig. 4. A vertical profile of four single (unaveraged) spectra, with a dwell time of 0.7 s and a velocity resolution of 0.15 m $s^{-1}$, from the vertical beam of a 915-MHz wind profiler operated in Montreal, Canada. The amplitude of each spectrum is scaled independently.

Fig. 5. A vertical profile of 1-min averaged spectra from the 404-MHz WPDN profiler at Lamont, Oklahoma, taken at 6-min intervals between 0818 and 0848 UTC on 26 September 1993. The lowest level is at 2750 m AGL (range gate 10) and the highest is at 4250 m AGL (range gate 16). The vertical scale of each profile is set to 72.3 dB (the maximum value, obtained at range gate 11), and the horizontal scale corresponds to ±12.6 m $s^{-1}$. The open

circles denote the centroid of the spectrum (radial velocity) and the horizontal bars the spectral width. The portion of each spectrum shown with a thin line was determined to be below the noise level by the WPDN processing algorithm, while the portion with a heavy line was accepted as the atmospheric signal. This latter portion was subsequently used in the calculation of moments.

Fig. 6. Time-height cross sections of 3-min values of (a) range-corrected $C_n^2$, (b) radial velocity, and (c) spectral width for a 24-h period starting at 2300 UTC, 21 August 1993, from a 915-MHz wind profiler at Oroville, California. The $C_n^2$ range is $10^{-13.9}$ to $10^{-9}$; velocity, $\pm 6$ m $s^{-1}$; and spectral width, 0-4 m $s^{-1}$. The profiler was operating with a 400-m range resolution with 4 times oversampling. Arrows indicate times of civil twilight at sunrise and sunset.

Fig. 7. 700-mb analysis at 0000 UTC, 26 September 1993. Geopotential heights in decameters (solid) and temperature in °C (dashed) are contoured. The location of the Lamont, Oklahoma, profiler is marked with an "O."

Fig. 8. Time-height cross sections of 6-min values of (a) signal power, (b) radial velocity, (c) velocity variance, and (d) hourly radial velocities, for a 15-h period starting at 0000 UTC, 26 September 1993, from the 250-m resolution north beam of a 404-MHz WPDN profiler at Lamont, Oklahoma. Time increases from right to left. Arrows indicate times of civil twilight at sunrise (SRCT) and sunset (SSCT).

Fig. 9. Time-height cross section of hourly, consensus-averaged, vector profiler winds and surface winds at Lamont, Oklahoma, between 0200 and 1300 UTC on 26 September 1993.

Fig. 10. Contour map of maximum height (AGL) of bird contamination existing in hourly consensus winds at 0400 UTC, 26 September 1993, with a contour interval of 1000 m. The dashed contour denotes no bird contamination. Solid circles show the location of each WPDN profiler, with the open circle showing the location of the Lamont, Oklahoma, profiler. Arrows show the direction of migration at the height of maximum contamination.

Fig. 11. As in Fig. 7, except at 850 mb at 0000 UTC, 5 May 1993. The location of the Fairbury, Nebraska, profiler is marked with an "O."

Fig. 12. As in Fig. 8, except on 5 May 1993 at Fairbury, Nebraska, between 0100 and 1300 UTC.

Fig. 13. Time-height cross section of vector profiler winds and surface winds at Fairbury, Nebraska, between 1000 and 1200 UTC on 5 May 1993.

Fig. 14. As in Fig. 10, except at 0500 UTC on 5 May 1993. The open circle shows the location of the Fairbury, Nebraska, profiler.

Fig. 15. Time series of the percent of 17 WPDN profilers showing obvious contamination of 6-min velocity data each day for the months of March, April, and May 1993.

Fig. 16. The average duration of contamination in 6-min spectral moment data as a function of latitude during May 1993 (bold, solid), and the average length of night during May determined from sunrise to sunset (thin, solid) and from civil twilight (dashed).

Fig. 17. FM-CW radar cross section for each radar resolution volume as a function of height, showing ten consecutive scans over a 45-s period. The dashed line indicates the minimum value used to indicate the presence of a bird.

Fig. 18. Time-height cross section of north beam radial velocity for a 24-h period starting at 0000 UTC on 18 August 1991 at Oroville, California, for (a) original data, and (b) after applying threshold limits of -10.5 log $C_n^2$ and 2.5 m $s^{-1}$ on spectral width.

Fig. 19. Schematic of power probability distribution function, with (dashed line) and without (solid line) bird contamination.

Fig. 20. Schematic of contaminated Doppler frequency spectra as a function of time.

Fig. 21. Doppler velocity spectra as a function of height from the north beam of the WPDN profiler at White Sands, New Mexico, at 0452 UTC, 7 May 1993, for (a) individual spectra, (b) an arithmetic average of 34 spectra collected over a 120-s period, (c) the medians of these spectra, and (d) average spectra after applying the exponential power distribution algorithm outlined in section 8.

Fig. 22. Time-height cross section from the south beam of a portable 915-MHz wind profiler for an approximately 1-h period on 26 September 1993, operated at the Boulder Atmospheric Observatory near Boulder, Colorado. The top panel shows range-corrected $C_n^2$; the middle panel, radial velocity; and the bottom panel, the corresponding vector winds every 3 min, with no data editing. The right half of the figure shows data processed with the conventional method, and the left half, data processed using the exponential power distribution algorithm.

Fig. 23. Comparison of 5-min values of portable 915-MHz profiler and *in situ* measured wind speed and direction at 200 m AGL at the BAO tower. Profiler data are solid lines; tower data are dashed lines. The profiler data were processed using standard techniques before 0600 UTC, and with the exponential power test after 0600 UTC.

Table 1. Frequency and maximum altitude of occurrence of bird contamination in WPDN network.

| Month | | March | April | May | Total |
|---|---|---|---|---|---|
| Number of stations examined | | 17 | 17 | 16 | |
| Number of days examined | | 31 | 30 | 30 | 91 |
| Station days with bird contamination | | (29%) | (43%) | (64%) | (43%) |
| Average maximum altitude | km AGL | 2.9 | 2.7 | 2.4 | 2.6 |
| Network average of the maximum observed at each station during that month | km AGL | 3.7 | 3.5 | 3.3 | 3.5 |

Table 2. Beam width, range reduction, and spectral averaging time for three types of wind profilers.

| | 404 MHz | 915-MHz Portable | 915-MHz Stapleton |
|---|---|---|---|
| Beam width (1-way, 3 db) | 4.2° | 9.9° | 2.8° |
| Range resolution | 250 m | 100 m | 200 m |
| Spectral averaging time | 60 s | 30 s | 30 s |

Table 3. Minimum bird densities required for continuous spectral contamination.
$D_{min} \times 10^{-7}\ m^{-3}$

| | 1000 m | | | 3000 m | | |
|---|---|---|---|---|---|---|
| | single (10 m $s^{-1}$) | avg (10 m $s^{-1}$) | avg (30 m $s^{-1}$) | single (10 m $s^{-1}$) | avg (10 m $s^{-1}$) | avg (30 m $s^{-1}$) |
| 404 MHz | 6.6 | 0.81 | 0.29 | 0.79 | 0.22 | 0.09 |
| 915-MHz Portable | 3.2 | 1.20 | 0.54 | 0.37 | 0.23 | 0.14 |
| 915-MHz Stapleton | 17.0 | 2.94 | 1.08 | 2.20 | 0.76 | 0.14 |

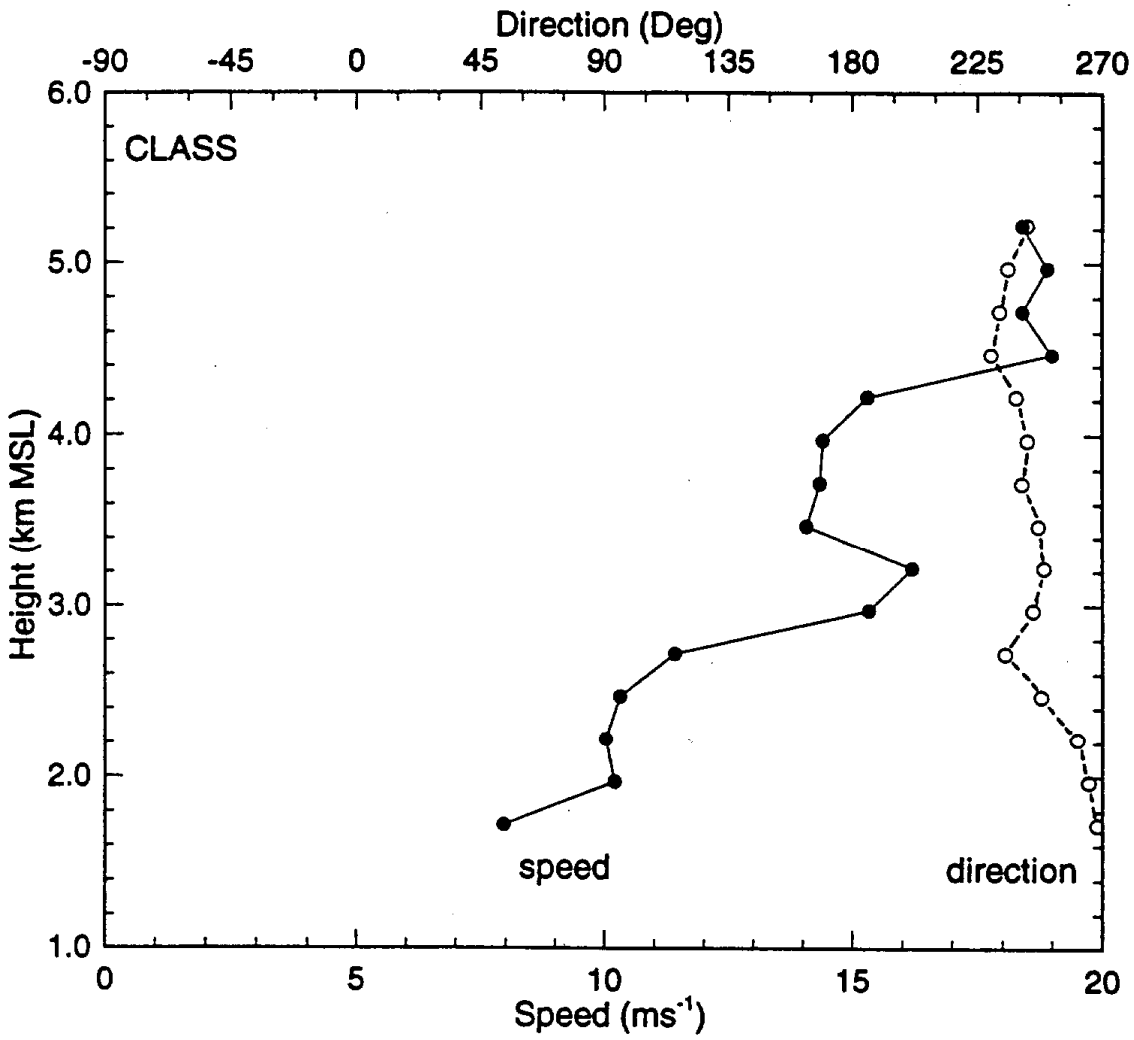
Direction (Deg)
-90
-45
0
45
90
135
180
225
270
6.0
5.0
4.0
3.0
2.0
1.0
CLASS
Height (km MSL)
speed
direction
0
5
10
15
20
Speed (ms-1)

Fig. 1

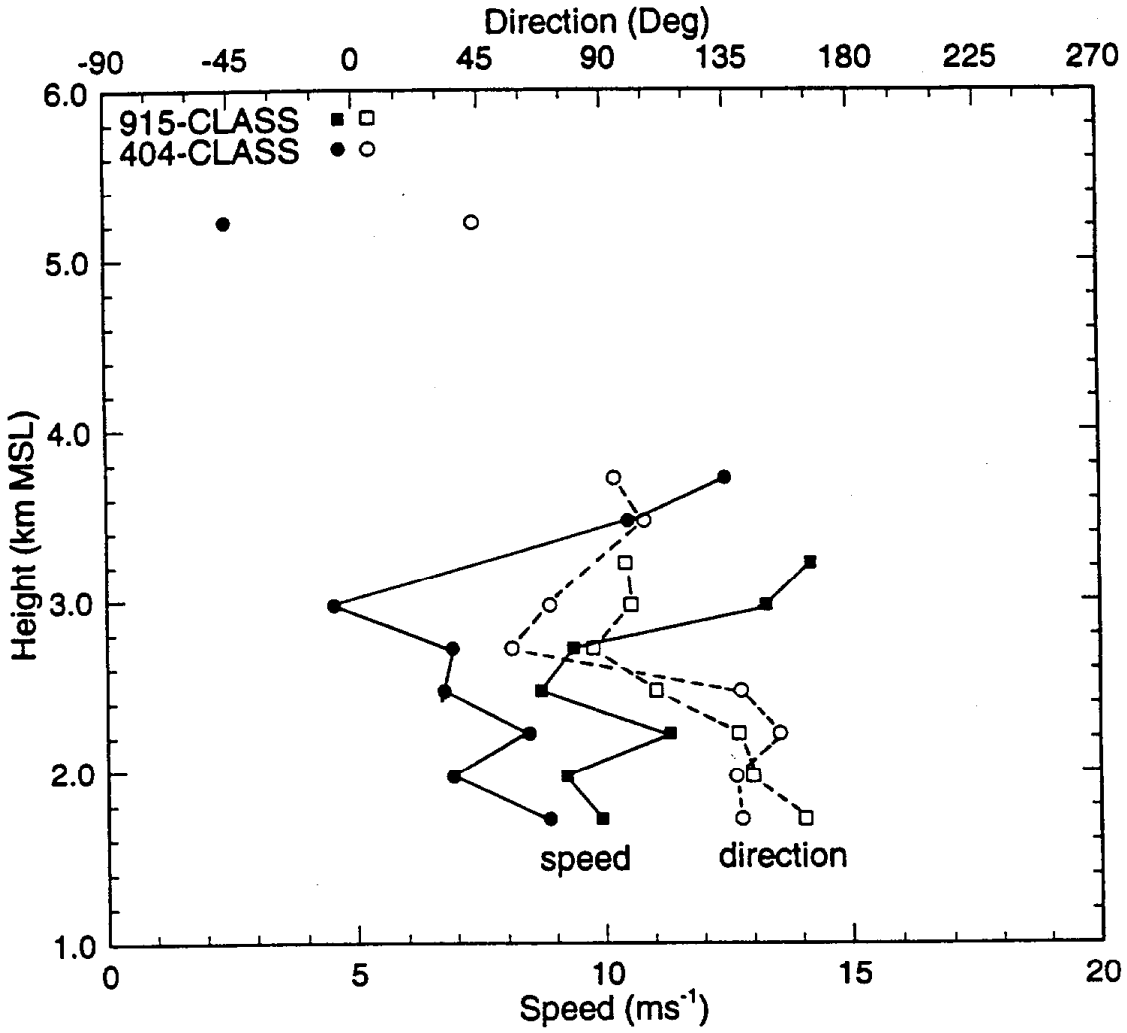
Direction (Deg)
-90
-45
0
45
90
135
180
225
270
915-CLASS
404-CLASS
Height (km MSL)
6.0
5.0
4.0
3.0
2.0
1.0
speed
direction
0
5
10
15
20
Speed (ms-1)

Fig. 2

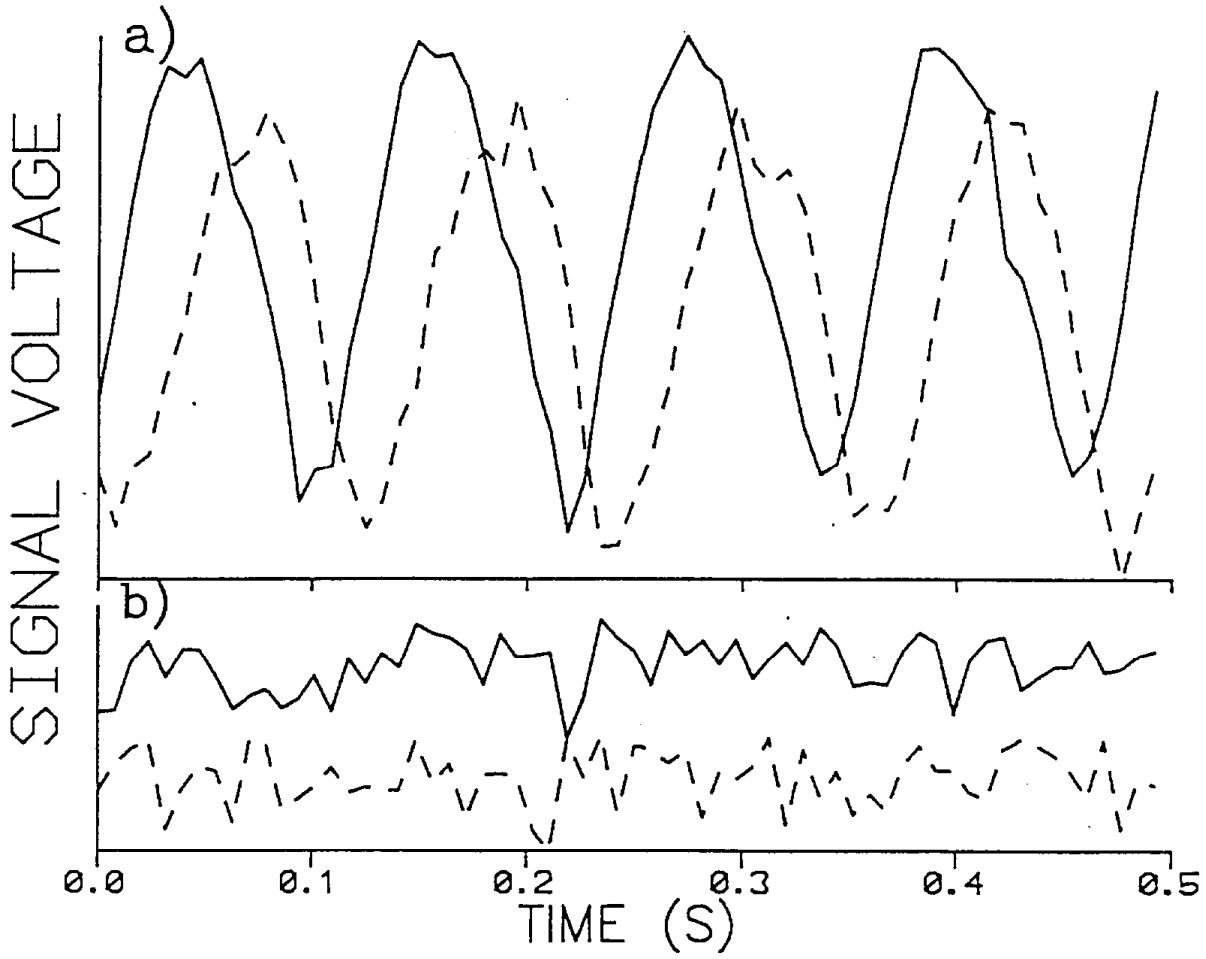


Fig. 3

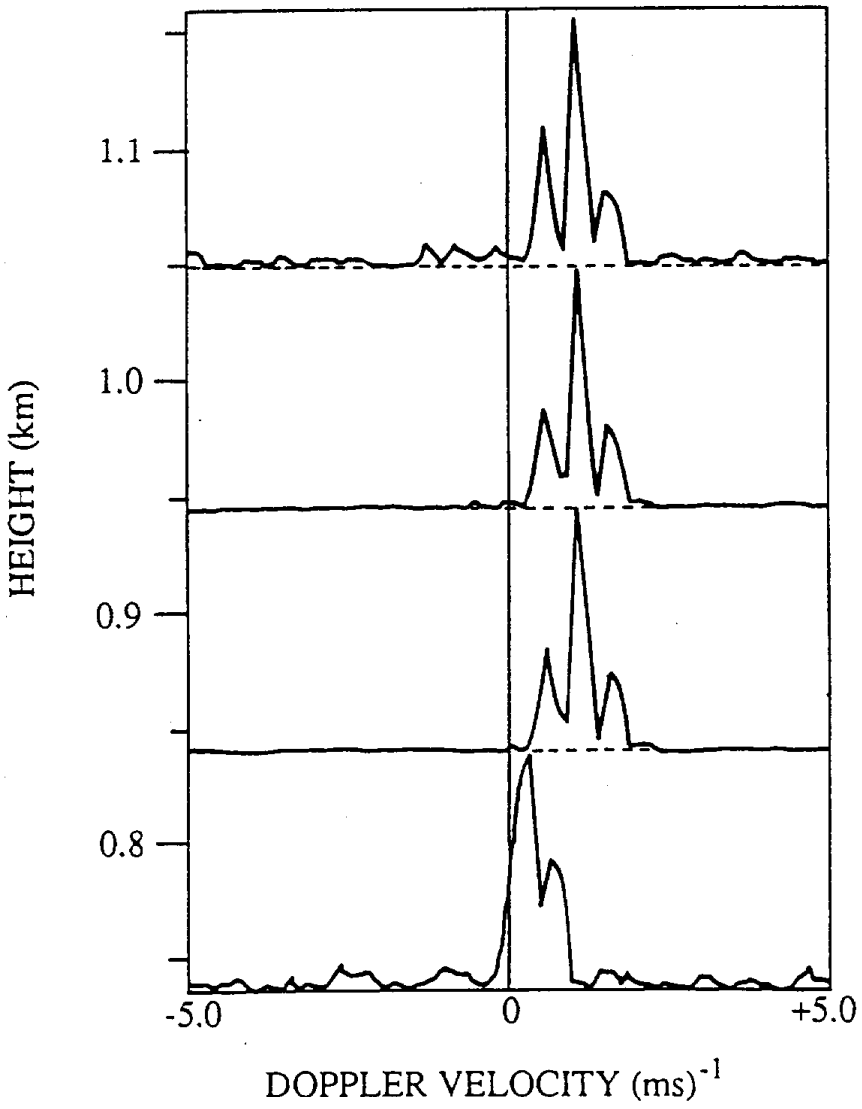


Fig. 4

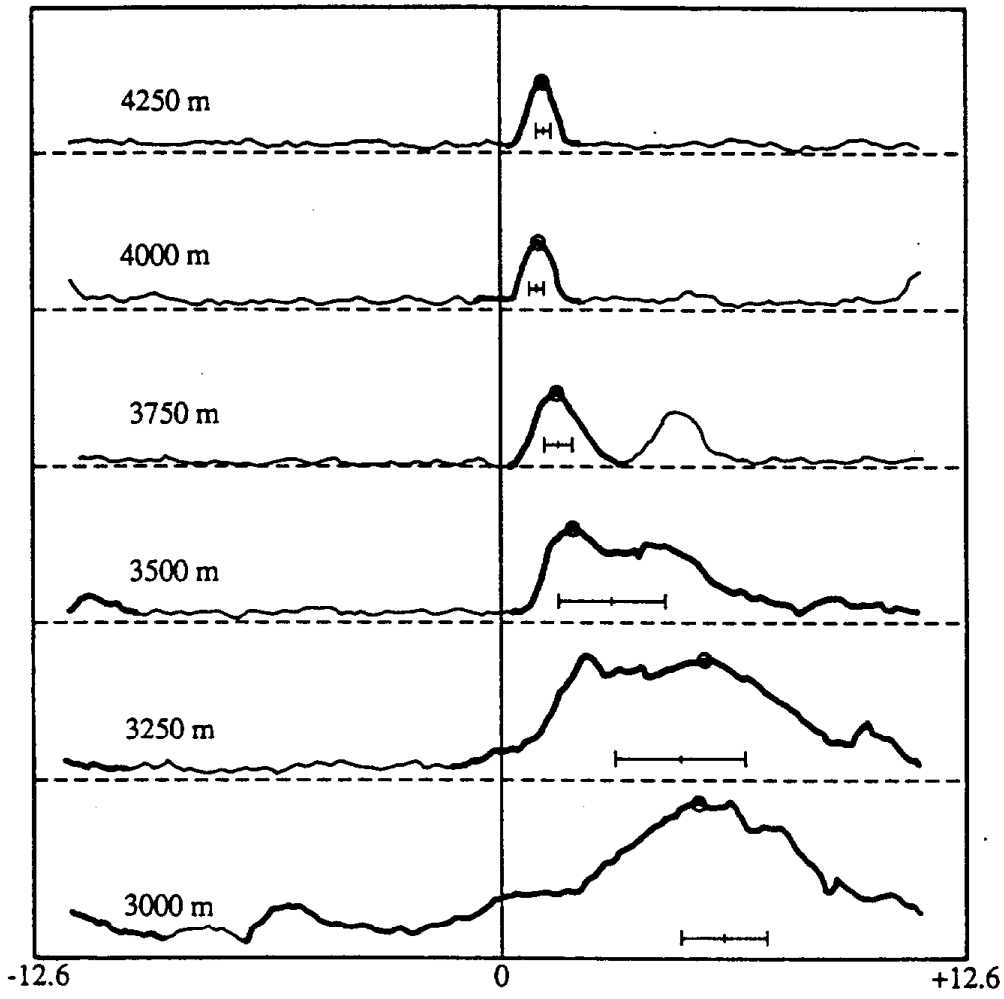
4250 m
4000 m
3750 m
3500 m
3250 m
3000 m
-12.6
0
+12.6
DOPPLER VELOCITY (ms-1)

Fig. 5

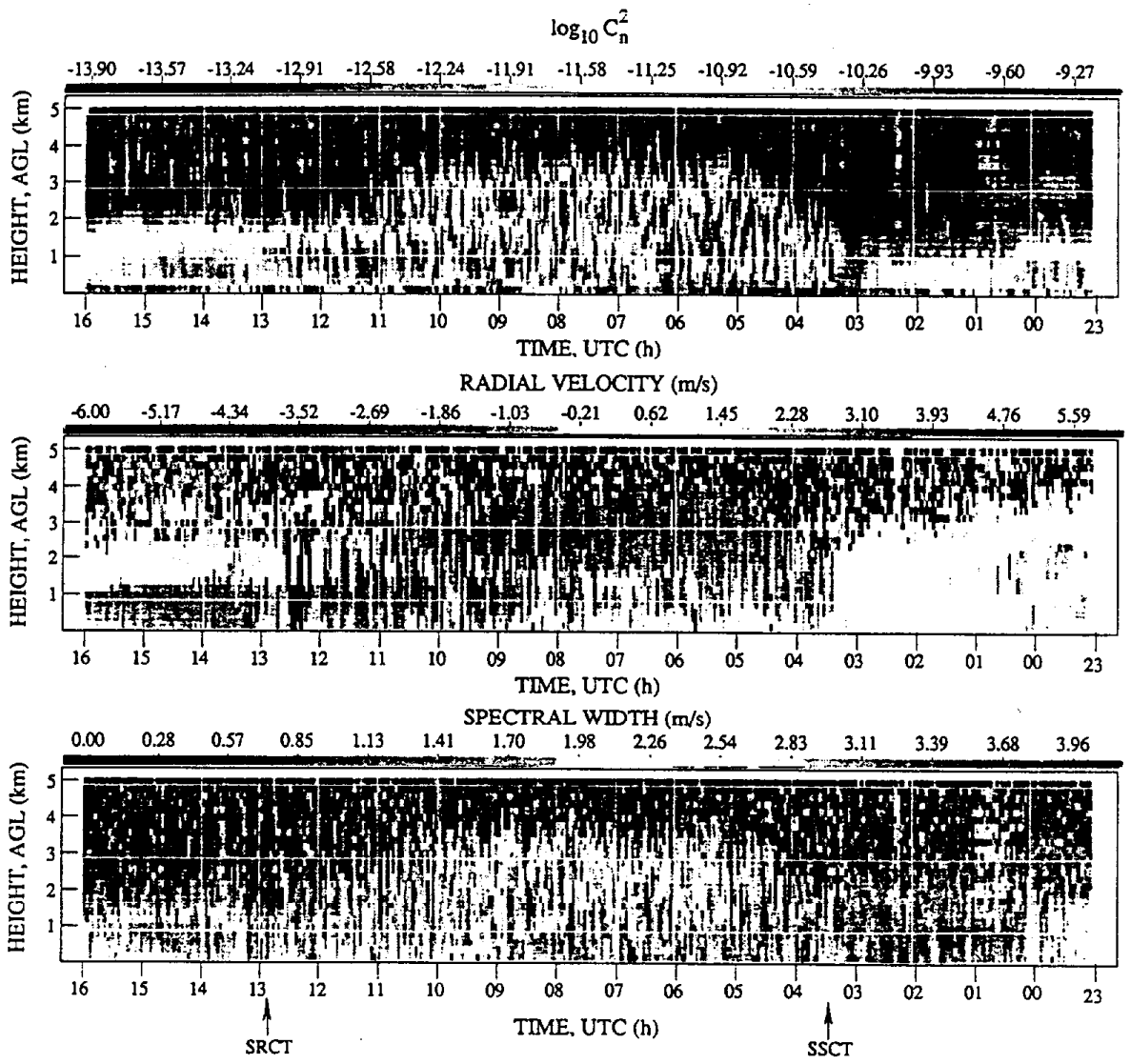
$\log_{10} C_n^2$
-13.90 -13.57 -13.24 -12.91 -12.58 -12.24 -11.91 -11.58 -11.25 -10.92 -10.59 -10.26 -9.93 -9.60 -9.27
HEIGHT, AGL (km)
5 4 3 2 1
16 15 14 13 12 11 10 09 08 07 06 05 04 03 02 01 00 23
TIME, UTC (h)
RADIAL VELOCITY (m/s)
-6.00 -5.17 -4.34 -3.52 -2.69 -1.86 -1.03 -0.21 0.62 1.45 2.28 3.10 3.93 4.76 5.59
HEIGHT, AGL (km)
5 4 3 2 1
16 15 14 13 12 11 10 09 08 07 06 05 04 03 02 01 00 23
TIME, UTC (h)
SPECTRAL WIDTH (m/s)
0.00 0.28 0.57 0.85 1.13 1.41 1.70 1.98 2.26 2.54 2.83 3.11 3.39 3.68 3.96
HEIGHT, AGL (km)
5 4 3 2 1
16 15 14 13 12 11 10 09 08 07 06 05 04 03 02 01 00 23
SRCT
TIME, UTC (h)
SSCT

Fig. 6

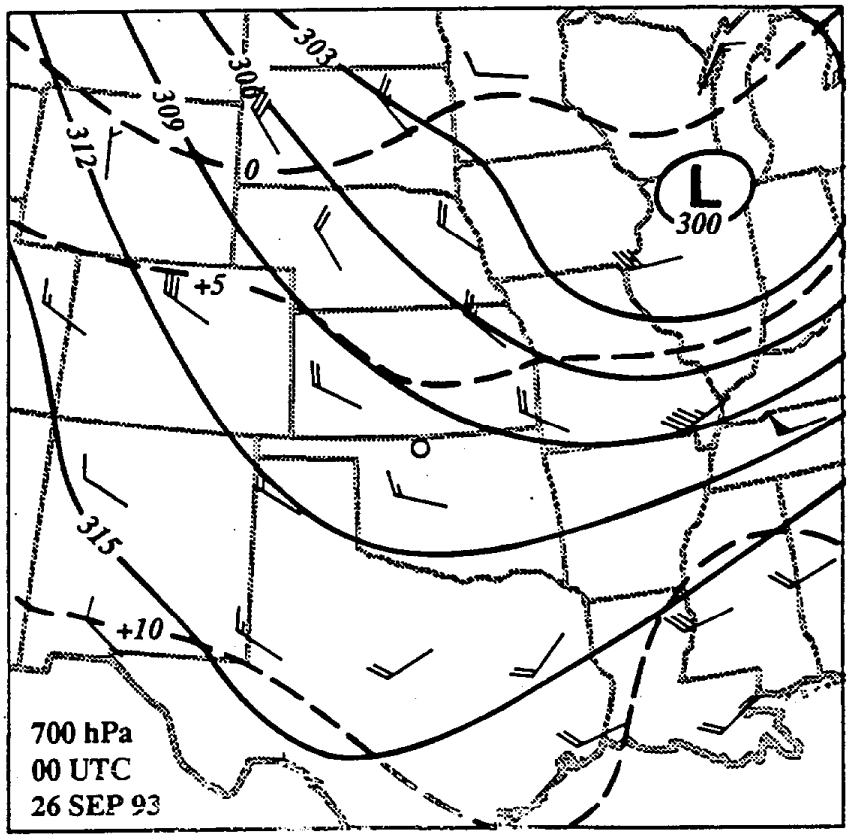


Fig. 7

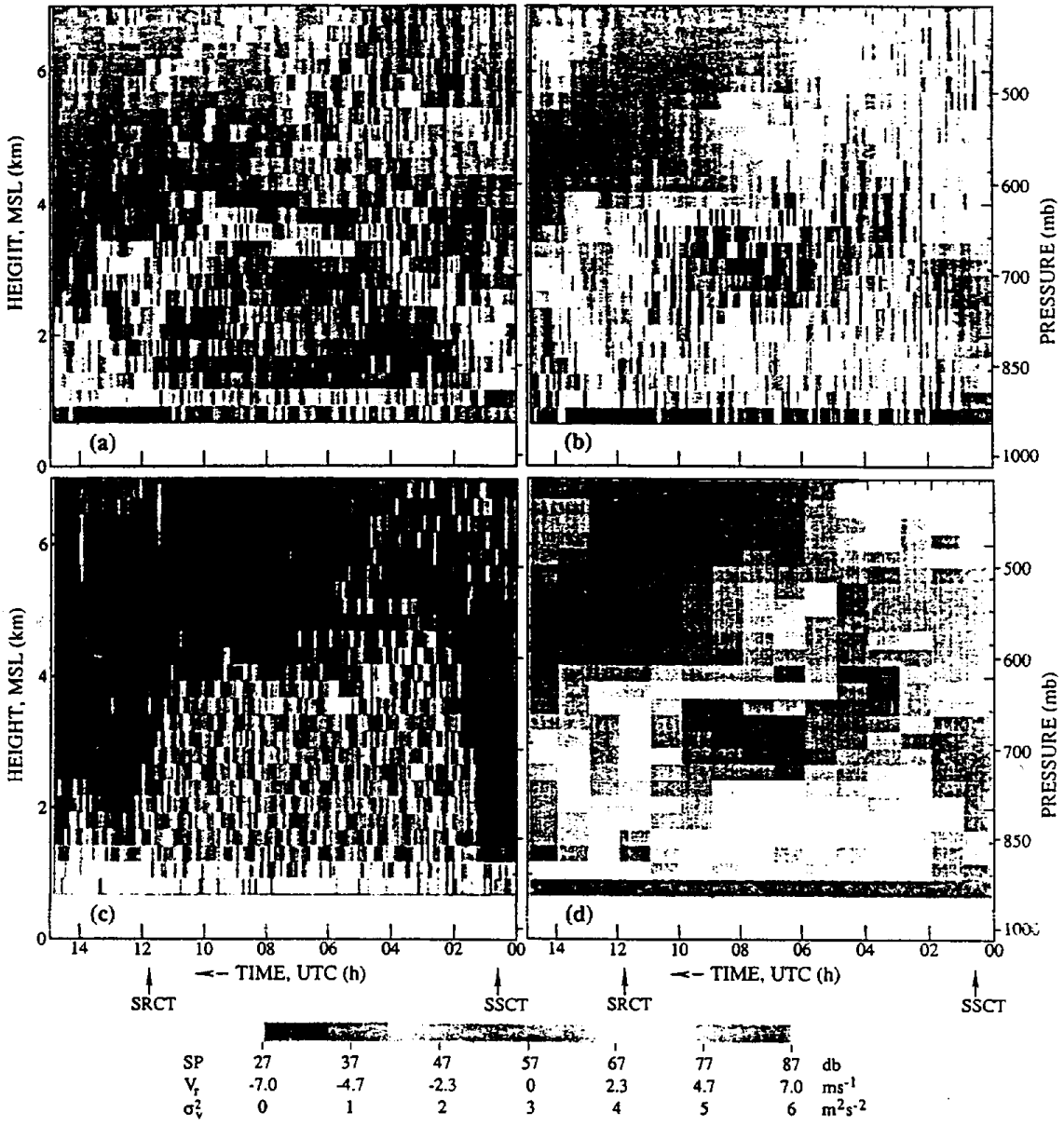
HEIGHT, MSL (km)
PRESSURE (mb)
(a)
(b)
(c)
(d)
TIME, UTC (h)
SRCT
SSCT
SP 27 37 47 57 67 77 87 db
$V_r$ -7.0 -4.7 -2.3 0 2.3 4.7 7.0 ms$^{-1}$
$\sigma_v^2$ 0 1 2 3 4 5 6 m$^2$s$^{-2}$

Fig. 8

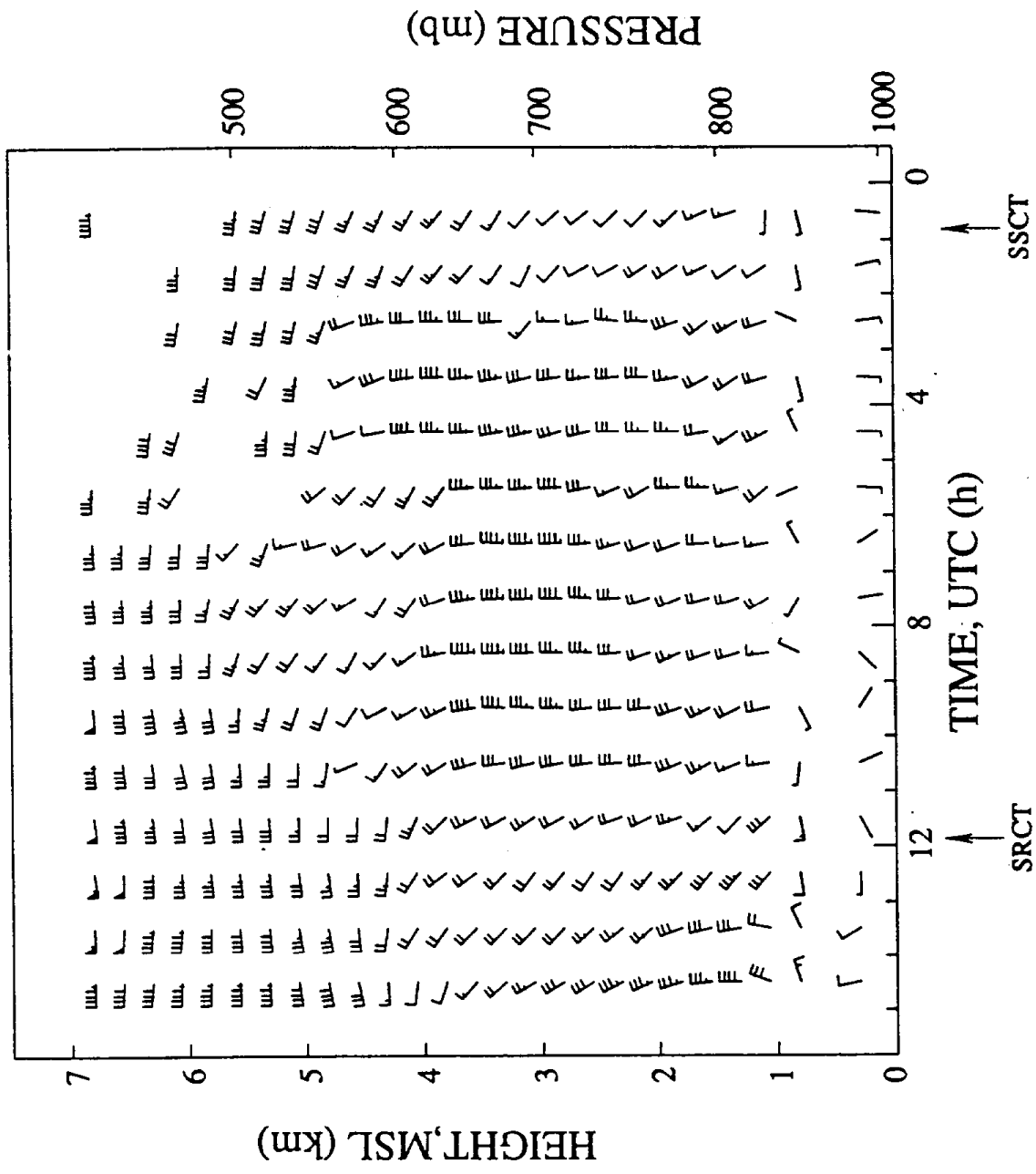
HEIGHT,MSL (km)
0
1
2
3
4
5
6
7
PRESSURE (mb)
500
600
700
800
1000
TIME, UTC (h)
0
4
8
12
SRCT
SSCT

Fig. 9

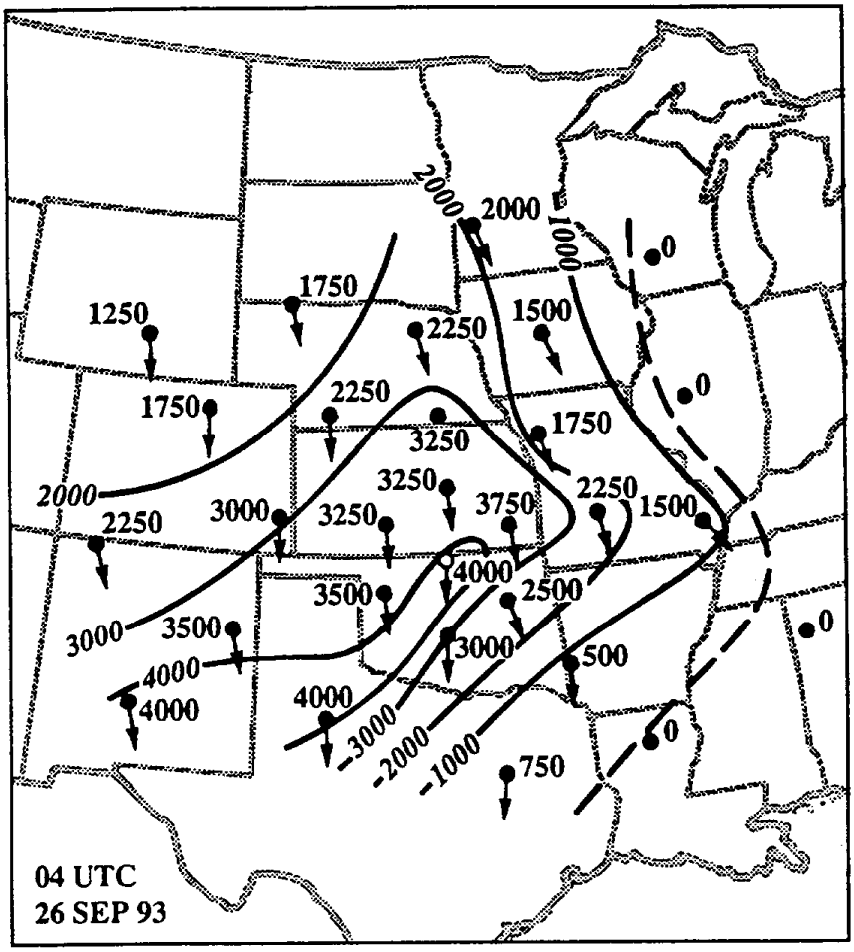
2000
2000
1000
0
1750
1250
2250
1500
0
2250
1750
3250
1750
2000
3250
2250
1500
3000
3250
3750
2250
4000
3500
2500
0
3000
3500
3000
500
4000
4000
4000
3000
2000
1000
0
750
04 UTC
26 SEP 93

Fig. 10

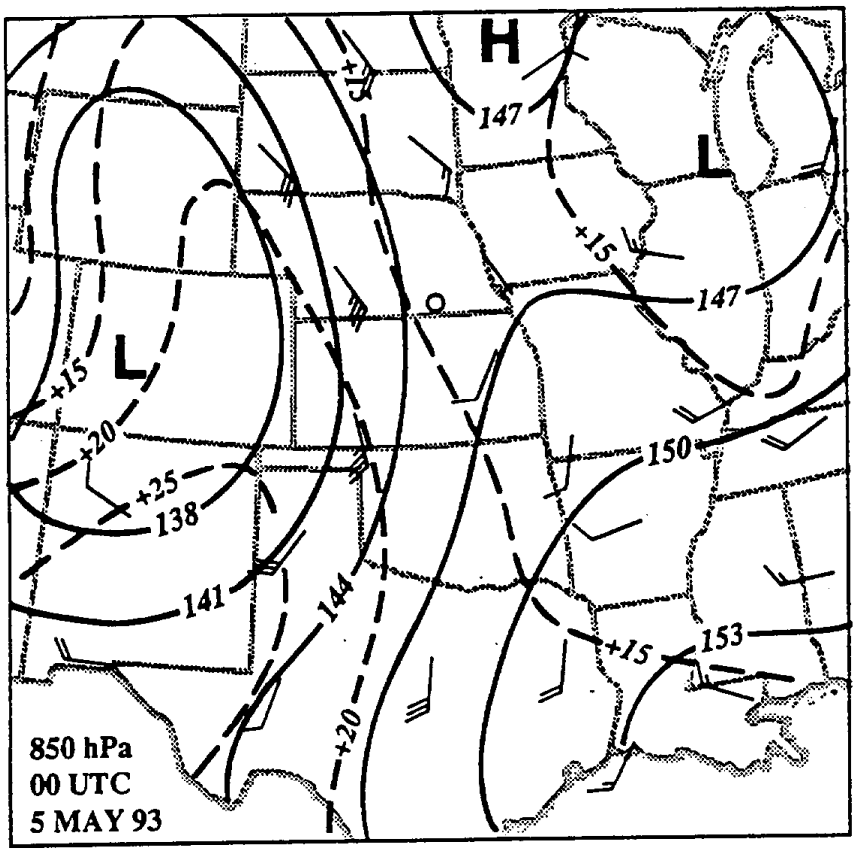
H
L
L
147
147
150
153
138
141
144
+15
+15
+15
+20
+20
+25
850 hPa
00 UTC
5 MAY 93

Fig. 11

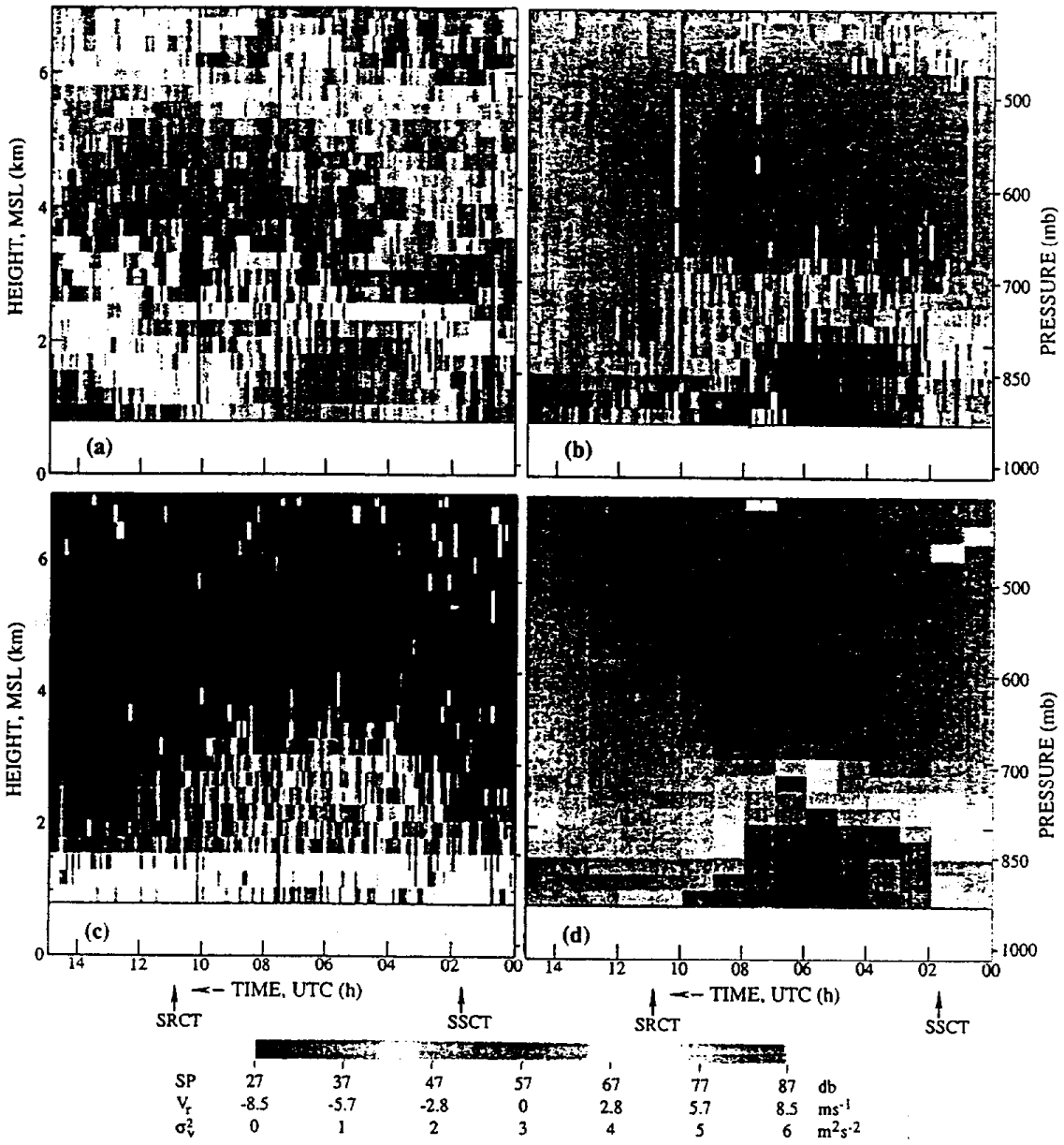
HEIGHT, MSL (km)
PRESSURE (mb)
(a)
(b)
(c)
(d)
TIME, UTC (h)
SRCT
SSCT
SP
$V_r$
$\sigma_v^2$
db
ms$^{-1}$
m$^2$s$^{-2}$

Fig. 12

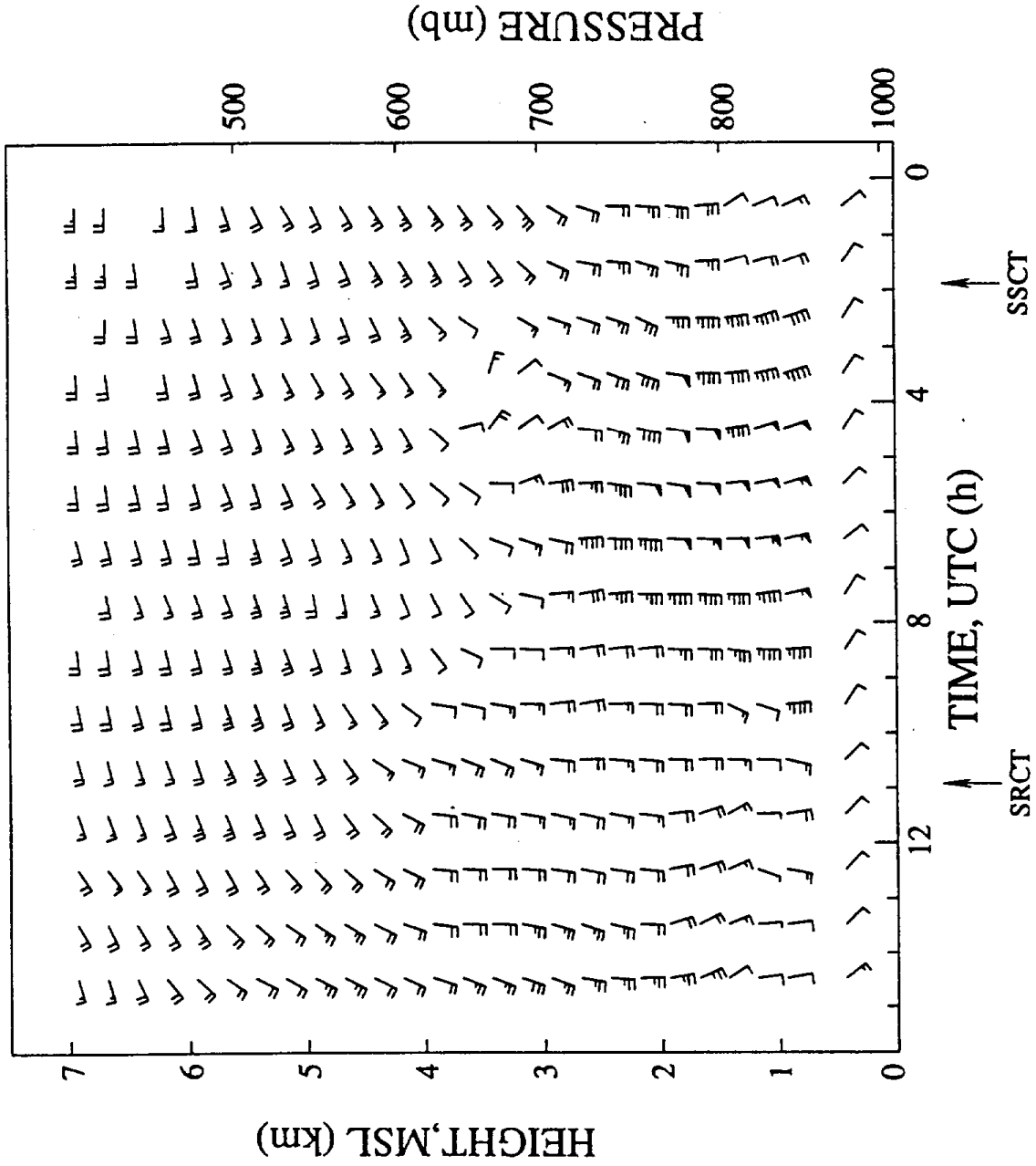
HEIGHT,MSL (km)
0
1
2
3
4
5
6
7
PRESSURE (mb)
500
600
700
800
1000
TIME, UTC (h)
0
4
8
12
SRCT
SSCT

Fig. 13

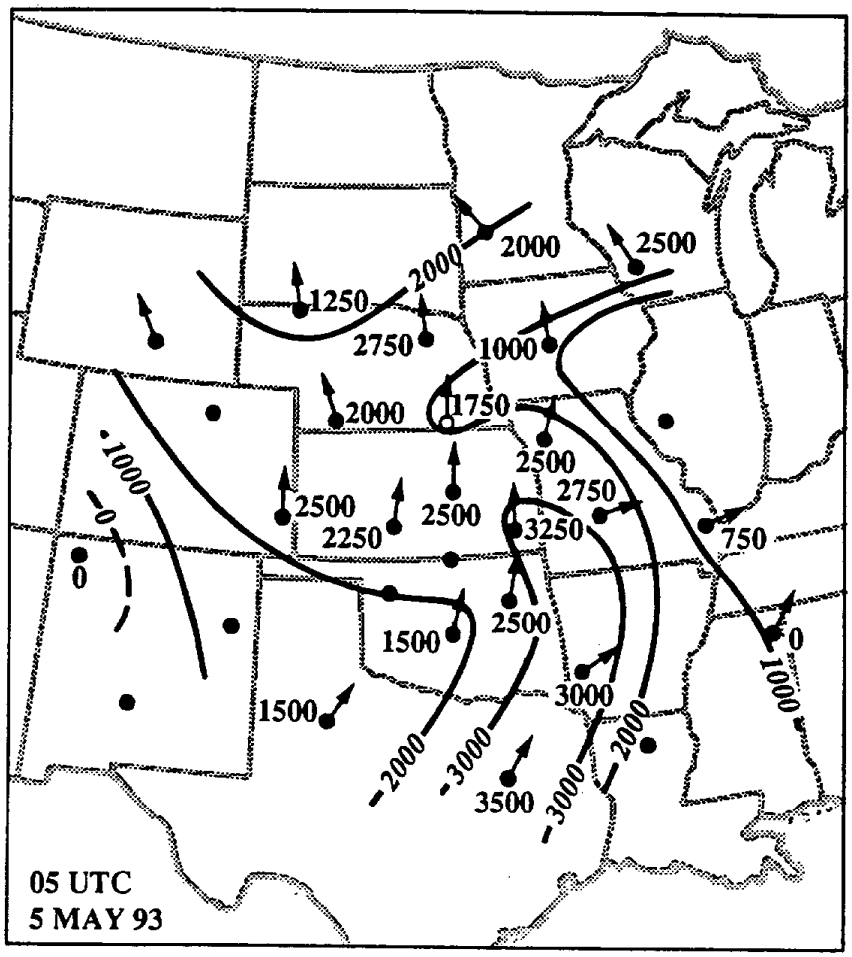
2000
2500
1250
2000
2750
1000
2000
1750
2500
2750
2500
2500
2250
3250
750
0
-1000
-0
2500
1500
0
1000
3000
1500
2000
-3000
-2000
3500
-3000
05 UTC
5 MAY 93

Fig. 14

Fig. 15

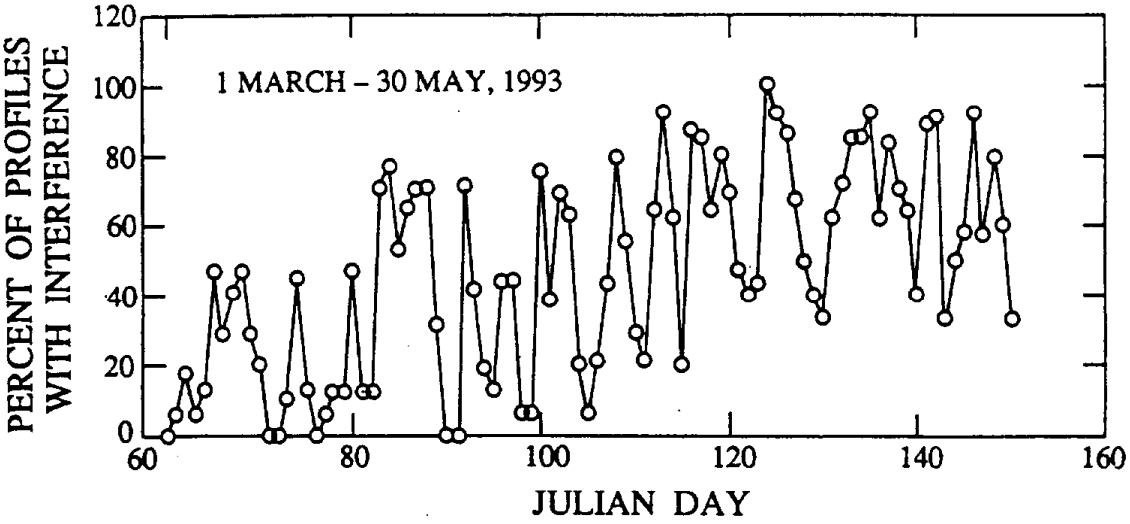
PERCENT OF PROFILES WITH INTERFERENCE
1 MARCH – 30 MAY, 1993
120
100
80
60
40
20
0
60
80
100
120
140
160
JULIAN DAY

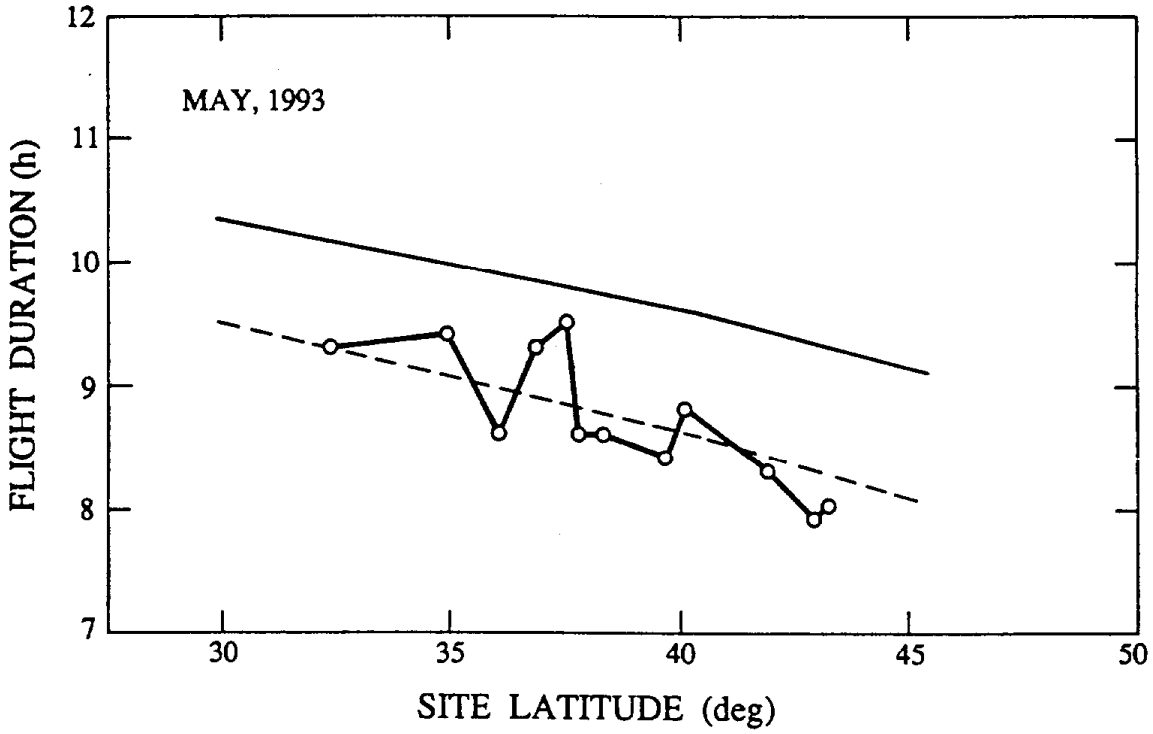
FLIGHT DURATION (h)
MAY, 1993
12
11
10
9
8
7
30
35
40
45
50
SITE LATITUDE (deg)

Fig. 16

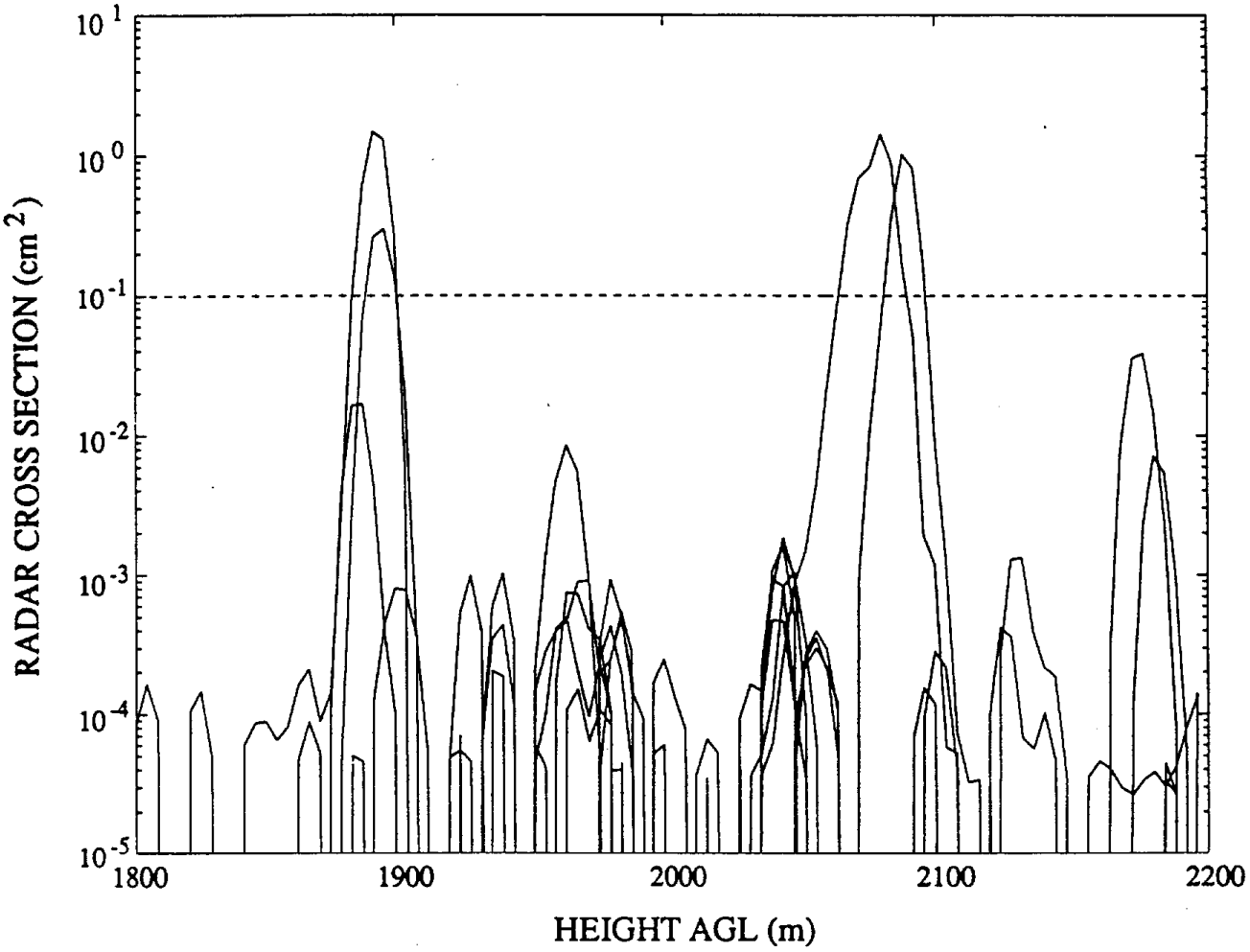
RADAR CROSS SECTION (cm 2)
10 1
10 0
10-1
10-2
10-3
10-4
10-5
1800
1900
2000
2100
2200
HEIGHT AGL (m)

Fig. 17

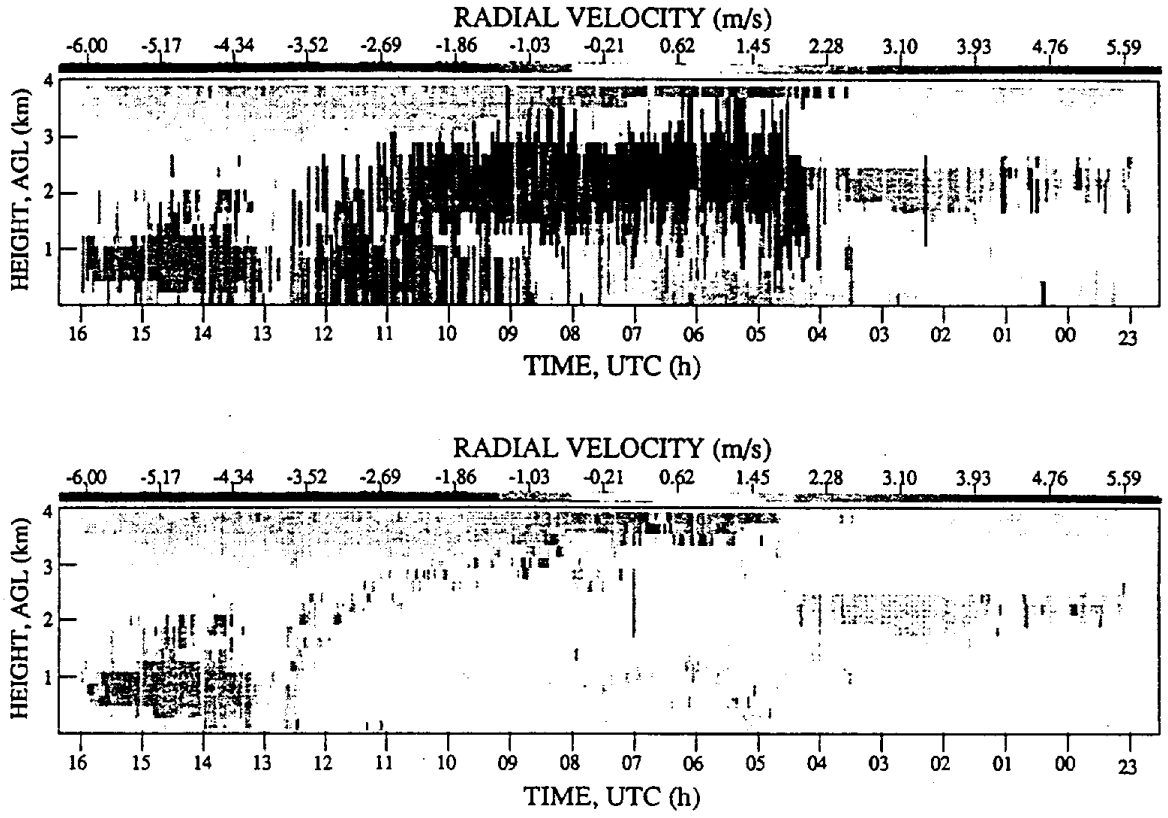
RADIAL VELOCITY (m/s)
-6.00 -5.17 -4.34 -3.52 -2.69 -1.86 -1.03 -0.21 0.62 1.45 2.28 3.10 3.93 4.76 5.59
HEIGHT, AGL (km)
4
3
2
1
16 15 14 13 12 11 10 09 08 07 06 05 04 03 02 01 00 23
TIME, UTC (h)
RADIAL VELOCITY (m/s)
-6.00 -5.17 -4.34 -3.52 -2.69 -1.86 -1.03 -0.21 0.62 1.45 2.28 3.10 3.93 4.76 5.59
HEIGHT, AGL (km)
4
3
2
1
16 15 14 13 12 11 10 09 08 07 06 05 04 03 02 01 00 23
TIME, UTC (h)

Fig. 18

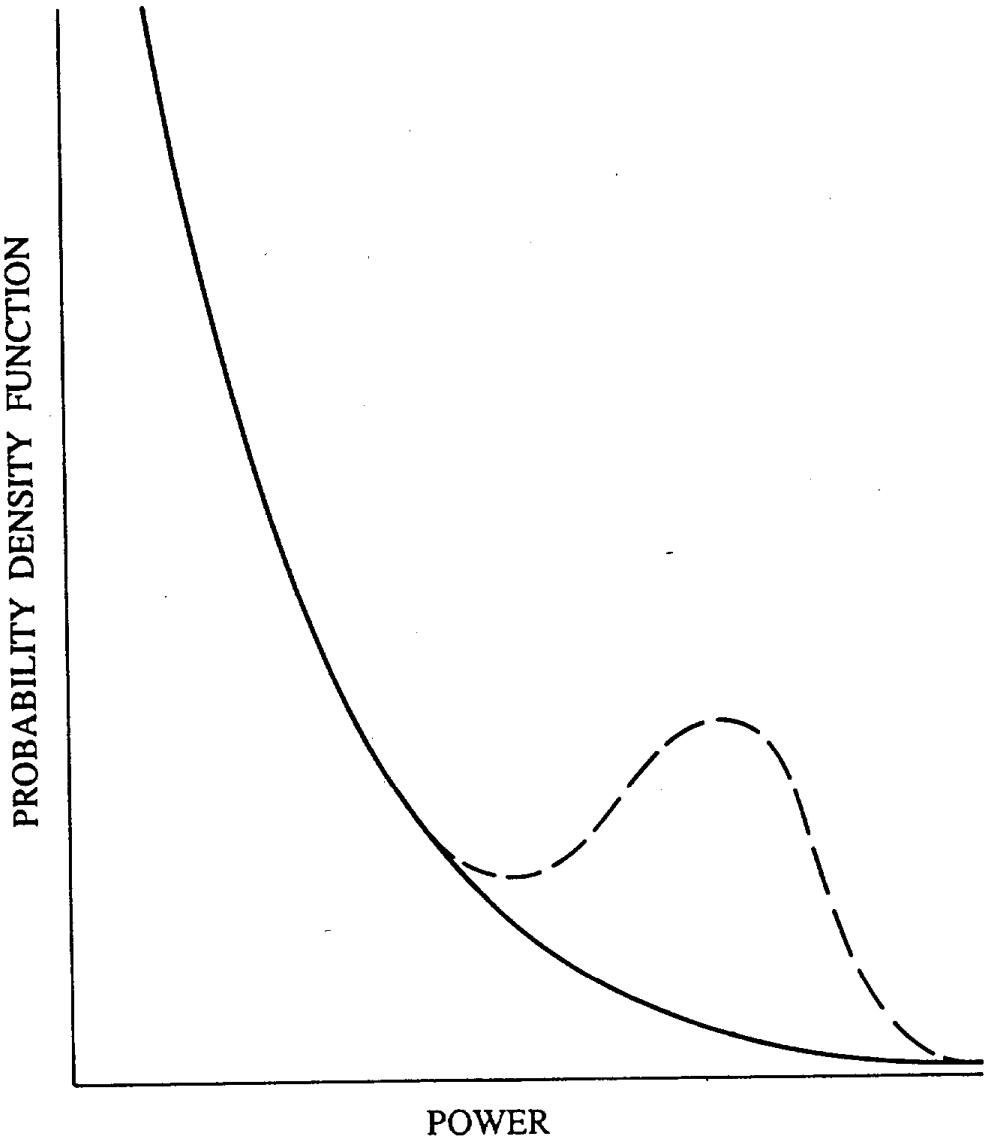


Fig. 19

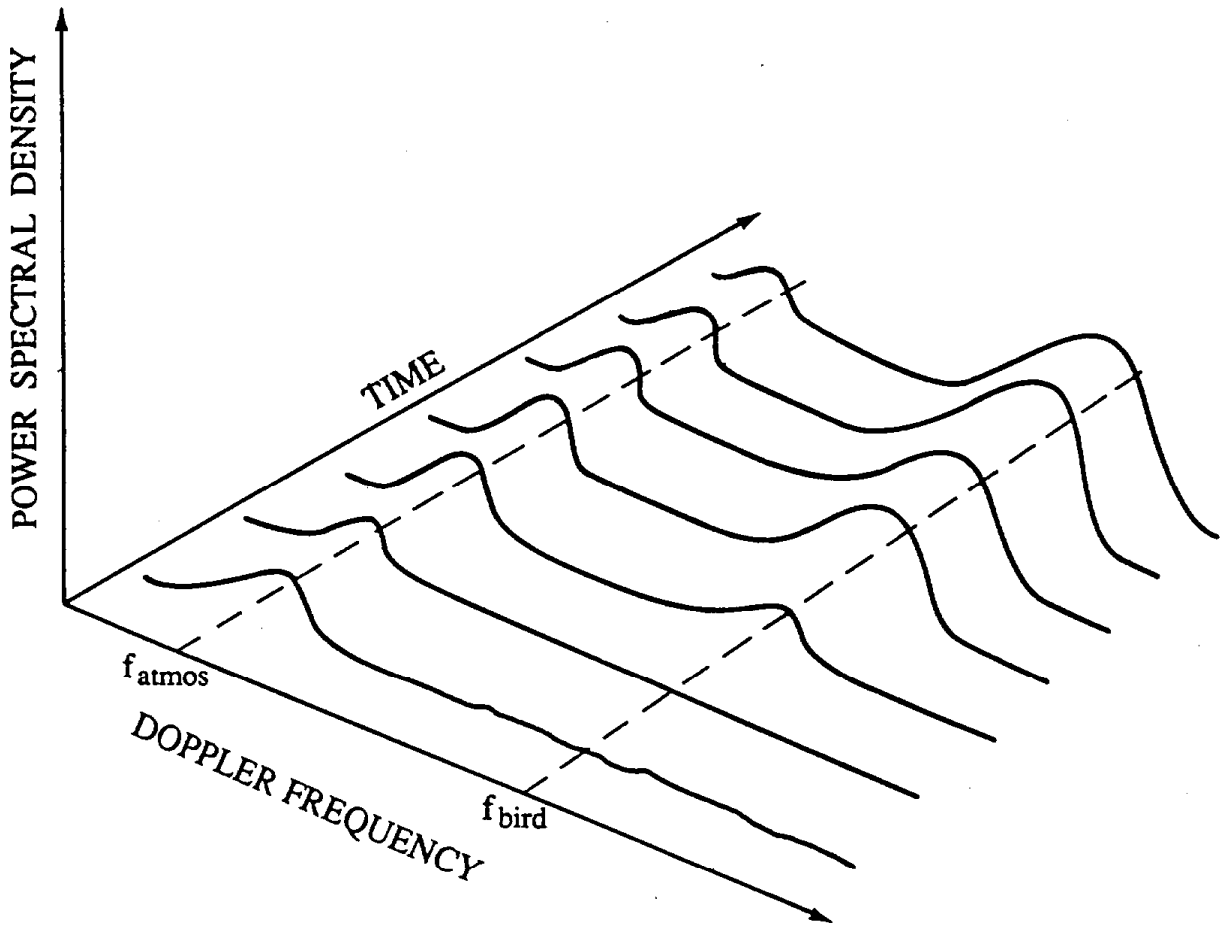
POWER SPECTRAL DENSITY
TIME
f atmos
DOPPLER FREQUENCY
f bird

Fig. 20

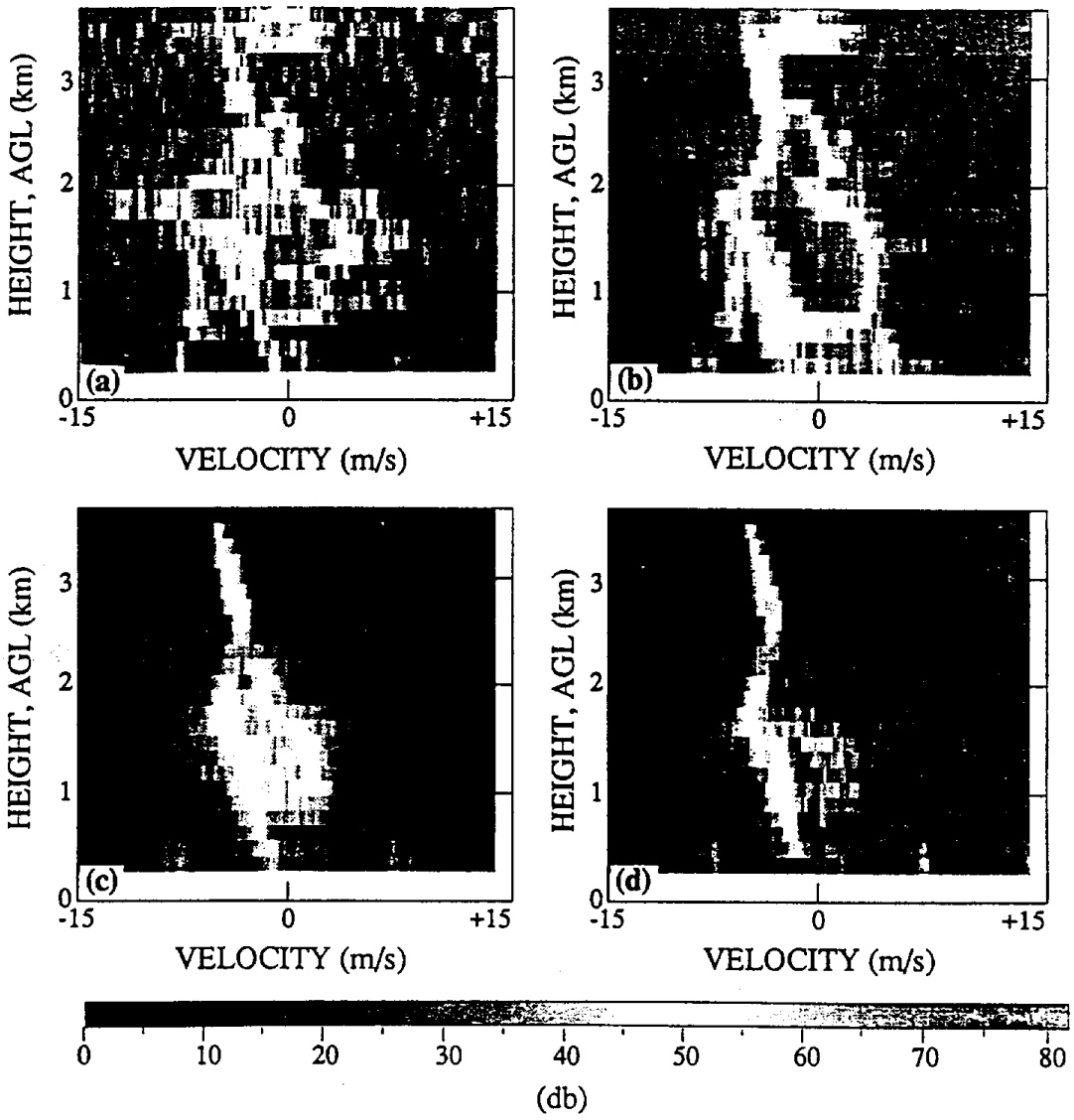
HEIGHT, AGL (km)
3
2
1
0
(a)
-15
0
+15
VELOCITY (m/s)
(b)
(c)
(d)
0
10
20
30
40
50
60
70
80
(db)

Fig. 21

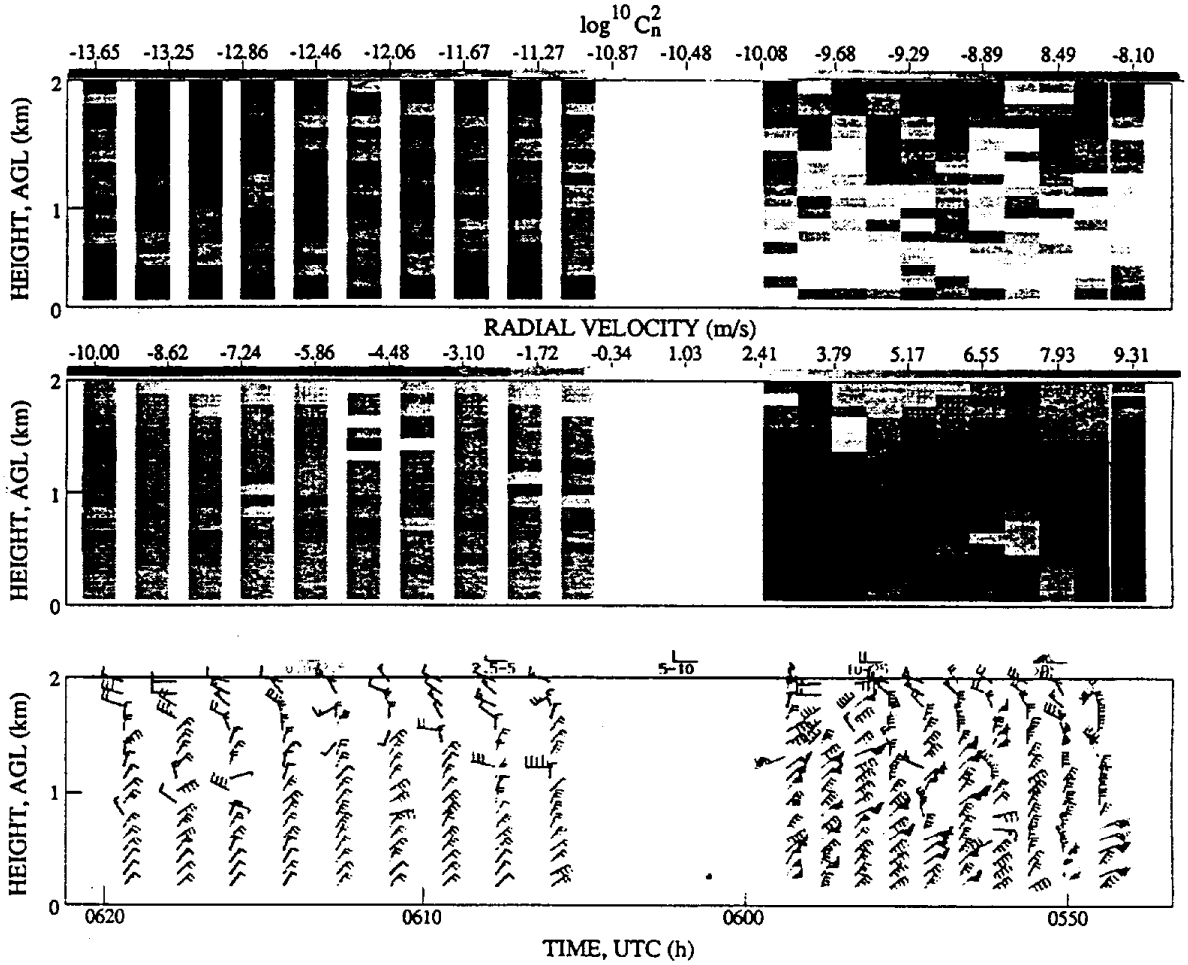
log10 Cn2
-13.65 -13.25 -12.86 -12.46 -12.06 -11.67 -11.27 -10.87 -10.48 -10.08 -9.68 -9.29 -8.89 8.49 -8.10
HEIGHT, AGL (km)
RADIAL VELOCITY (m/s)
-10.00 -8.62 -7.24 -5.86 -4.48 -3.10 -1.72 -0.34 1.03 2.41 3.79 5.17 6.55 7.93 9.31
HEIGHT, AGL (km)
HEIGHT, AGL (km)
0620 0610 0600 0550
TIME, UTC (h)

Fig. 22

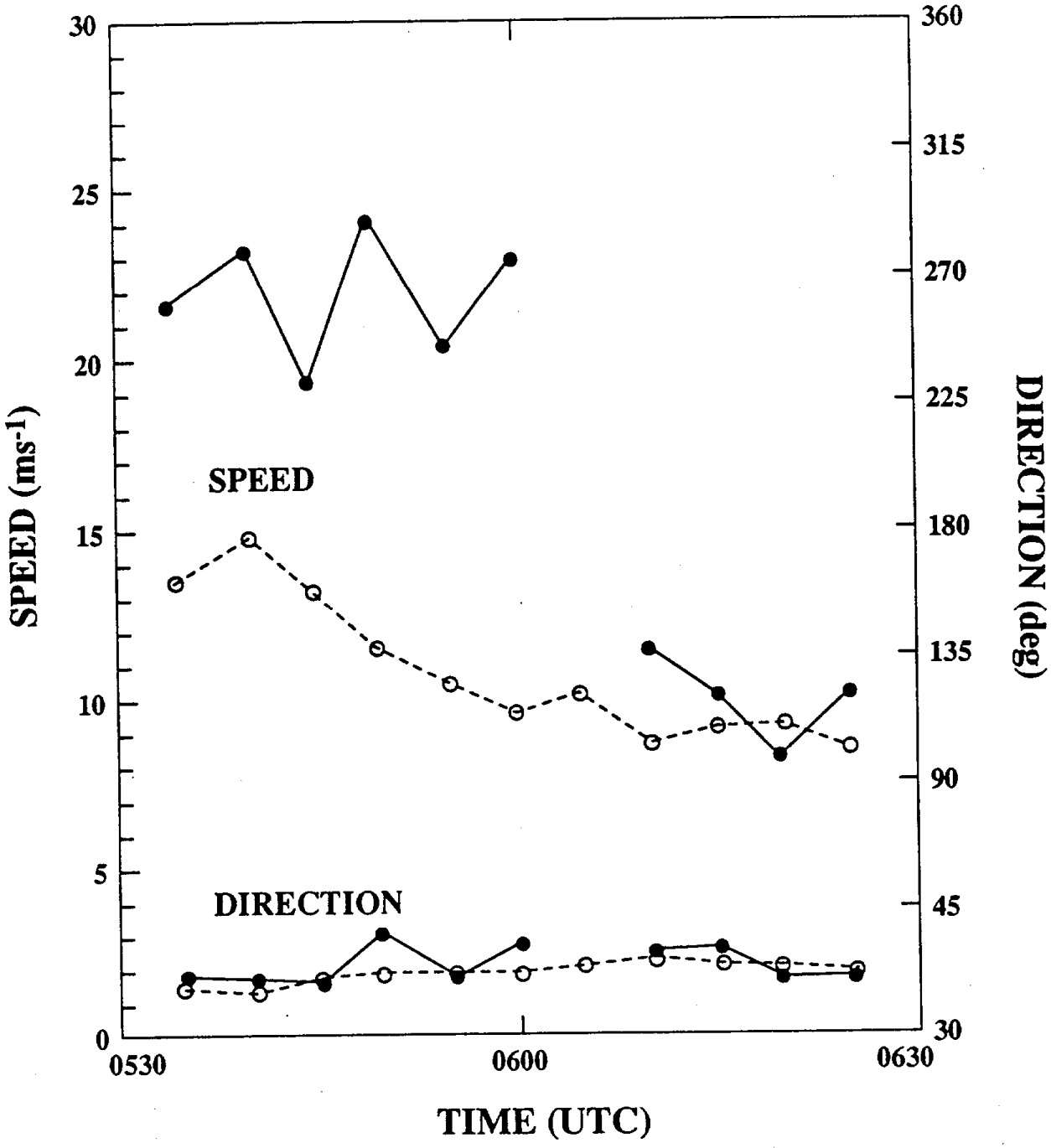
30
25
20
15
10
5
0
360
315
270
225
180
135
90
45
30
SPEED (ms-1)
DIRECTION (deg)
SPEED
DIRECTION
0530
0600
0630
TIME (UTC)

Fig. 23

# APPENDIX B

RAWINSONDE/PROFILER COMPARISONS

# NORTHERN CALIFORNIA TRANSPORT (NCT) 1991
# 915 MHz WIND PROFILER/RAWINSONDE COMPARISON

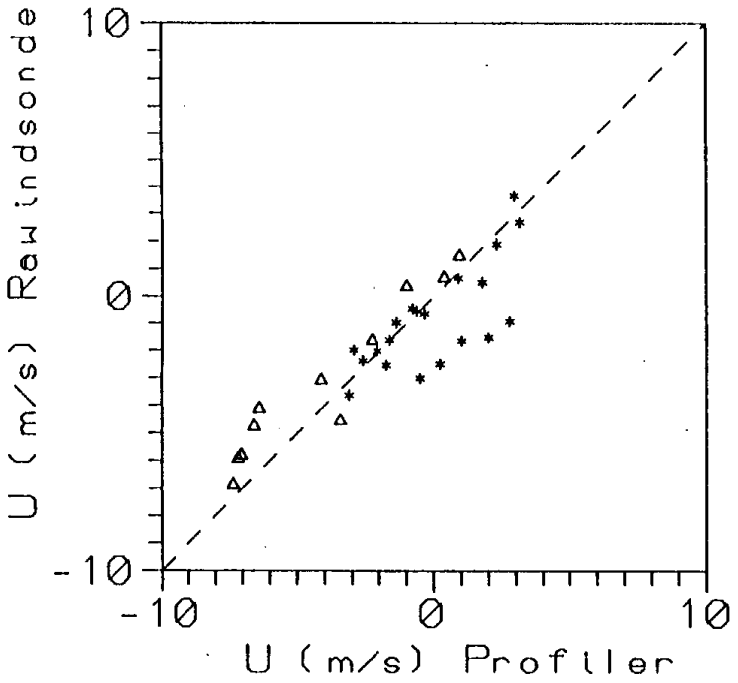


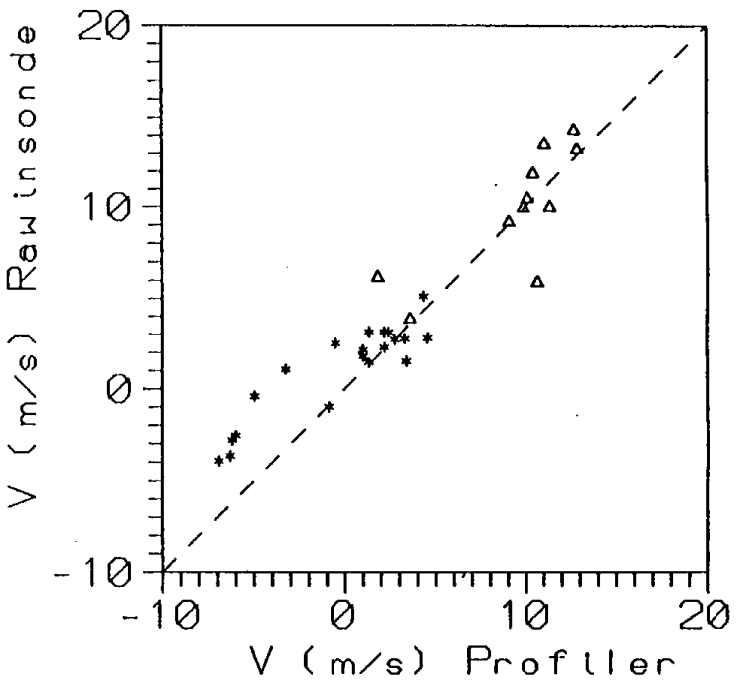


* * * * * 0-3000 m
△ △ △ △ △ > 3000 m

* RMSE for data <= 3000 m

| Var | n | min | max | Mean | SD | r | $r^2$ | SE | RMSE |
|---|---|---|---|---|---|---|---|---|---|
| RU | 31 | -7 | 4 | -1.6 | 2.5 | 0.88 | 0.77 | 1.23 | 1.6 |
| PU | 31 | -7 | 3 | -1.4 | 3.1 | 0.88 | 0.77 | 1.23 | 1.6 |
| RV | 31 | -4 | 14 | 4.2 | 5.2 | 0.94 | 0.89 | 1.72 | 2.3 |
| PV | 31 | -7 | 13 | 3.2 | 6.0 | 0.94 | 0.89 | 1.72 | 2.3 |

Arbuckle (JD: 229-230)
Night: 1900 - 0800 PDT
Threshold/low res

# NORTHERN CALIFORNIA TRANSPORT (NCT) 1991
# 915 MHz WIND PROFILER/RAWINSONDE COMPARISON

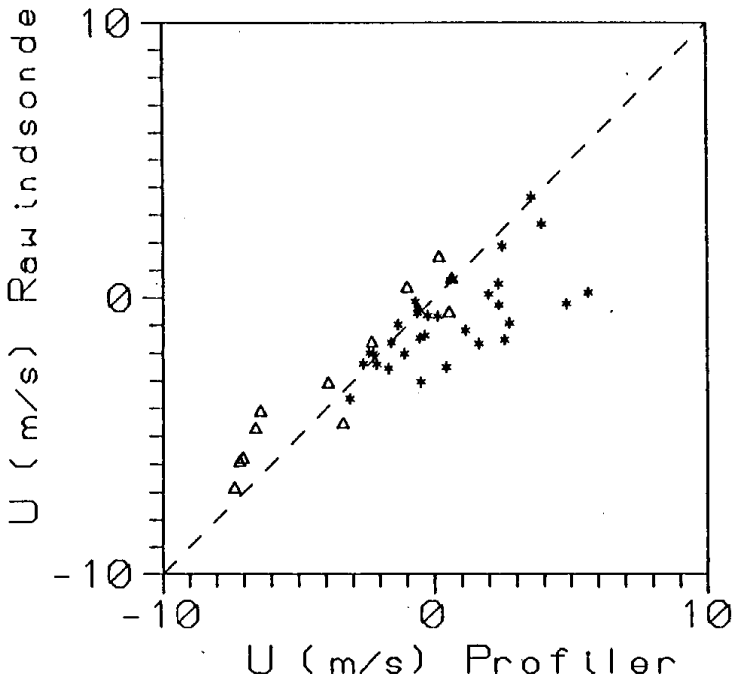


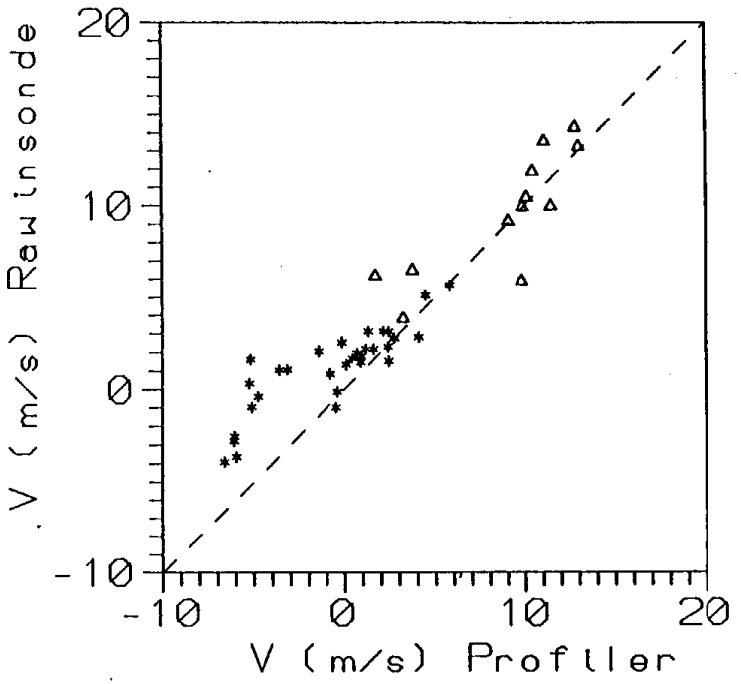


* * * * * 0-3000 m
△ △ △ △ △ > 3000 m

* RMSE for data <= 3000 m

| Var | n | min | max | Mean | SD | r | $r^2$ | SE | RMSE |
|---|---|---|---|---|---|---|---|---|---|
| RU | 44 | -7 | 4 | -1.4 | 2.2 | 0.83 | 0.70 | 1.22 | 2.1 |
| PU | 44 | -7 | 6 | -0.7 | 3.1 | 0.83 | 0.70 | 1.22 | 2.1 |
| RV | 44 | -4 | 14 | 3.5 | 4.6 | 0.94 | 0.88 | 1.63 | 2.7 |
| PV | 44 | -7 | 13 | 2.0 | 5.5 | 0.94 | 0.88 | 1.63 | 2.7 |

Arbuckle (JD: 229-230)
Night: 1900 - 0800 PDT
No threshold/low res

# NORTHERN CALIFORNIA TRANSPORT (NCT) 1991
# 915 MHz WIND PROFILER/RAWINSONDE COMPARISON

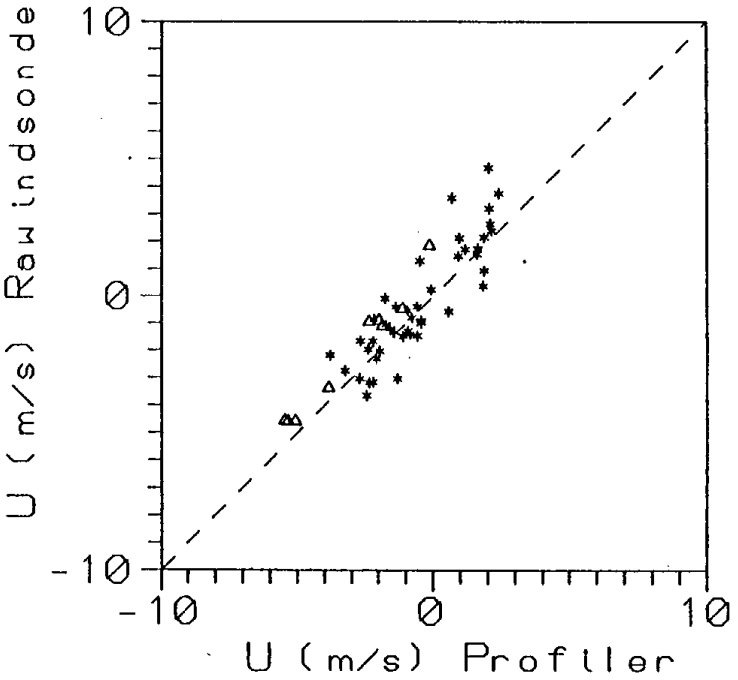


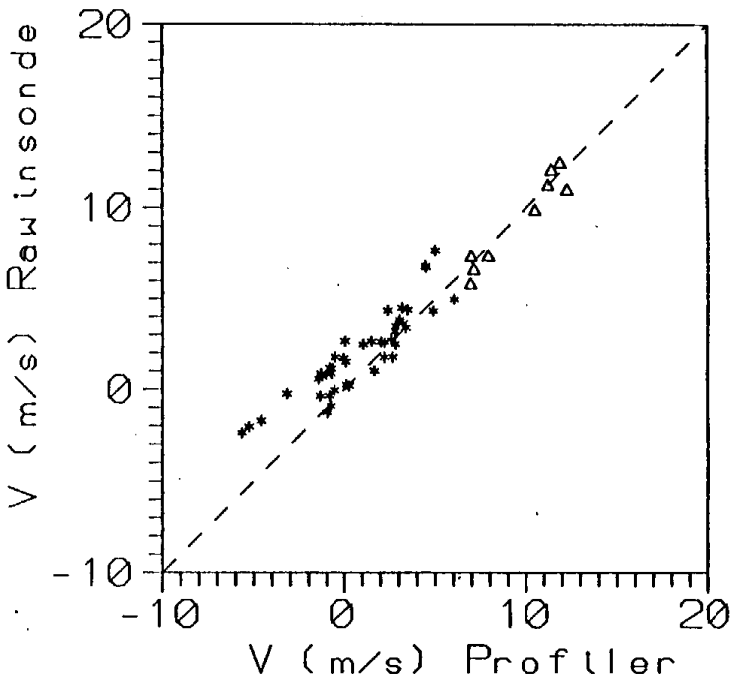


* * * * * 0-3000 m
△ △ △ △ △ > 3000 m

* RMSE for data <= 3000 m

| Var | n | min | max | Mean | SD | r | $r^2$ | SE | RMSE |
|---|---|---|---|---|---|---|---|---|---|
| RU | 53 | -5 | 5 | -0.6 | 2.2 | 0.90 | 0.80 | 1.00 | 1.0 |
| PU | 53 | -5 | 2 | -0.9 | 2.0 | 0.90 | 0.80 | 1.00 | 1.0 |
| RV | 53 | -2 | 12 | 3.2 | 3.6 | 0.96 | 0.92 | 1.00 | 1.6 |
| PV | 53 | -6 | 12 | 2.3 | 4.2 | 0.96 | 0.92 | 1.00 | 1.6 |

Arbuckle (JD: 229-230)
Day: 0800 - 1900 PDT
Threshold/low res

# NORTHERN CALIFORNIA TRANSPORT (NCT) 1991
# 915 MHz WIND PROFILER/RAWINSONDE COMPARISON

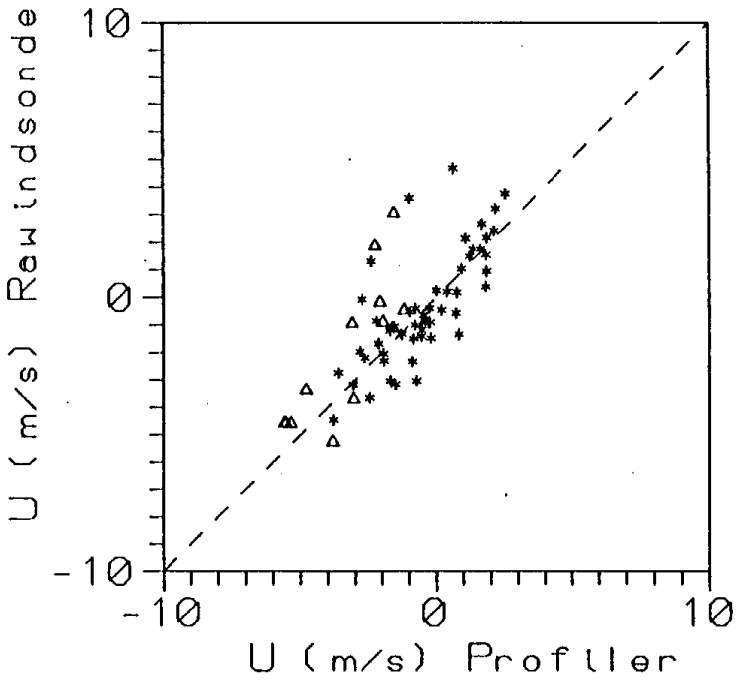


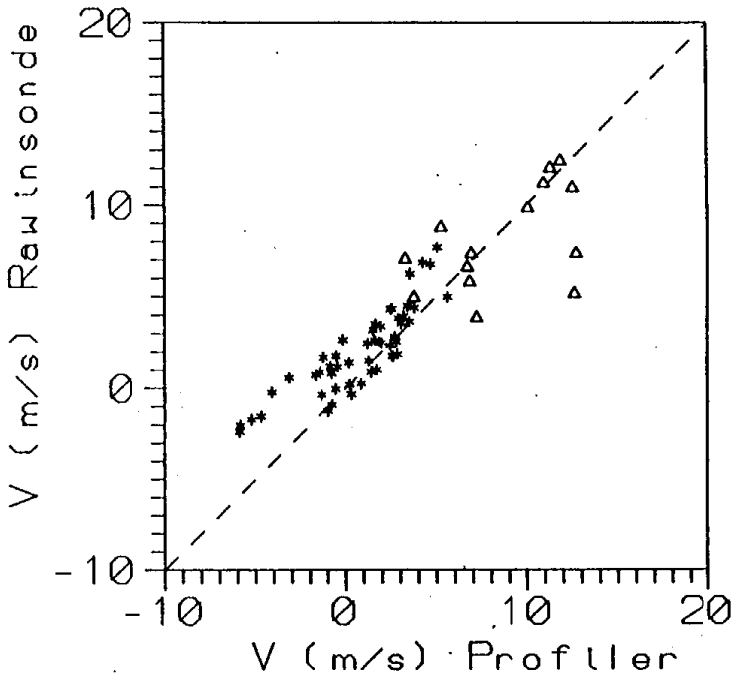


* * * * * 0-3000 m
△ △ △ △ △ > 3000 m

* RMSE for data <= 3000 m

| Var | n | min | max | Mean | SD | r | $r^2$ | SE | RMSE |
|---|---|---|---|---|---|---|---|---|---|
| RU | 68 | -5 | 5 | -0.7 | 2.2 | 0.75 | 0.57 | 1.46 | 1.3 |
| PU | 68 | -6 | 3 | -1.0 | 1.9 | 0.75 | 0.57 | 1.46 | 1.3 |
| RV | 68 | -2 | 12 | 3.3 | 3.4 | 0.89 | 0.80 | 1.55 | 1.8 |
| PV | 68 | -6 | 13 | 2.5 | 4.3 | 0.89 | 0.80 | 1.55 | 1.8 |

Arbuckle (JD: 229-230)
Day: 0800 - 1900 PDT
No threshold/low pass

# NORTHERN CALIFORNIA TRANSPORT (NCT) 1991
# 915 MHz WIND PROFILER/RAWINSONDE COMPARISON

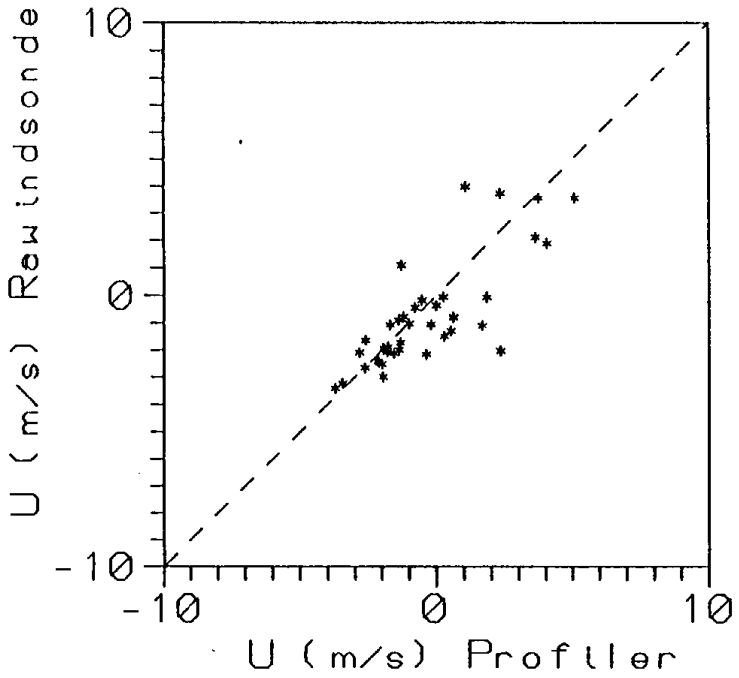


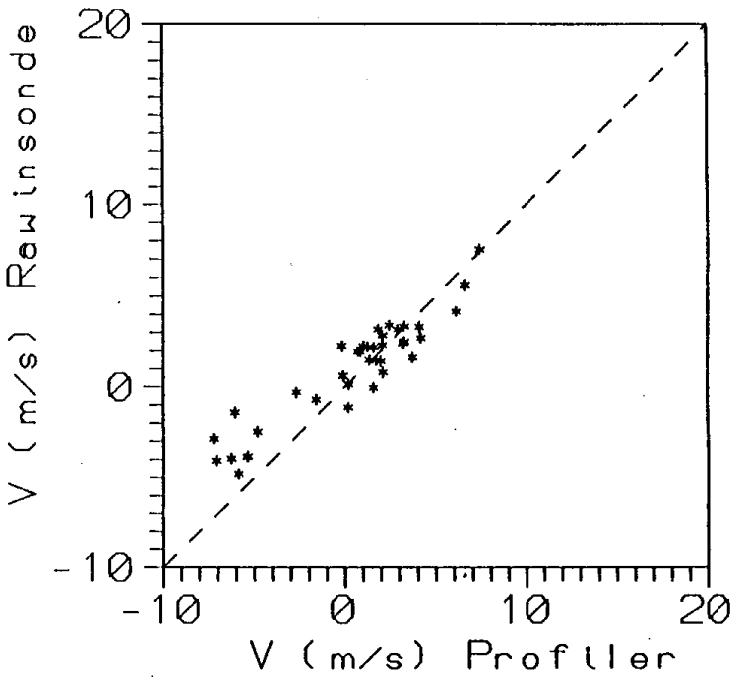


* * * * * 0-3000 m
∆ ∆ ∆ ∆ ∆ > 3000 m

* RMSE for data <= 3000 m

| Var | n | min | max | Mean | SD | r | $r^2$ | SE | RMSE |
|---|---|---|---|---|---|---|---|---|---|
| RU | 38 | -3 | 4 | -0.8 | 2.0 | 0.79 | 0.63 | 1.23 | 1.4 |
| PU | 38 | -4 | 5 | -0.4 | 2.2 | 0.79 | 0.63 | 1.23 | 1.4 |
| RV | 38 | -5 | 8 | 1.0 | 2.8 | 0.94 | 0.87 | 1.01 | 1.7 |
| PV | 38 | -7 | 7 | 0.4 | 3.9 | 0.94 | 0.87 | 1.01 | 1.7 |

Arbuckle (JD: 229-230)
Night: 1900 - 0800 PDT
Threshold/high res

# NORTHERN CALIFORNIA TRANSPORT (NCT) 1991
# 915 MHz WIND PROFILER/RAWINSONDE COMPARISON

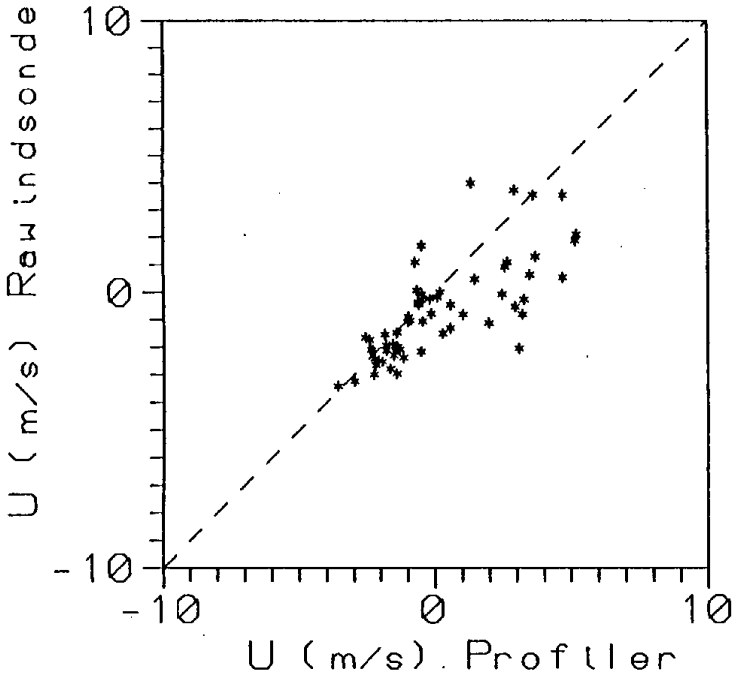


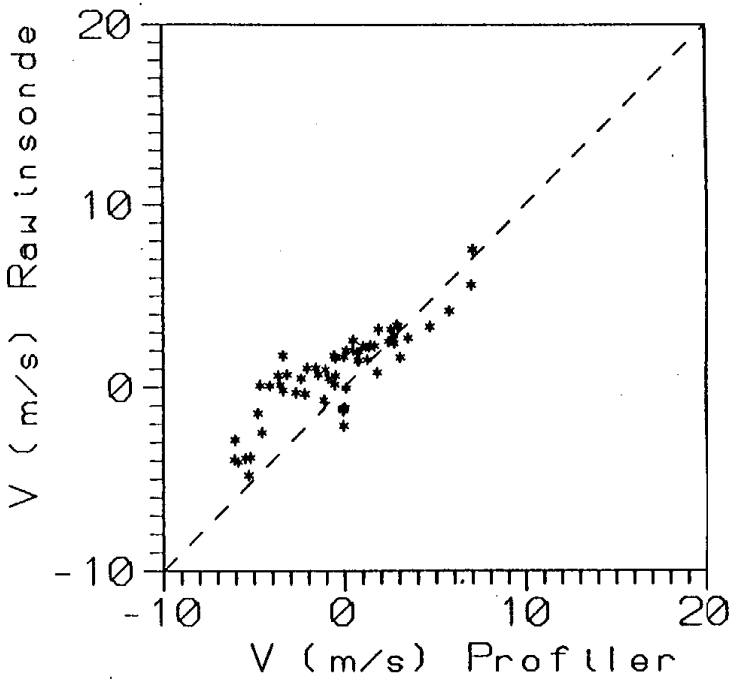


* * * * * 0-3000 m
△ △ △ △ △ > 3000 m

* RMSE for data <= 3000 m

| Var | n | min | max | Mean | SD | r | $r^2$ | SE | RMSE |
|---|---|---|---|---|---|---|---|---|---|
| RU | 62 | -3 | 4 | -0.7 | 1.8 | 0.75 | 0.56 | 1.19 | 1.7 |
| PU | 62 | -4 | 5 | 0.1 | 2.3 | 0.75 | 0.56 | 1.19 | 1.7 |
| RV | 62 | -5 | 8 | 0.9 | 2.3 | 0.86 | 0.74 | 1.20 | 2.0 |
| PV | 62 | -6 | 7 | -0.3 | 3.1 | 0.86 | 0.74 | 1.20 | 2.0 |

Arbuckle (JD: 229-230)
Night: 1900 - 0800 PDT
No threshold/high res

# NORTHERN CALIFORNIA TRANSPORT (NCT) 1991
# 915 MHz WIND PROFILER/RAWINSONDE COMPARISON

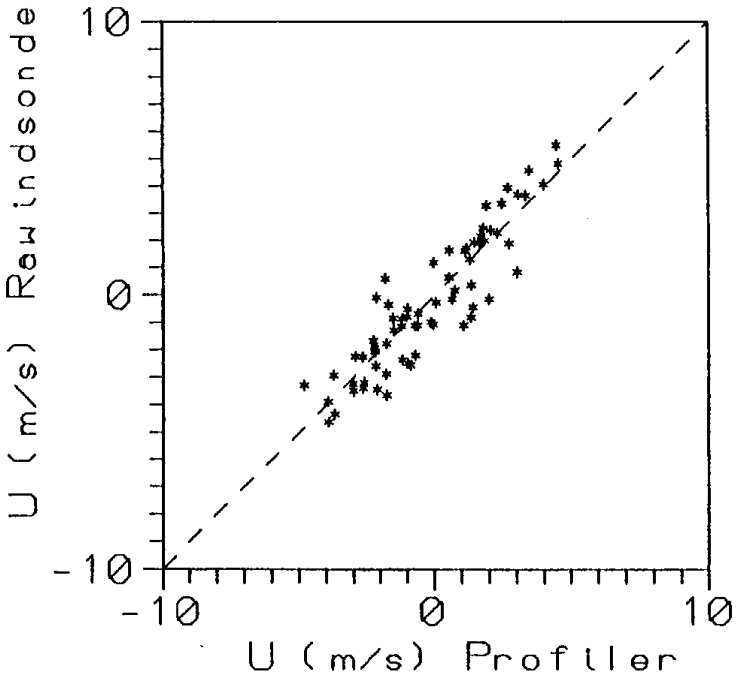


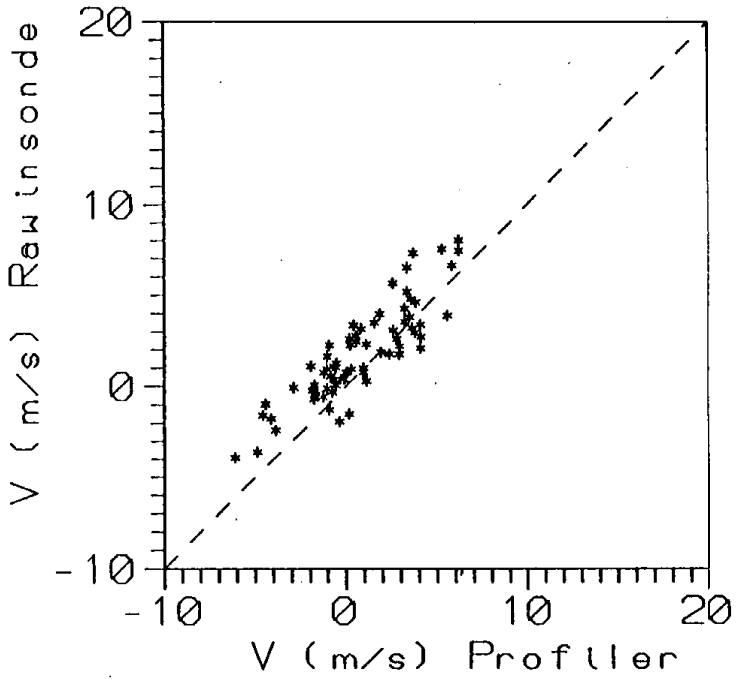


* * * * * 0-3000 m
Δ Δ Δ Δ Δ > 3000 m

* RMSE for data <= 3000 m

| Var | n | min | max | Mean | SD | r | $r^2$ | SE | RMSE |
|---|---|---|---|---|---|---|---|---|---|
| RU | 70 | -5 | 6 | -0.3 | 2.5 | 0.91 | 0.83 | 1.04 | 1.0 |
| PU | 70 | -5 | 5 | -0.2 | 2.3 | 0.91 | 0.83 | 1.04 | 1.0 |
| RV | 70 | -4 | 8 | 1.8 | 2.6 | 0.87 | 0.76 | 1.29 | 1.7 |
| PV | 70 | -6 | 6 | 0.7 | 2.8 | 0.87 | 0.76 | 1.29 | 1.7 |

Arbuckle (JD: 229-230)
Day: 0800 - 1900 PDT
Threshold/high res

# NORTHERN CALIFORNIA TRANSPORT (NCT) 1991
# 915 MHz WIND PROFILER/RAWINSONDE COMPARISON

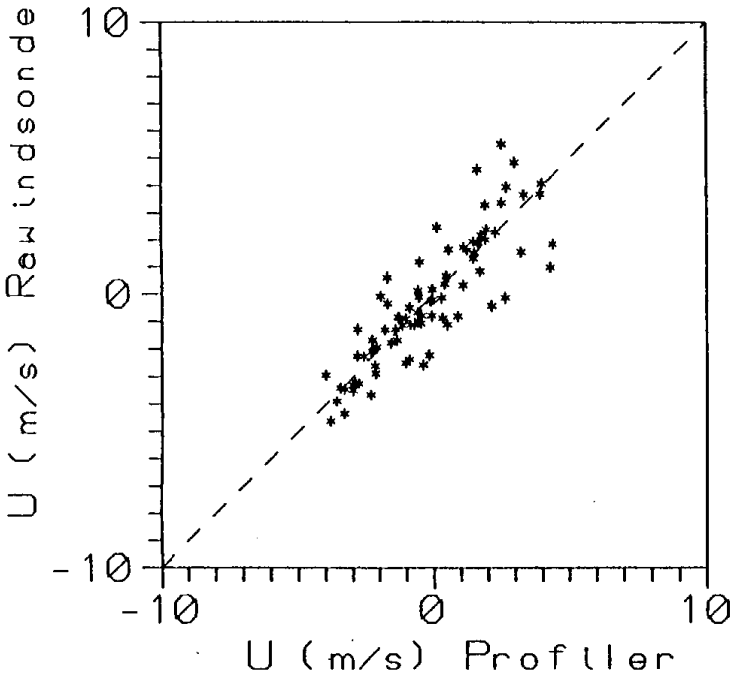


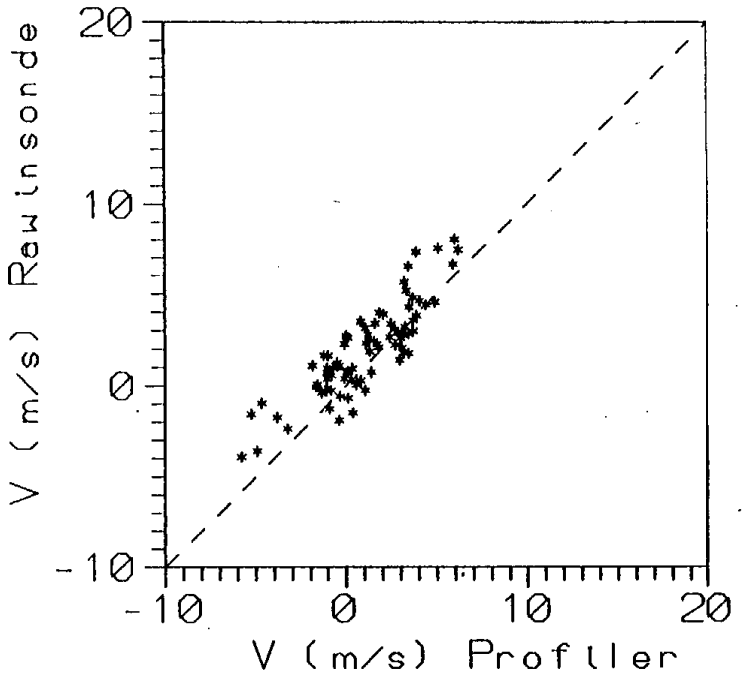


* * * * * 0-3000 m
Δ Δ Δ Δ Δ > 3000 m

* RMSE for data <= 3000 m

| Var | n | min | max | Mean | SD | r | $r^2$ | SE | RMSE |
|---|---|---|---|---|---|---|---|---|---|
| RU | 84 | -5 | 6 | -0.2 | 2.3 | 0.86 | 0.74 | 1.18 | 1.2 |
| PU | 84 | -4 | 4 | -0.2 | 2.1 | 0.86 | 0.74 | 1.18 | 1.2 |
| RV | 84 | -4 | 8 | 1.9 | 2.4 | 0.86 | 0.74 | 1.24 | 1.6 |
| PV | 84 | -6 | 6 | 1.0 | 2.6 | 0.86 | 0.74 | 1.24 | 1.6 |

Arbuckle (JD: 229-230)
Day: 0800 - 1900 PDT
No threshold/high res

# NORTHERN CALIFORNIA TRANSPORT (NCT) 1991
# 915 MHz WIND PROFILER/RAWINSONDE COMPARISON

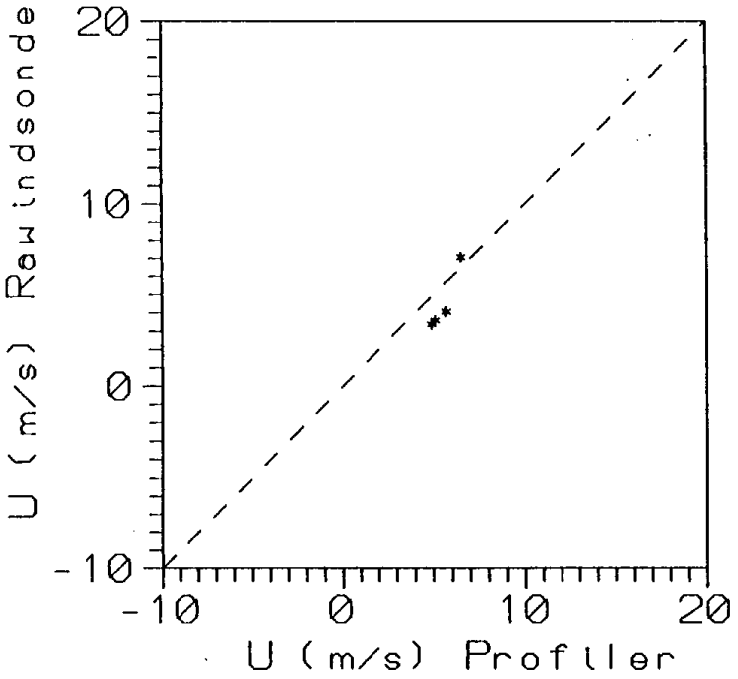


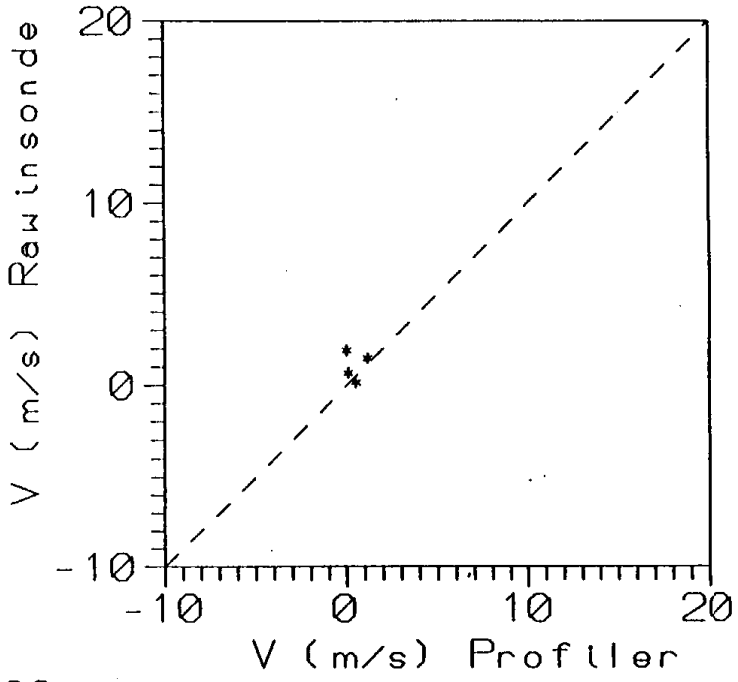


* * * * * 0-3000 m
∆ ∆ ∆ ∆ ∆ > 3000 m

* RMSE for data <= 3000 m

| Var | n | min | max | Mean | SD | r | $r^2$ | SE | RMSE |
|---|---|---|---|---|---|---|---|---|---|
| RU | 4 | 3 | 7 | 4.5 | 1.7 | 0.95 | 0.90 | 0.65 | 1.4 |
| PU | 4 | 5 | 7 | 5.5 | 0.7 | 0.95 | 0.90 | 0.65 | 1.4 |
| RV | 4 | 0 | 2 | 1.0 | 0.8 | 0.01 | 0.00 | 0.96 | 1.0 |
| PV | 4 | 0 | 1 | 0.4 | 0.5 | 0.01 | 0.00 | 0.96 | 1.0 |

Delta Island (JD: 236-237)
Night: 1900 - 0800 PDT
Threshold/low res

# NORTHERN CALIFORNIA TRANSPORT (NCT) 1991
# 915 MHz WIND PROFILER/RAWINSONDE COMPARISON

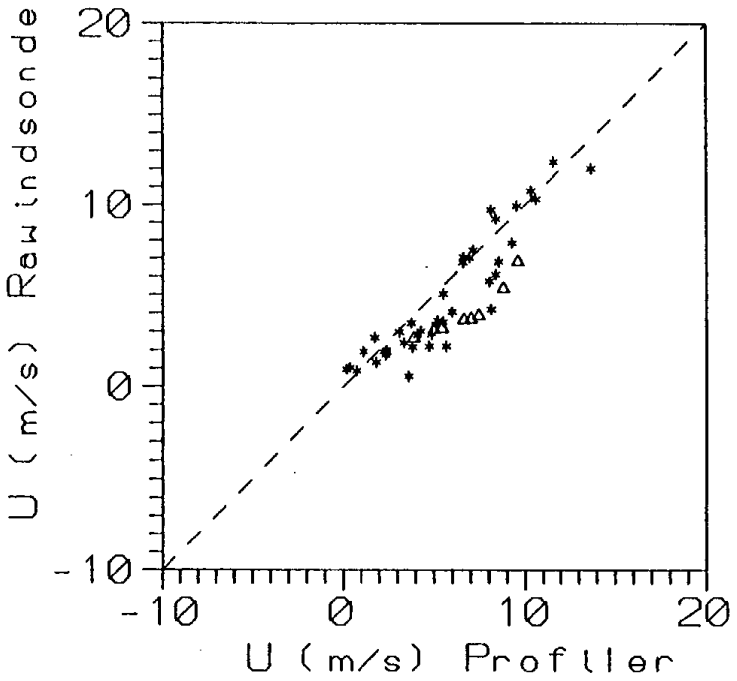


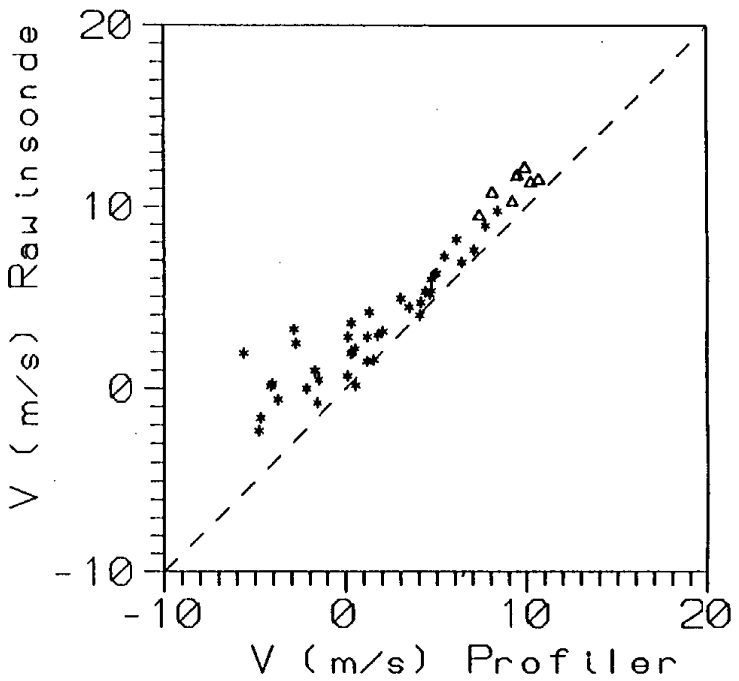


* * * * * 0-3000 m
△ △ △ △ △ > 3000 m

* RMSE for data <= 3000 m

| Var | n | min | max | Mean | SD | r | $r^2$ | SE | RMSE |
|---|---|---|---|---|---|---|---|---|---|
| RU | 49 | 1 | 12 | 4.6 | 3.1 | 0.90 | 0.80 | 1.40 | 1.5 |
| PU | 49 | 0 | 14 | 5.7 | 3.1 | 0.90 | 0.80 | 1.40 | 1.5 |
| RV | 49 | -2 | 12 | 4.5 | 4.0 | 0.94 | 0.89 | 1.36 | 2.5 |
| PV | 49 | -6 | 11 | 2.6 | 4.6 | 0.94 | 0.89 | 1.36 | 2.5 |

Delta Island (JD: 236-237)
Night: 1900 - 0800 PDT
No threshold/low res

# NORTHERN CALIFORNIA TRANSPORT (NCT) 1991
# 915 MHz WIND PROFILER/RAWINSONDE COMPARISON

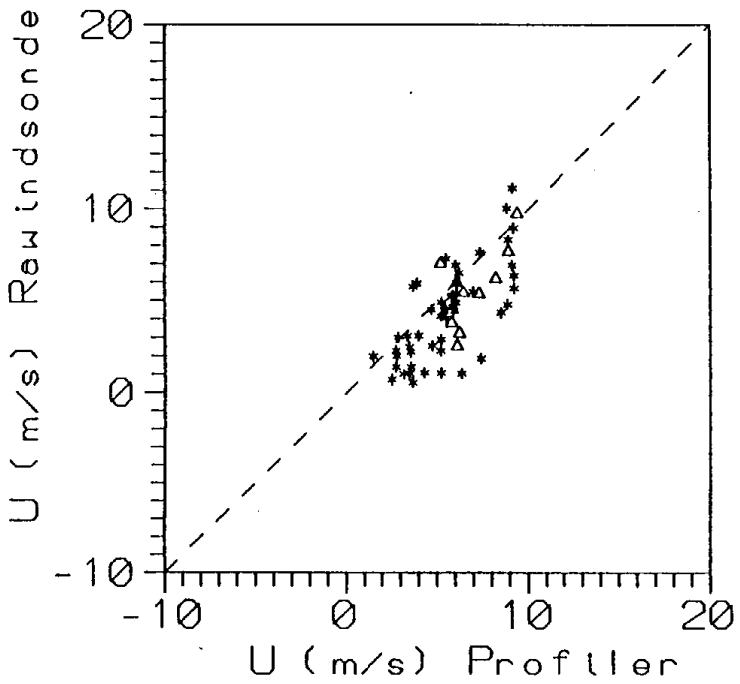


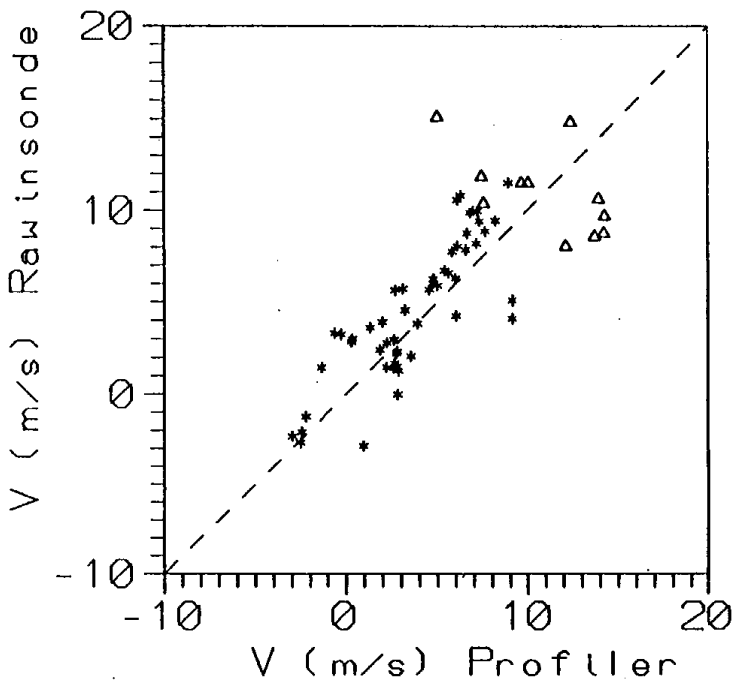


* * * * * 0-3000 m
△ △ △ △ △ > 3000 m

* RMSE for data <= 3000 m

| Var | n | min | max | Mean | SD | r | $r^2$ | SE | RMSE |
|---|---|---|---|---|---|---|---|---|---|
| RU | 64 | 1 | 11 | 4.6 | 2.4 | 0.71 | 0.51 | 1.73 | 2.1 |
| PU | 64 | 2 | 9 | 5.7 | 2.0 | 0.71 | 0.51 | 1.73 | 2.1 |
| RV | 64 | -3 | 15 | 5.7 | 4.3 | 0.78 | 0.60 | 2.71 | 2.3 |
| PV | 64 | -3 | 14 | 5.0 | 4.2 | 0.78 | 0.60 | 2.71 | 2.3 |

Delta Island (JD: 236-237)
Day: 0800 - 1900 PDT
Threshold/low res

# NORTHERN CALIFORNIA TRANSPORT (NCT) 1991
# 915 MHz WIND PROFILER/RAWINSONDE COMPARISON

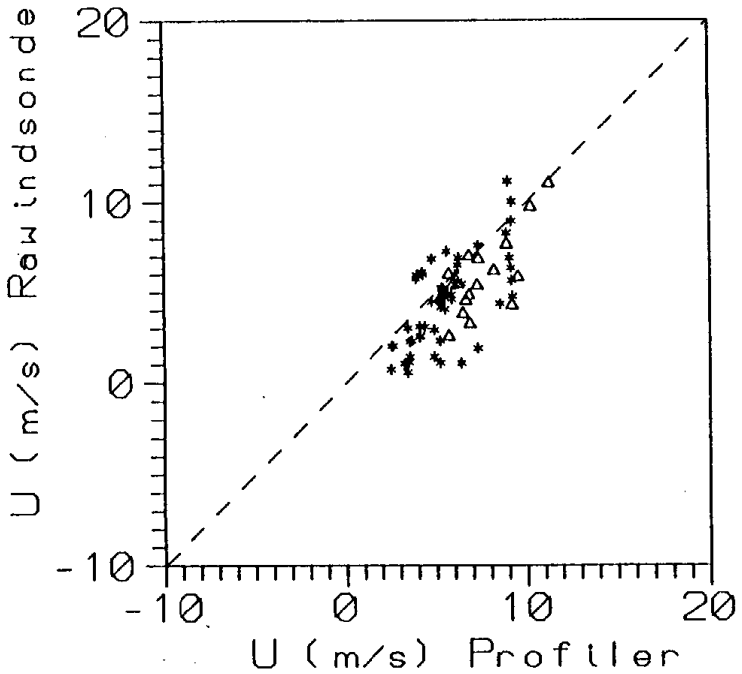


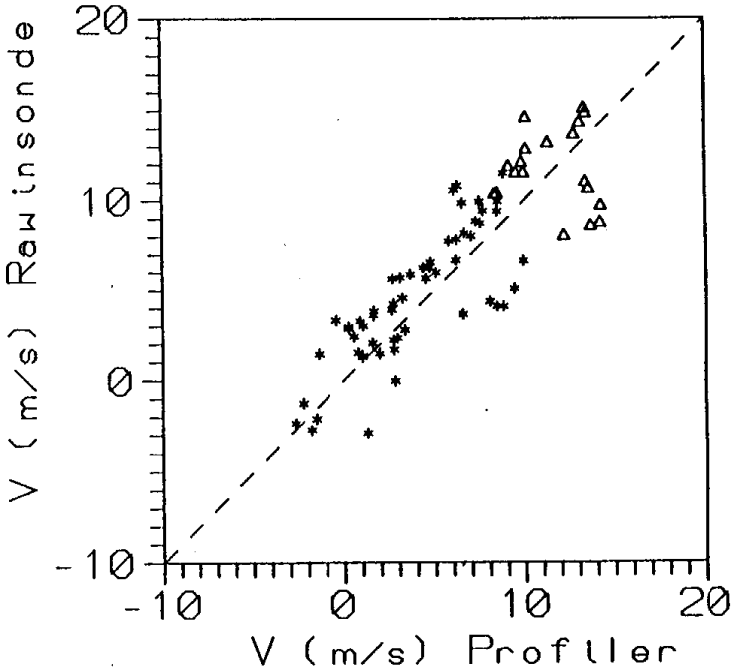


* * * * * 0-3000 m
△ △ △ △ △ > 3000 m

* RMSE for data <= 3000 m

| Var | n | min | max | Mean | SD | r | $r^2$ | SE | RMSE |
|---|---|---|---|---|---|---|---|---|---|
| RU | 75 | 1 | 11 | 4.8 | 2.4 | 0.70 | 0.49 | 1.74 | 2.1 |
| PU | 75 | 3 | 11 | 5.9 | 2.0 | 0.70 | 0.49 | 1.74 | 2.1 |
| RV | 75 | -3 | 15 | 6.4 | 4.5 | 0.85 | 0.73 | 2.39 | 2.3 |
| PV | 75 | -3 | 14 | 5.8 | 4.6 | 0.85 | 0.73 | 2.39 | 2.3 |

Delta Island (JD: 236-237)
Day: 0800 - 1900 PDT
No threshold/low pass

# NORTHERN CALIFORNIA TRANSPORT (NCT) 1991
# 915 MHz WIND PROFILER/RAWINSONDE COMPARISON

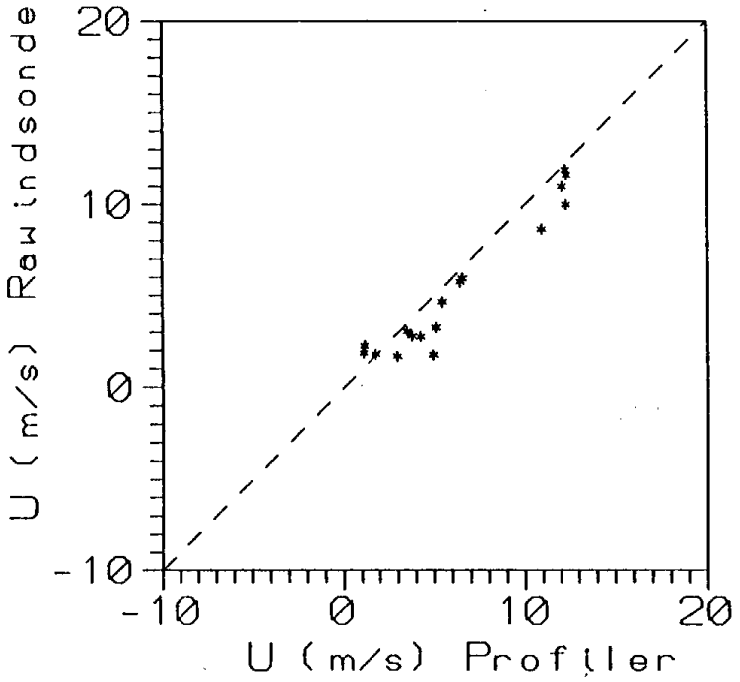


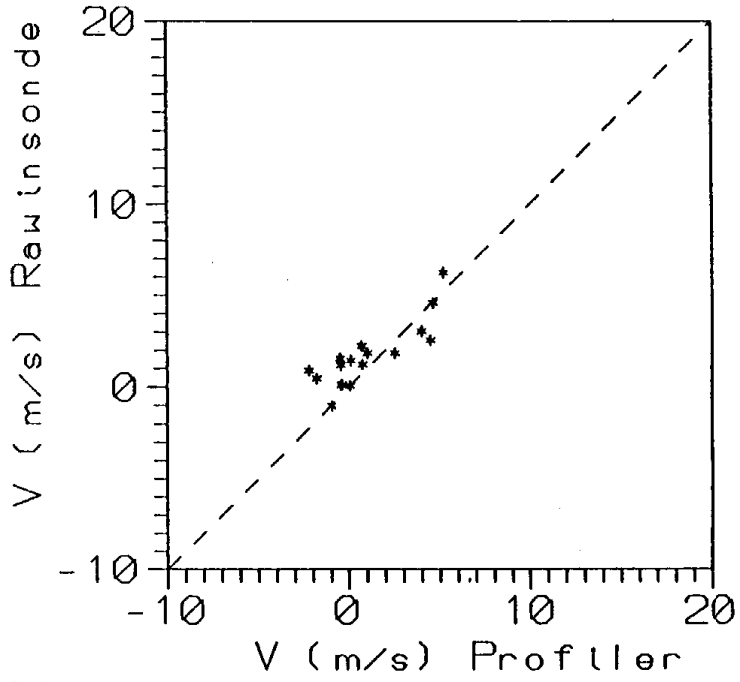


* * * * * 0-3000 m
∆ ∆ ∆ ∆ ∆ > 3000 m

* RMSE for data <= 3000 m

| Var | n | min | max | Mean | SD | r | $r^2$ | SE | RMSE |
|---|---|---|---|---|---|---|---|---|---|
| RU | 17 | 2 | 12 | 5.3 | 3.8 | 0.96 | 0.93 | 1.03 | 1.4 |
| PU | 17 | 1 | 12 | 6.3 | 4.1 | 0.96 | 0.93 | 1.03 | 1.4 |
| RV | 17 | -1 | 6 | 1.7 | 1.8 | 0.84 | 0.71 | 0.97 | 1.4 |
| PV | 17 | -2 | 5 | 1.0 | 2.3 | 0.84 | 0.71 | 0.97 | 1.4 |

Delta Island (JD: 236-237)
Night: 1900 - 0800 PDT
Threshold/high res

# NORTHERN CALIFORNIA TRANSPORT (NCT) 1991
# 915 MHz WIND PROFILER/RAWINSONDE COMPARISON

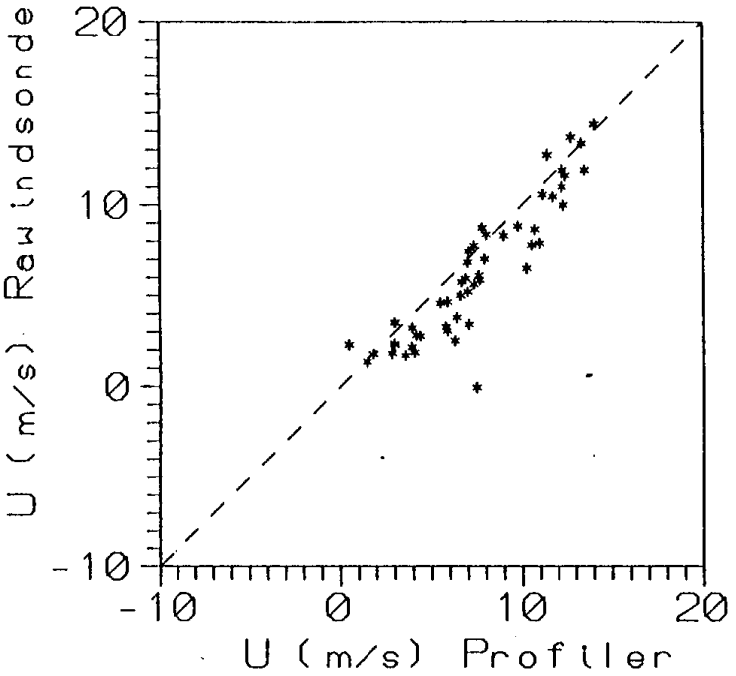


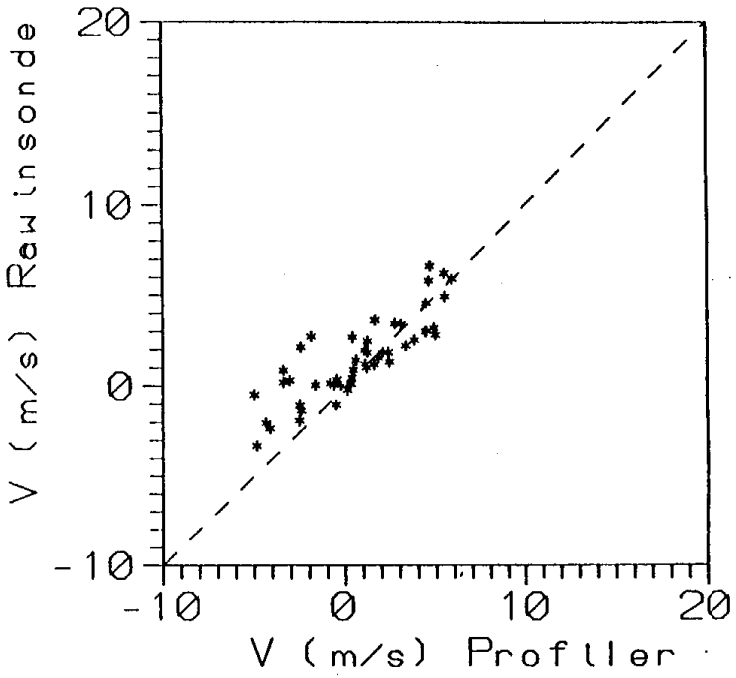


* * * * * 0-3000 m
∆ ∆ ∆ ∆ ∆ > 3000 m

* RMSE for data <= 3000 m

| Var | n | min | max | Mean | SD | r | $r^2$ | SE | RMSE |
|---|---|---|---|---|---|---|---|---|---|
| RU | 51 | 0 | 14 | 6.3 | 3.8 | 0.91 | 0.83 | 1.57 | 2.0 |
| PU | 51 | 0 | 14 | 7.5 | 3.5 | 0.91 | 0.83 | 1.57 | 2.0 |
| RV | 51 | -3 | 7 | 1.6 | 2.3 | 0.85 | 0.72 | 1.23 | 1.8 |
| PV | 51 | -5 | 6 | 0.8 | 3.0 | 0.85 | 0.72 | 1.23 | 1.8 |

Delta Island (JD: 236-237)
Night: 1900 - 0800 PDT
No threshold/high res

# NORTHERN CALIFORNIA TRANSPORT (NCT) 1991
## 915 MHz WIND PROFILER/RAWINSONDE COMPARISON

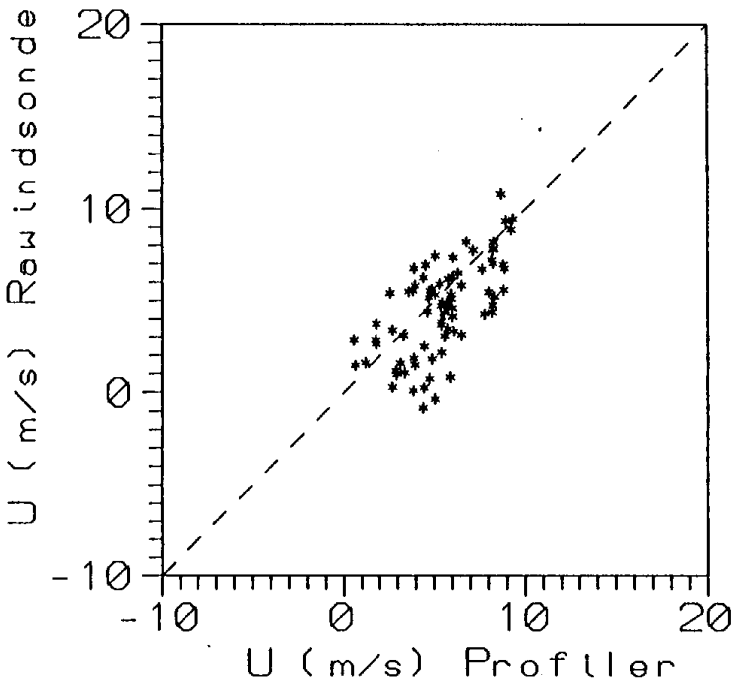


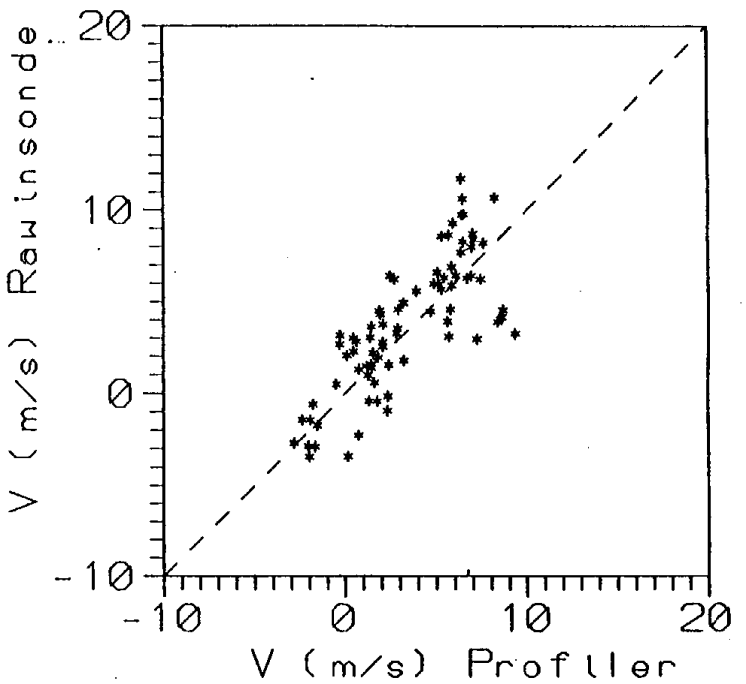


* * * * * 0-3000 m
∆ ∆ ∆ ∆ ∆ > 3000 m

* RMSE for data <= 3000 m

| Var | n | min | max | Mean | SD | r | $r^2$ | SE | RMSE |
|---|---|---|---|---|---|---|---|---|---|
| RU | 80 | -1 | 11 | 4.6 | 2.5 | 0.64 | 0.41 | 1.95 | 2.2 |
| PU | 80 | 1 | 9 | 5.4 | 2.1 | 0.64 | 0.41 | 1.95 | 2.2 |
| RV | 80 | -3 | 12 | 3.8 | 3.6 | 0.78 | 0.61 | 2.28 | 2.3 |
| PV | 80 | -3 | 9 | 3.4 | 3.2 | 0.78 | 0.61 | 2.28 | 2.3 |

Delta Island (JD: 236-237)
Day: 0800 - 1900 PDT
Threshold/high res

# NORTHERN CALIFORNIA TRANSPORT (NCT) 1991
# 915 MHz WIND PROFILER/RAWINSONDE COMPARISON

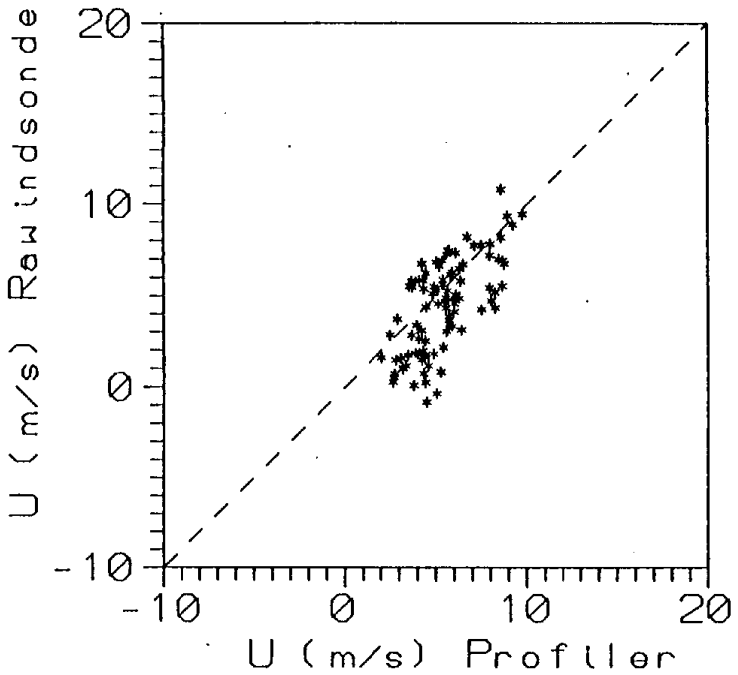


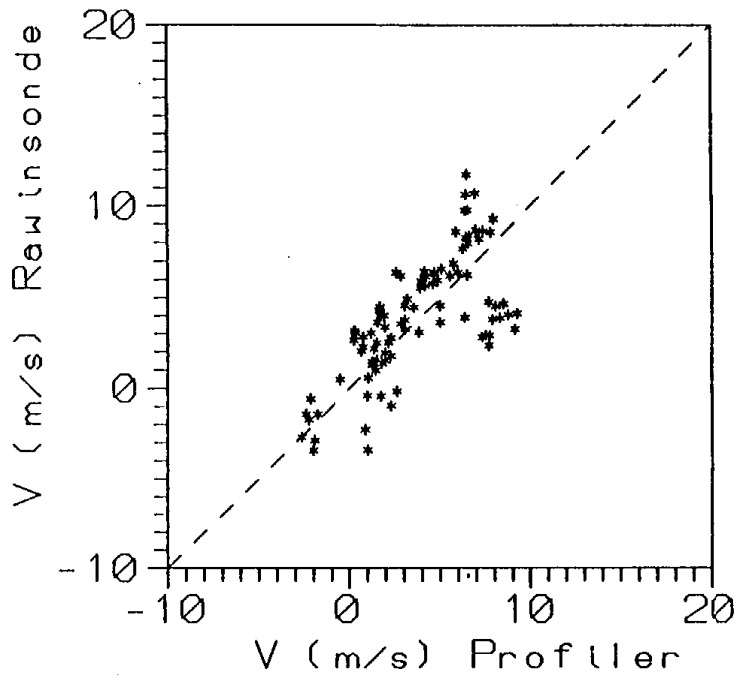


* * * * * 0-3000 m
∆ ∆ ∆ ∆ ∆ > 3000 m

* RMSE for data <= 3000 m

| Var | n | min | max | Mean | SD | r | $r^2$ | SE | RMSE |
|---|---|---|---|---|---|---|---|---|---|
| RU | 95 | -1 | 11 | 4.5 | 2.6 | 0.68 | 0.46 | 1.89 | 2.1 |
| PU | 95 | 2 | 10 | 5.4 | 1.8 | 0.68 | 0.46 | 1.89 | 2.1 |
| RV | 95 | -3 | 12 | 3.9 | 3.4 | 0.73 | 0.53 | 2.36 | 2.4 |
| PV | 95 | -3 | 9 | 3.6 | 3.1 | 0.73 | 0.53 | 2.36 | 2.4 |

Delta Island (JD: 236-237)
Day: 0800 - 1900 PDT
No threshold/high res

# NORTHERN CALIFORNIA TRANSPORT (NCT) 1991
## 915 MHz WIND PROFILER/RAWINSONDE COMPARISON

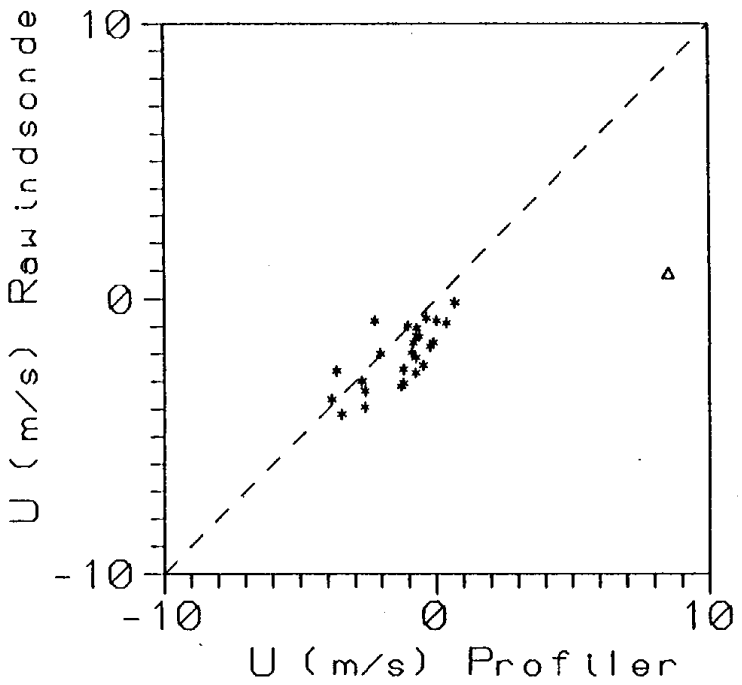


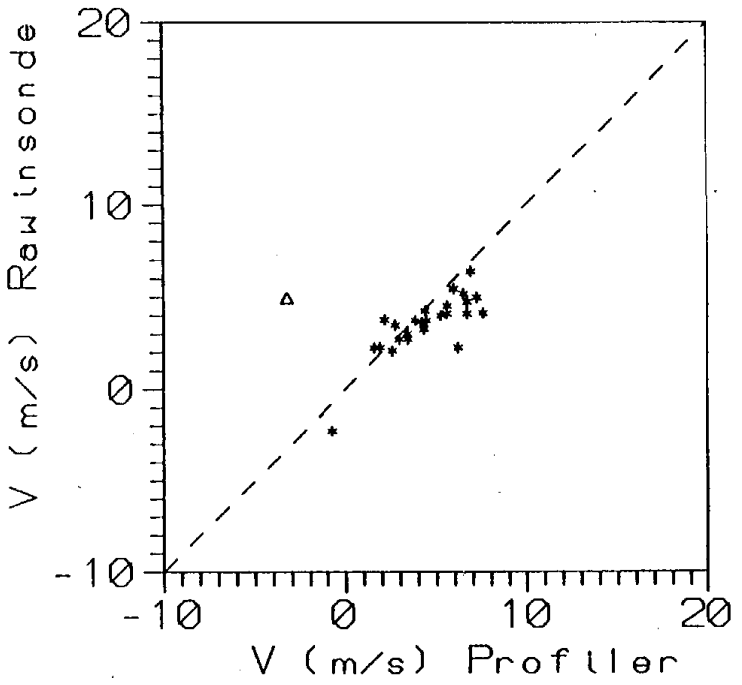


* * * * * 0-3000 m
△ △ △ △ △ > 3000 m

* RMSE for data <= 3000 m

| Var | n | min | max | Mean | SD | r | $r^2$ | SE | RMSE |
|---|---|---|---|---|---|---|---|---|---|
| RU | 27 | -4 | 1 | -1.9 | 1.2 | 0.75 | 0.56 | 0.83 | 1.1 |
| PU | 27 | -4 | 8 | -0.9 | 2.2 | 0.75 | 0.56 | 0.83 | 1.1 |
| RV | 27 | -2 | 6 | 3.6 | 1.6 | 0.53 | 0.28 | 1.38 | 1.5 |
| PV | 27 | -3 | 8 | 4.2 | 2.5 | 0.53 | 0.28 | 1.38 | 1.5 |

Oroville (JD: 232-232)
Night: 1900 - 0800 PDT
Threshold/low res

# NORTHERN CALIFORNIA TRANSPORT (NCT) 1991
# 915 MHz WIND PROFILER/RAWINSONDE COMPARISON

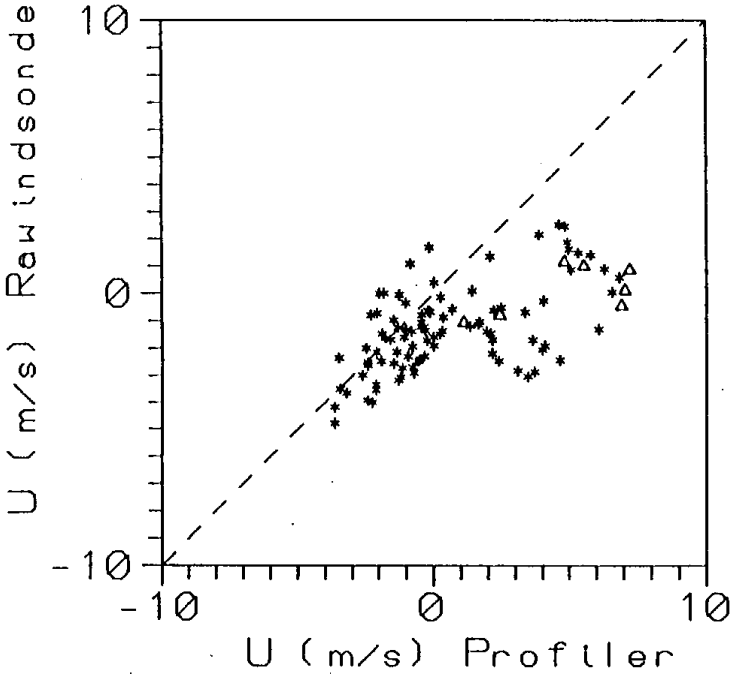


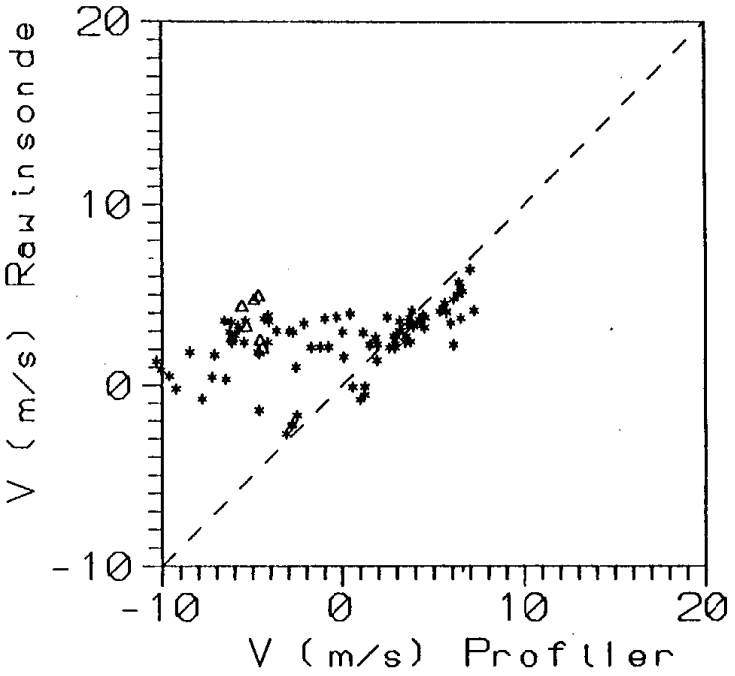


* * * * * 0-3000 m
△ △ △ △ △ > 3000 m

* RMSE for data <= 3000 m

| Var | n | min | max | Mean | SD | r | $r^2$ | SE | RMSE |
|---|---|---|---|---|---|---|---|---|---|
| RU | 100 | -5 | 3 | -1.2 | 1.6 | 0.60 | 0.36 | 1.26 | 2.9 |
| PU | 100 | -4 | 7 | 0.8 | 2.9 | 0.60 | 0.36 | 1.26 | 2.9 |
| RV | 100 | -3 | 6 | 2.6 | 1.8 | 0.45 | 0.20 | 1.58 | 4.9 |
| PV | 100 | -10 | 7 | -0.3 | 4.9 | 0.45 | 0.20 | 1.58 | 4.9 |

Oroville (JD: 232-232)
Night: 1900 - 0800 PDT
No threshold/low res

# NORTHERN CALIFORNIA TRANSPORT (NCT) 1991
# 915 MHz WIND PROFILER/RAWINSONDE COMPARISON

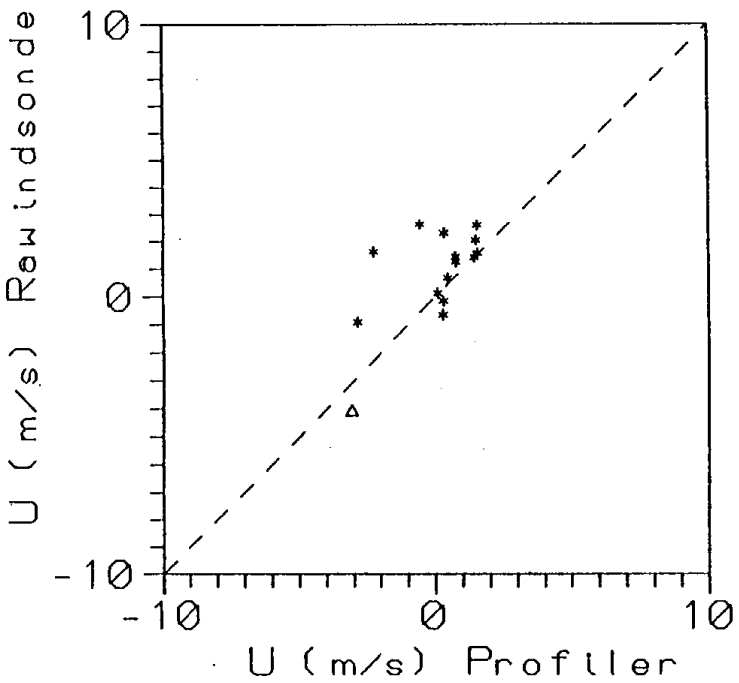


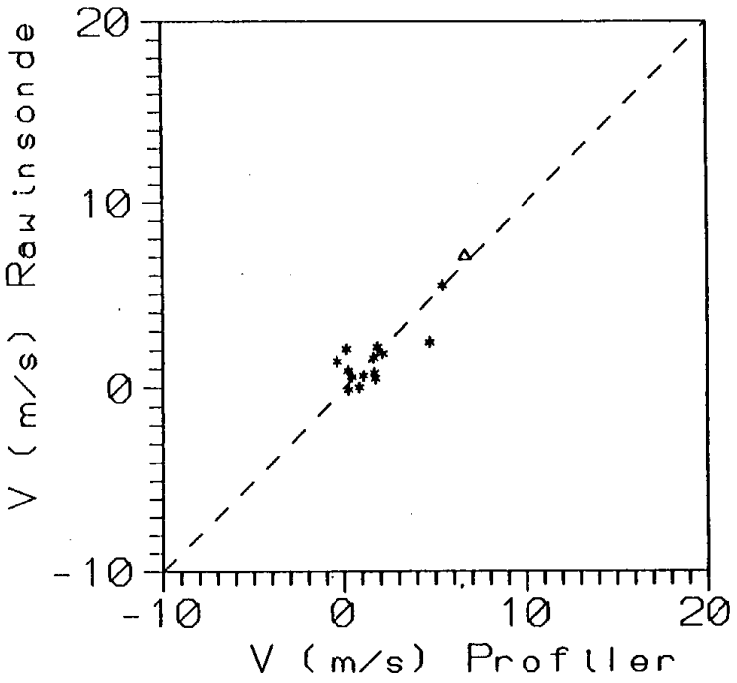


* * * * * 0-3000 m
△ △ △ △ △ > 3000 m

* RMSE for data <= 3000 m

| Var | n | min | max | Mean | SD | r | $r^2$ | SE | RMSE |
|---|---|---|---|---|---|---|---|---|---|
| RU | 15 | -4 | 3 | 0.8 | 1.7 | 0.64 | 0.40 | 1.40 | 1.6 |
| PU | 15 | -3 | 2 | 0.0 | 1.5 | 0.64 | 0.40 | 1.40 | 1.6 |
| RV | 15 | 0 | 7 | 1.8 | 2.0 | 0.86 | 0.74 | 1.05 | 1.1 |
| PV | 15 | 0 | 7 | 1.9 | 2.1 | 0.86 | 0.74 | 1.05 | 1.1 |

Oroville (JD: 232-232)
Day: 0800 - 1900 PDT
Threshold/low res

# NORTHERN CALIFORNIA TRANSPORT (NCT) 1991
# 915 MHz WIND PROFILER/RAWINSONDE COMPARISON

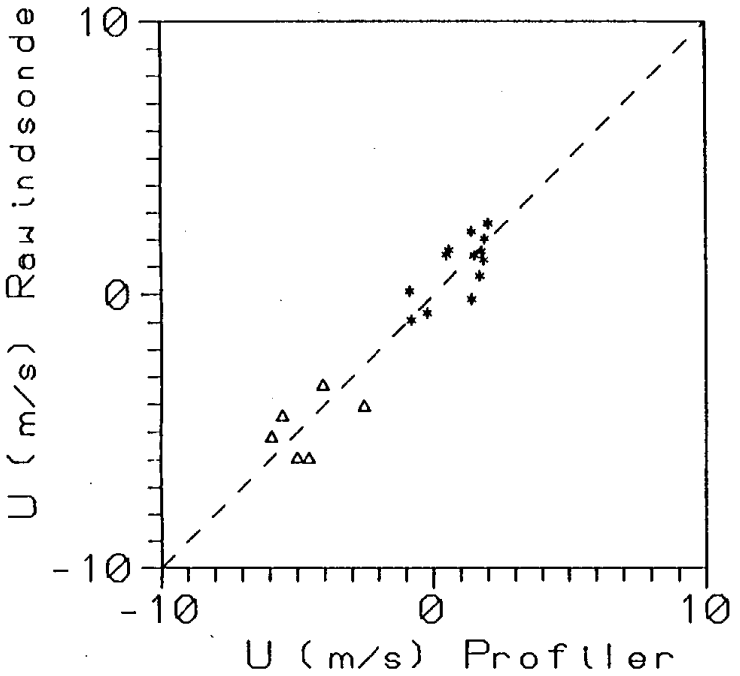


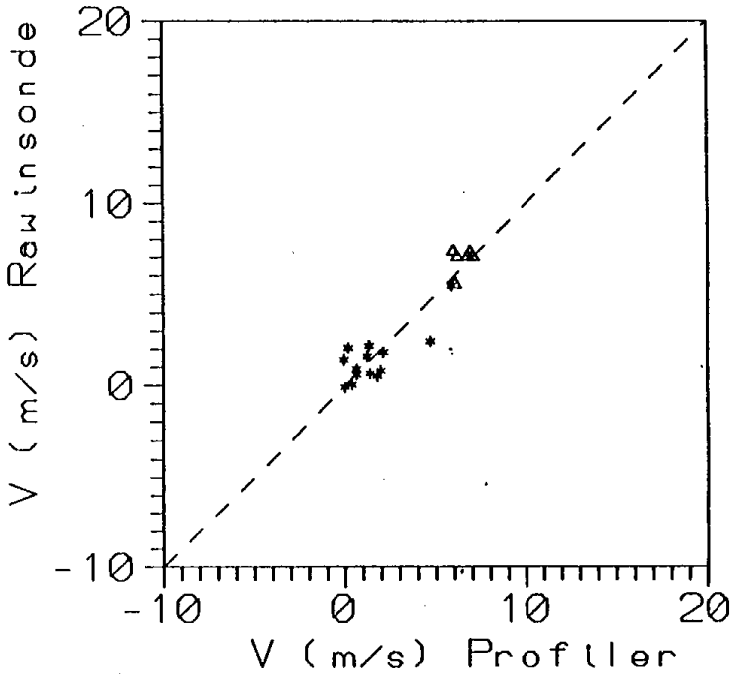


* * * * * 0-3000 m
△ △ △ △ △ > 3000 m

* RMSE for data <= 3000 m

| Var | n | min | max | Mean | SD | r | $r^2$ | SE | RMSE |
|---|---|---|---|---|---|---|---|---|---|
| RU | 20 | -6 | 3 | -0.6 | 3.0 | 0.95 | 0.91 | 0.94 | 0.8 |
| PU | 20 | -6 | 2 | -0.7 | 2.9 | 0.95 | 0.91 | 0.94 | 0.8 |
| RV | 20 | 0 | 7 | 3.1 | 2.9 | 0.94 | 0.88 | 1.03 | 1.1 |
| PV | 20 | 0 | 7 | 3.0 | 2.7 | 0.94 | 0.88 | 1.03 | 1.1 |

Oroville (JD: 232-232)
Day: 0800 - 1900 PDT
No threshold/low res

# NORTHERN CALIFORNIA TRANSPORT (NCT) 1991
# 915 MHz WIND PROFILER/RAWINSONDE COMPARISON

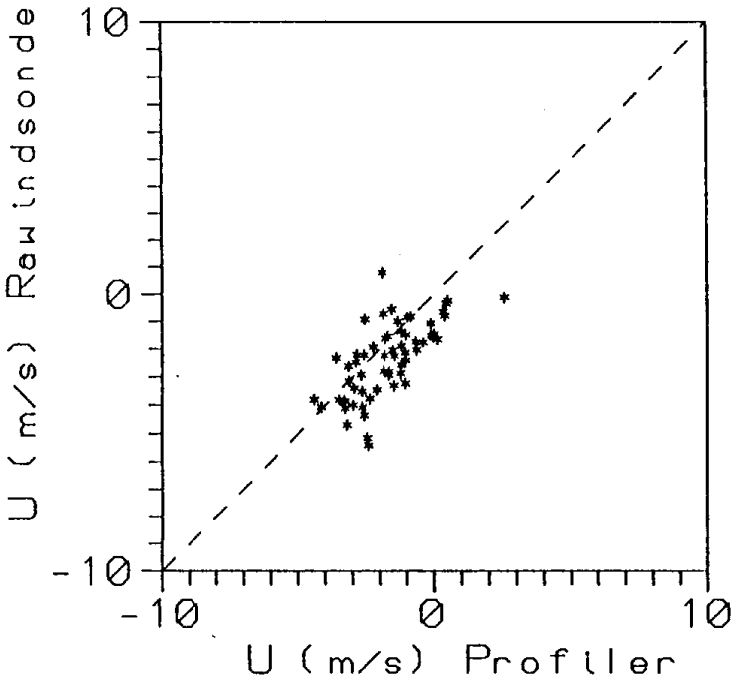


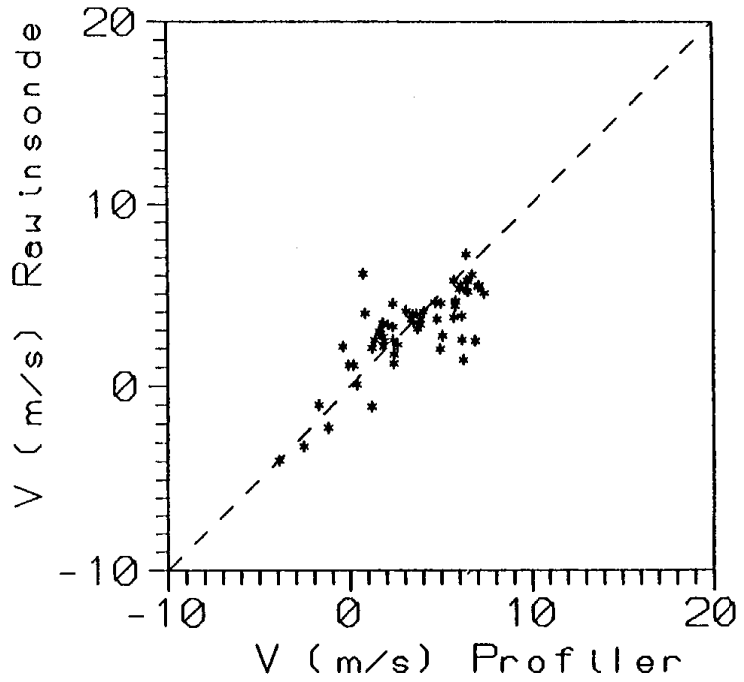


* * * * * 0-3000 m
Δ Δ Δ Δ Δ > 3000 m

* RMSE for data <= 3000 m

| Var | n | min | max | Mean | SD | r | $r^2$ | SE | RMSE |
|---|---|---|---|---|---|---|---|---|---|
| RU | 61 | -5 | 1 | -2.4 | 1.3 | 0.68 | 0.46 | 0.99 | 1.2 |
| PU | 61 | -4 | 3 | -1.7 | 1.3 | 0.68 | 0.46 | 0.99 | 1.2 |
| RV | 61 | -4 | 7 | 3.1 | 2.2 | 0.78 | 0.60 | 1.41 | 1.7 |
| PV | 61 | -4 | 7 | 3.5 | 2.7 | 0.78 | 0.60 | 1.41 | 1.7 |

Oroville (JD: 232-232)
Night: 1900 - 0800 PDT

# NORTHERN CALIFORNIA TRANSPORT (NCT) 1991
## 915 MHz WIND PROFILER/RAWINSONDE COMPARISON

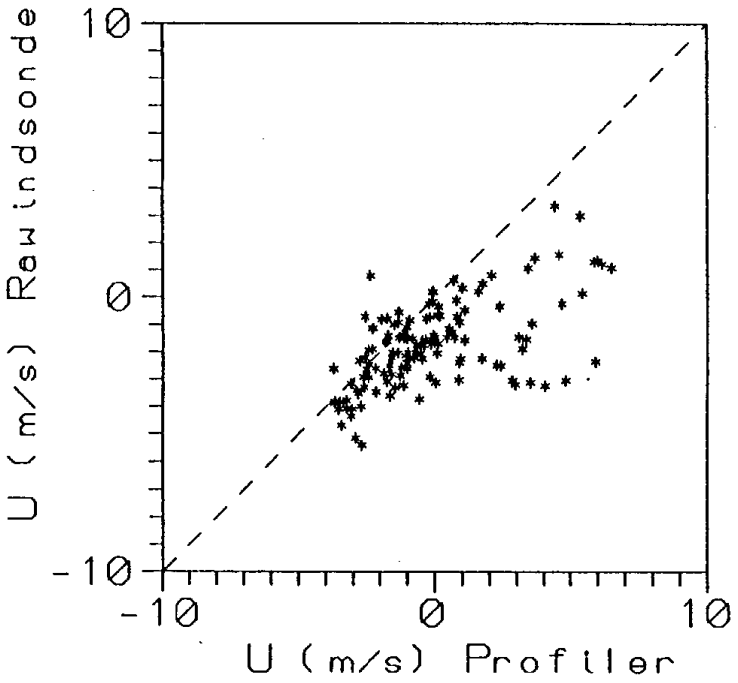


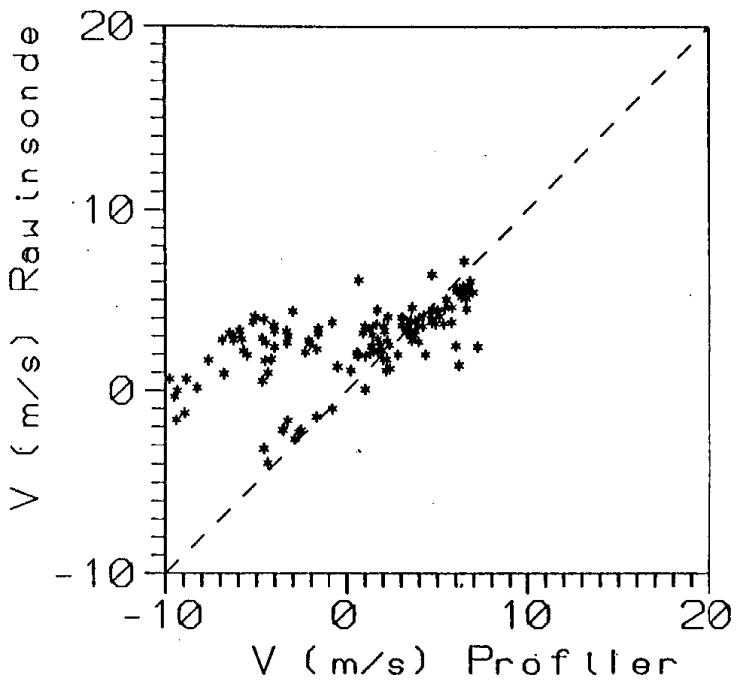


* * * * * 0-3000 m
△ △ △ △ △ > 3000 m

* RMSE for data <= 3000 m

| Var | n | min | max | Mean | SD | r | $r^2$ | SE | RMSE |
|---|---|---|---|---|---|---|---|---|---|
| RU | 140 | -5 | 3 | -1.7 | 1.5 | 0.61 | 0.37 | 1.23 | 2.5 |
| PU | 140 | -4 | 7 | -0.2 | 2.4 | 0.61 | 0.37 | 1.23 | 2.5 |
| RV | 140 | -4 | 7 | 2.7 | 2.0 | 0.61 | 0.37 | 1.62 | 4.2 |
| PV | 140 | -10 | 7 | 0.6 | 4.5 | 0.61 | 0.37 | 1.62 | 4.2 |

Oroville (JD: 232-232)
Night: 1900 - 0800 PDT
No threshold/high ras

# NORTHERN CALIFORNIA TRANSPORT (NCT) 1991
# 915 MHz WIND PROFILER/RAWINSONDE COMPARISON

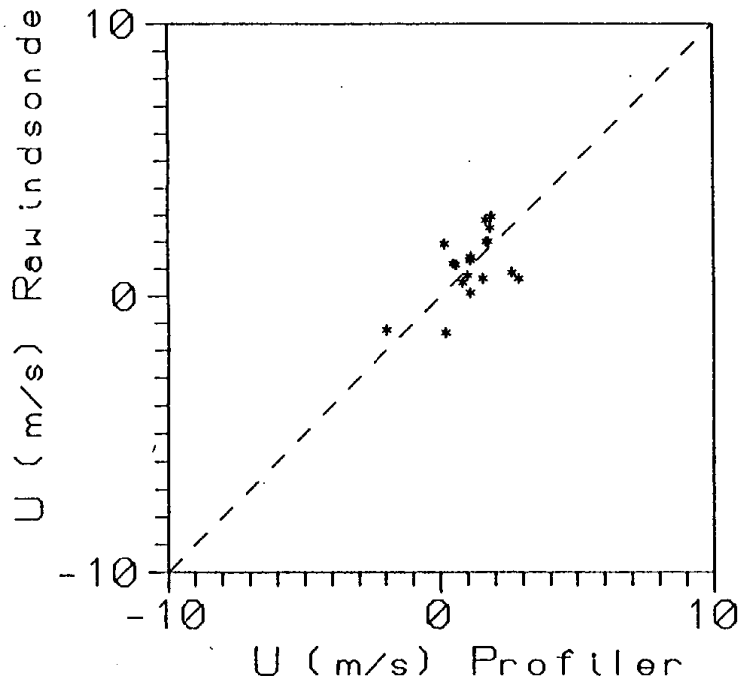


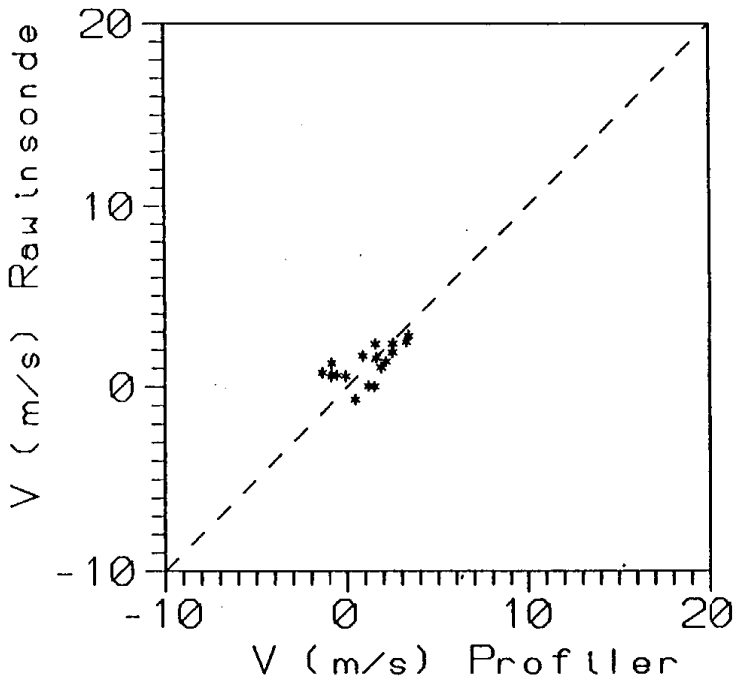


* * * * * 0-3000 m
Δ Δ Δ Δ Δ > 3000 m

* RMSE for data <= 3000 m

| Var | n | min | max | Mean | SD | r | $r^2$ | SE | RMSE |
|---|---|---|---|---|---|---|---|---|---|
| RU | 18 | -1 | 3 | 1.1 | 1.2 | 0.55 | 0.30 | 1.03 | 1.1 |
| PU | 18 | -2 | 3 | 1.1 | 1.1 | 0.55 | 0.30 | 1.03 | 1.1 |
| RV | 18 | -1 | 3 | 1.2 | 0.9 | 0.62 | 0.38 | 0.77 | 1.2 |
| PV | 18 | -1 | 3 | 1.0 | 1.5 | 0.62 | 0.38 | 0.77 | 1.2 |

Oroville (JD: 232-232)
Day: 0800 - 1900 PDT
Threshold/high res

# NORTHERN CALIFORNIA TRANSPORT (NCT) 1991
# 915 MHz WIND PROFILER/RAWINSONDE COMPARISON

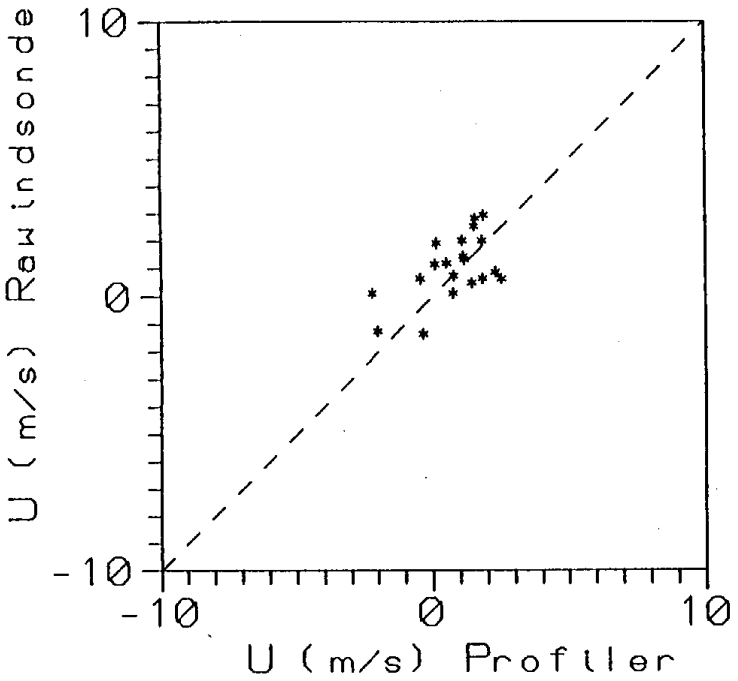


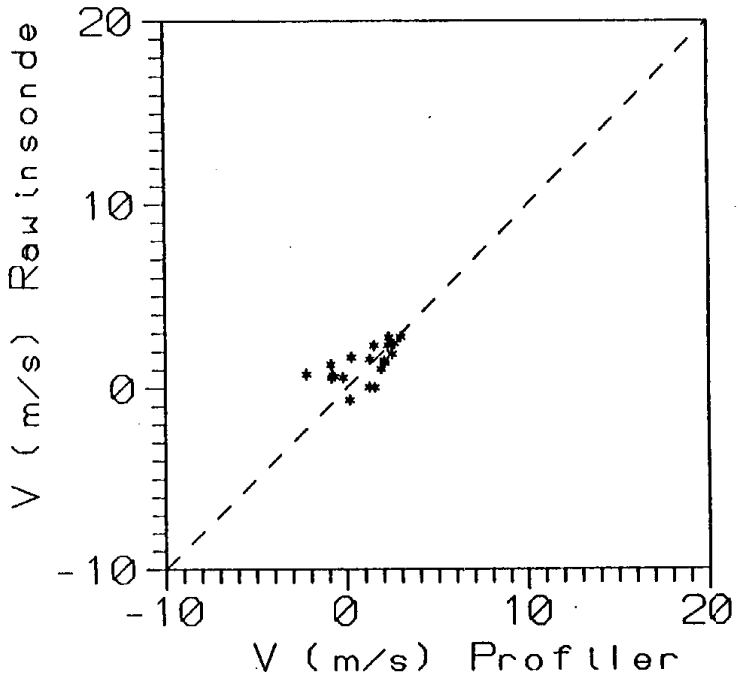


* * * * * 0-3000 m
^ ^ ^ ^ ^ > 3000 m

* RMSE for data <= 3000 m

| Var | n | min | max | Mean | SD | r | $r^2$ | SE | RMSE |
|---|---|---|---|---|---|---|---|---|---|
| RU | 20 | -1 | 3 | 1.1 | 1.2 | 0.57 | 0.33 | 0.98 | 1.1 |
| PU | 20 | -2 | 3 | 0.8 | 1.3 | 0.57 | 0.33 | 0.98 | 1.1 |
| RV | 20 | -1 | 3 | 1.3 | 1.0 | 0.59 | 0.35 | 0.80 | 1.2 |
| PV | 20 | -2 | 3 | 0.9 | 1.5 | 0.59 | 0.35 | 0.80 | 1.2 |

Oroville (JD: 232-232)
Day: 0800 - 1900 PDT

# NORTHERN CALIFORNIA TRANSPORT (NCT) 1991
# 915 MHz WIND PROFILER/RAWINSONDE COMPARISON

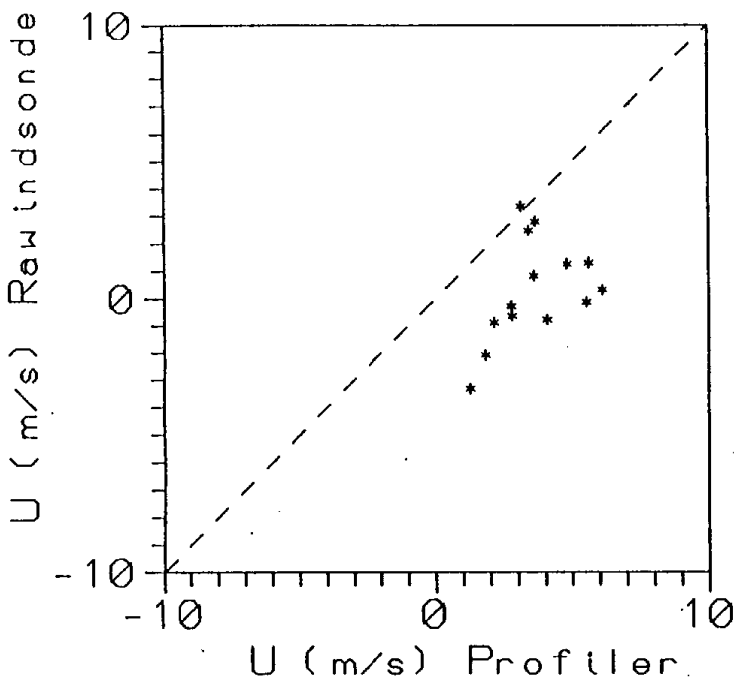


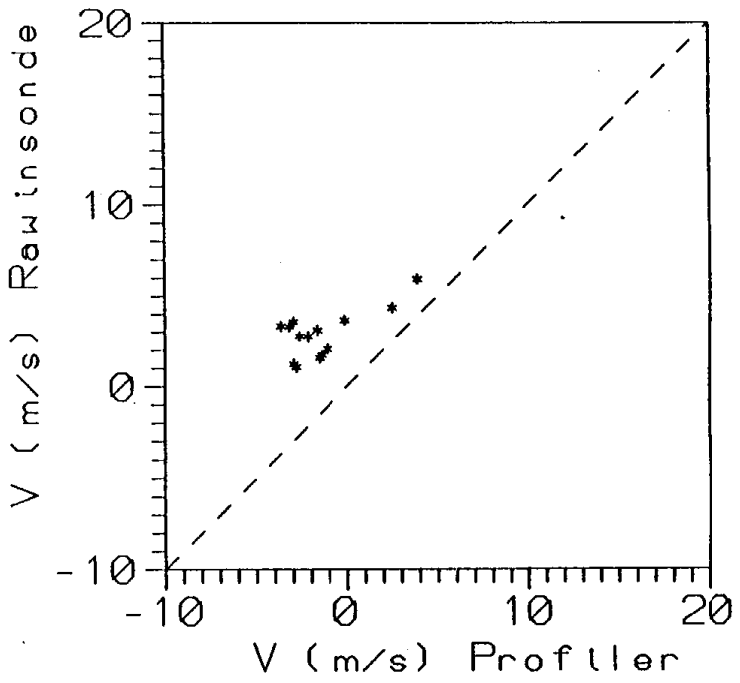


* * * * * 0-3000 m
Δ Δ Δ Δ Δ > 3000 m

* RMSE for data <= 3000 m

| Var | n | min | max | Mean | SD | r | $r^2$ | SE | RMSE |
|---|---|---|---|---|---|---|---|---|---|
| RU | 14 | -3 | 3 | 0.3 | 1.9 | 0.44 | 0.19 | 1.74 | 3.7 |
| PU | 14 | 1 | 6 | 3.6 | 1.5 | 0.44 | 0.19 | 1.74 | 3.7 |
| RV | 14 | 1 | 6 | 2.9 | 1.3 | 0.67 | 0.45 | 1.01 | 4.6 |
| PV | 14 | -4 | 4 | -1.4 | 2.2 | 0.67 | 0.45 | 1.01 | 4.6 |

Pleasant Grove (JD: 230-231)
Night: 1900 - 0800 PDT
No threshold/low res

# NORTHERN CALIFORNIA TRANSPORT (NCT) 1991
# 915 MHz WIND PROFILER/RAWINSONDE COMPARISON

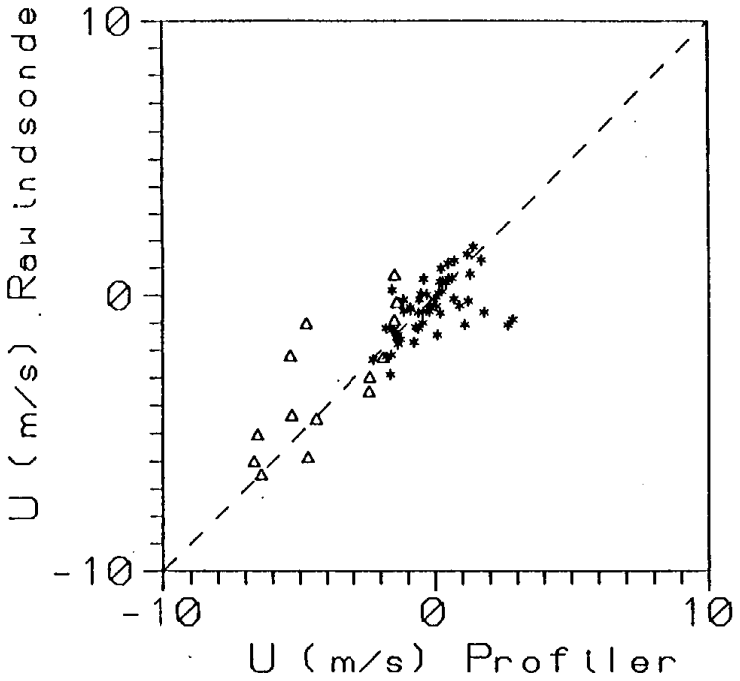


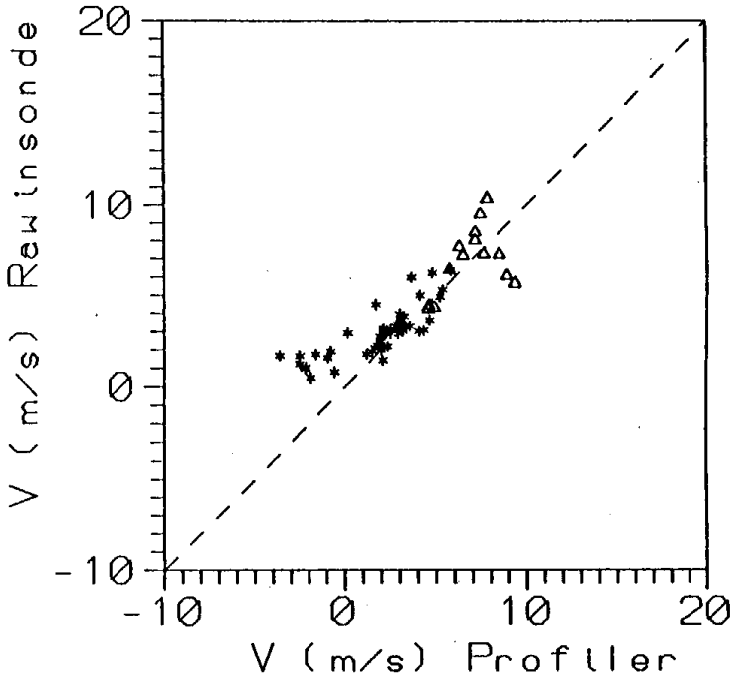


* * * * * 0-3000 m
△ △ △ △ △ > 3000 m

* RMSE for data <= 3000 m

| Var | n | min | max | Mean | SD | r | $r^2$ | SE | RMSE |
|---|---|---|---|---|---|---|---|---|---|
| RU | 70 | -6 | 2 | -1.0 | 1.7 | 0.81 | 0.66 | 1.02 | 1.0 |
| PU | 70 | -7 | 3 | -0.9 | 2.0 | 0.81 | 1.66 | 1.02 | 1.0 |
| RV | 70 | 0 | 10 | 3.7 | 2.2 | 0.86 | 0.74 | 1.11 | 1.6 |
| PV | 70 | -4 | 9 | 3.0 | 2.8 | 0.86 | 0.74 | 1.11 | 1.6 |

Pleasant Grove (JD: 230-231)
Day: 0800 - 1900 PDT
No threshold/low res

# NORTHERN CALIFORNIA TRANSPORT (NCT) 1991
# 915 MHz WIND PROFILER/RAWINSONDE COMPARISON

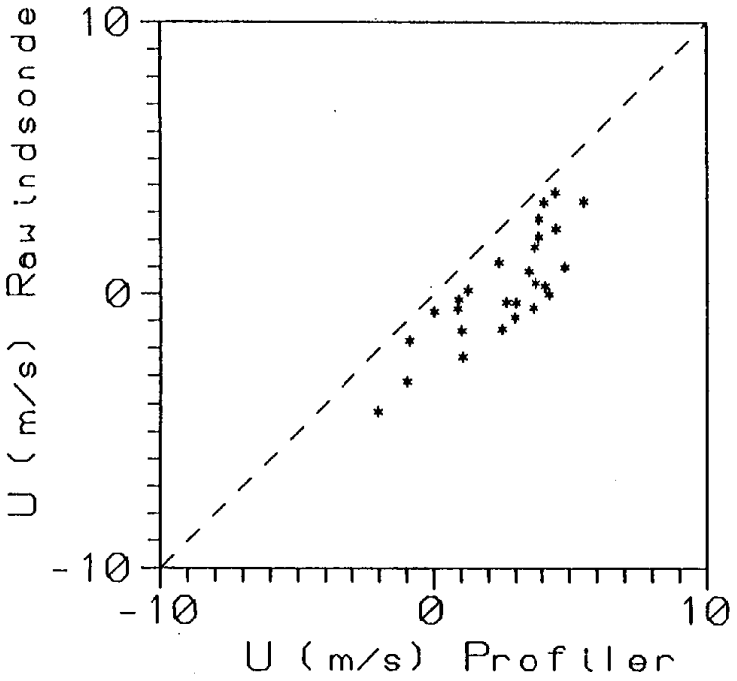


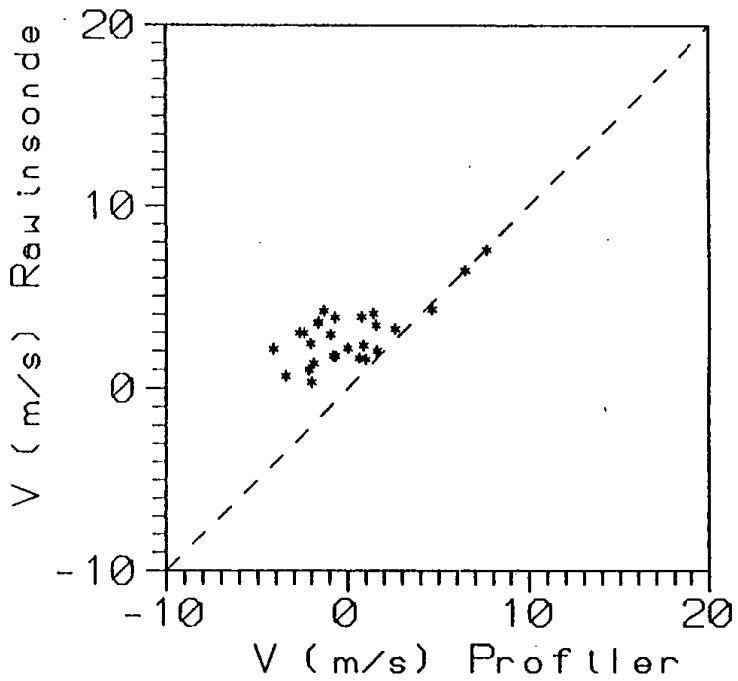


* * * * * 0-3000 m

∆ ∆ ∆ ∆ ∆ > 3000 m

* RMSE for data <= 3000 m

| Var | n | min | max | Mean | SD | r | $r^2$ | SE | RMSE |
|---|---|---|---|---|---|---|---|---|---|
| RU | 27 | -4 | 4 | 0.2 | 2.0 | 0.82 | 0.67 | 1.16 | 2.6 |
| PU | 27 | -2 | 6 | 2.5 | 2.0 | 0.82 | 0.67 | 1.16 | 2.6 |
| RV | 27 | 0 | 8 | 2.9 | 1.6 | 0.72 | 0.52 | 1.15 | 3.5 |
| PV | 27 | -4 | 8 | 0.0 | 2.8 | 0.72 | 0.52 | 1.15 | 3.5 |

Pleasant Grove (JD: 230-231)
Night: 1900 - 0800 PDT

# NORTHERN CALIFORNIA TRANSPORT (NCT) 1991
## 915 MHz WIND PROFILER/RAWINSONDE COMPARISON

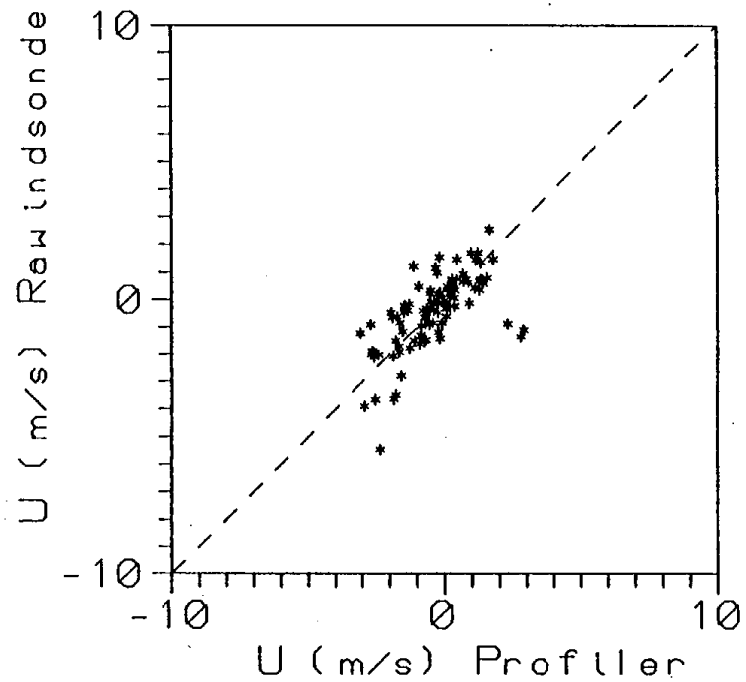


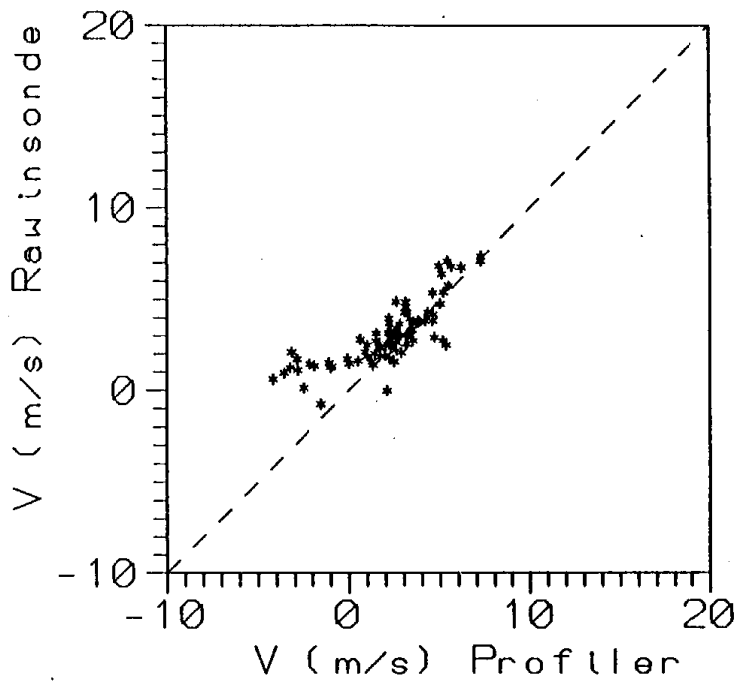


* * * * * 0-3000 m
∆ ∆ ∆ ∆ ∆ > 3000 m

* RMSE for data <= 3000 m

| Var | n | min | max | Mean | SD | r | $r^2$ | SE | RMSE |
|---|---|---|---|---|---|---|---|---|---|
| RU | 102 | -5 | 3 | -0.4 | 1.3 | 0.66 | 0.44 | 0.99 | 1.1 |
| PU | 102 | -3 | 3 | -0.4 | 1.3 | 0.66 | 0.44 | 0.99 | 1.1 |
| RV | 102 | -1 | 7 | 3.0 | 1.6 | 0.79 | 0.63 | 0.96 | 1.6 |
| PV | 102 | -4 | 7 | 2.3 | 2.3 | 0.79 | 0.63 | 0.96 | 1.6 |

Pleasant Grove (JD: 230-231)
Day: 0800 - 1900 PDT
No threshold/high res

# NORTHERN CALIFORNIA TRANSPORT (NCT) 1991
# 915 MHz WIND PROFILER/RAWINSONDE COMPARISON

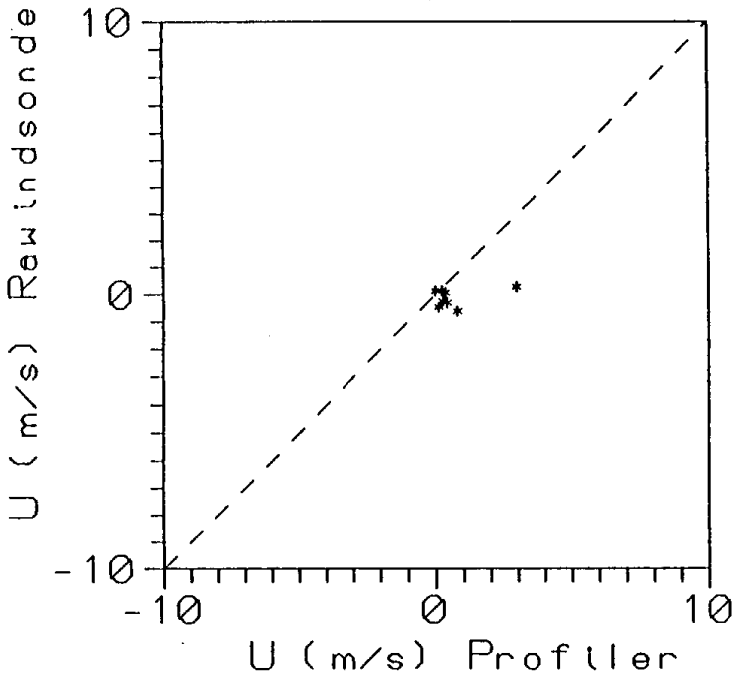


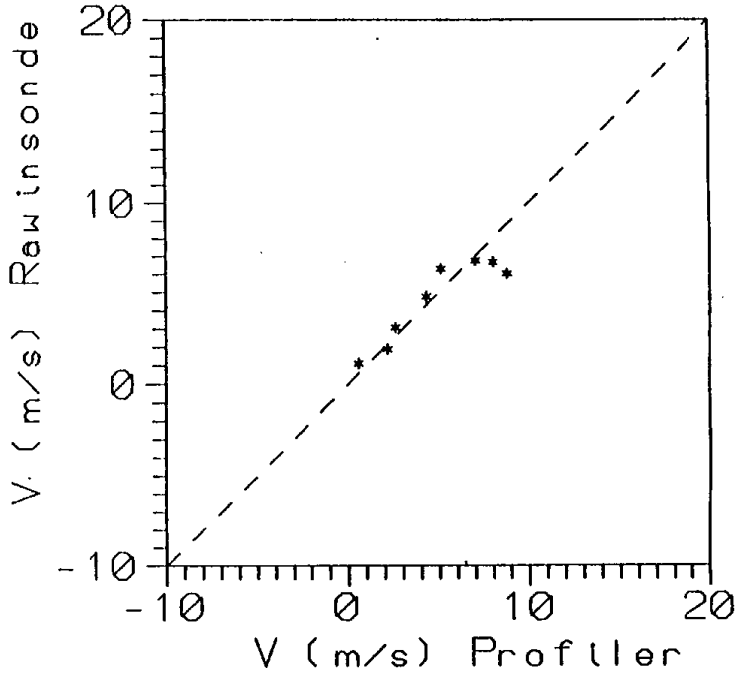


* * * * * 0-3000 m
∆ ∆ ∆ ∆ ∆ > 3000 m

* RMSE for data <= 3000 m

| Var | n | min | max | Mean | SD | r | $r^2$ | SE | RMSE |
|---|---|---|---|---|---|---|---|---|---|
| RU | 8 | -1 | 0 | -0.1 | 0.3 | 0.36 | 0.13 | 0.32 | 1.1 |
| PU | 8 | 0 | 3 | 0.6 | 1.0 | 0.36 | 0.13 | 0.32 | 1.1 |
| RV | 8 | 1 | 7 | 4.6 | 2.2 | 0.92 | 0.84 | 0.98 | 1.2 |
| PV | 8 | 1 | 9 | 4.8 | 2.9 | 0.92 | 0.84 | 0.98 | 1.2 |

Rancho Seco (JD: 235-236)
Night: 1900 - 0800 PDT
Threshold/low res.

# NORTHERN CALIFORNIA TRANSPORT (NCT) 1991
# 915 MHz WIND PROFILER/RAWINSONDE COMPARISON

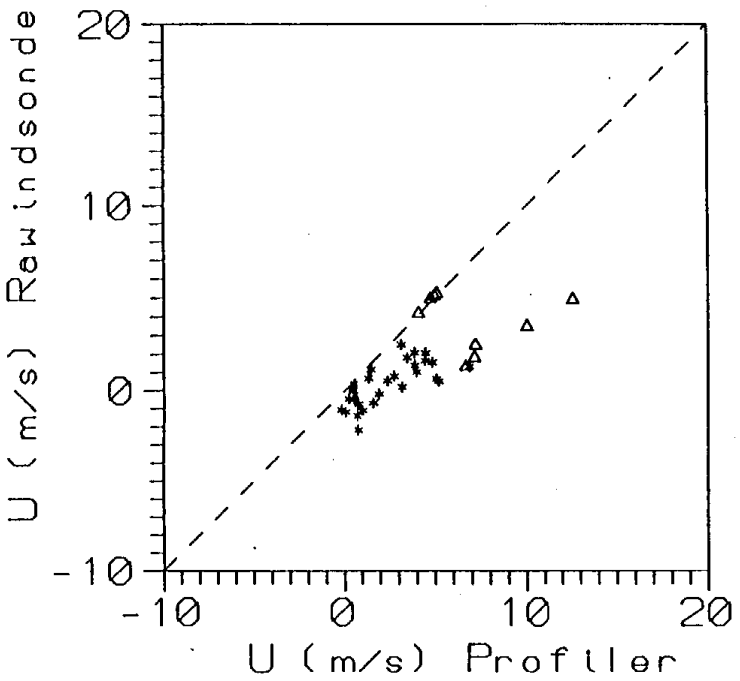


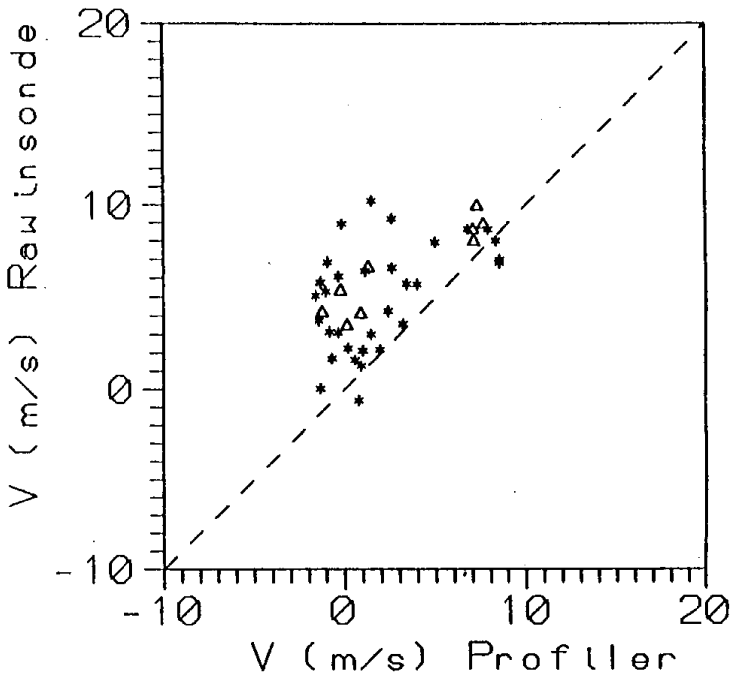


* * * * * 0-3000 m
△ △ △ △ △ > 3000 m

* RMSE for data <= 3000 m

| Var | n | min | max | Mean | SD | r | $r^2$ | SE | RMSE |
|---|---|---|---|---|---|---|---|---|---|
| RU | 42 | -2 | 5 | 1.0 | 1.9 | 0.74 | 0.55 | 1.29 | 2.3 |
| PU | 42 | 0 | 13 | 3.2 | 2.9 | 0.74 | 0.55 | 1.29 | 2.3 |
| RV | 42 | -1 | 10 | 5.3 | 2.8 | 0.59 | 0.35 | 2.32 | 4.2 |
| PV | 42 | -2 | 8 | 2.2 | 3.3 | 0.59 | 0.35 | 2.32 | 4.2 |

Rancho Seco (JD: 235-236)
Night: 1900 - 0800 PDT
No threshold/low res

# NORTHERN CALIFORNIA TRANSPORT (NCT) 1991
## 915 MHz WIND PROFILER/RAWINSONDE COMPARISON

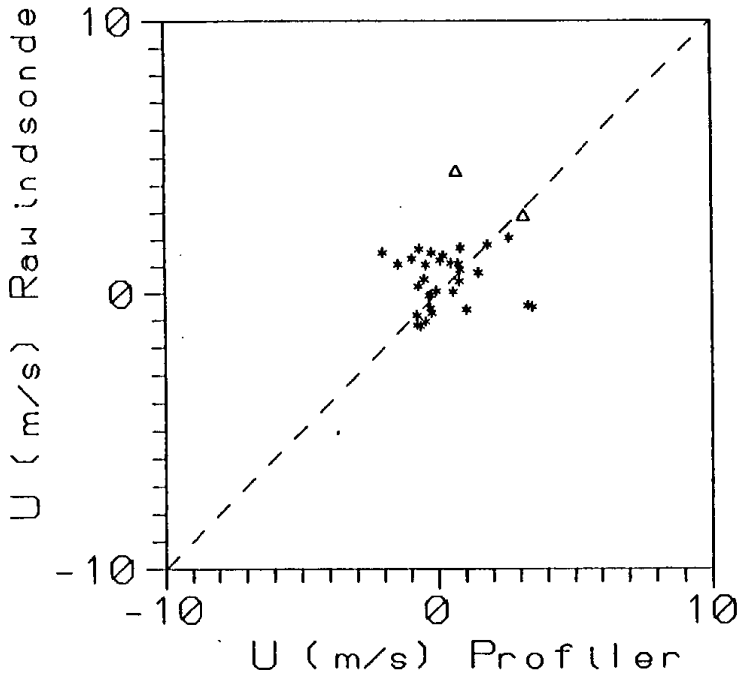


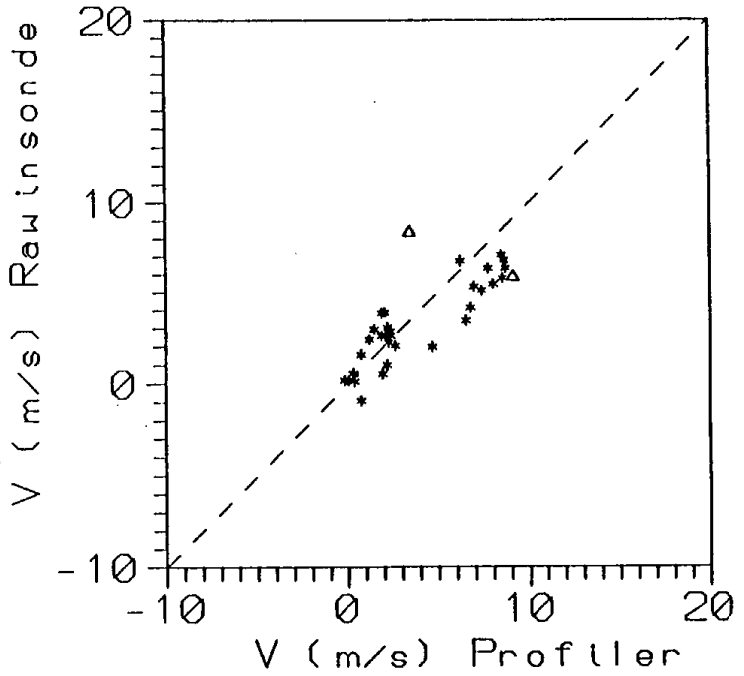


* * * * * 0-3000 m.
Δ Δ Δ Δ Δ > 3000 m

* RMSE for data <= 3000 m

| Var | n | min | max | Mean | SD | r | $r^2$ | SE | RMSE |
|---|---|---|---|---|---|---|---|---|---|
| RU | 33 | -1 | 5 | 0.7 | 1.3 | 0.18 | 0.03 | 1.26 | 1.6 |
| PU | 33 | -2 | 3 | 0.3 | 1.3 | 0.18 | 0.03 | 1.26 | 1.6 |
| RV | 33 | -1 | 8 | 3.4 | 2.4 | 0.82 | 0.67 | 1.42 | 1.6 |
| PV | 33 | 0 | 9 | 3.9 | 3.1 | 0.82 | 0.67 | 1.42 | 1.6 |

Rancho Seco (JD: 235-236)
Day: 0800 - 1900 PDT
Threshold/low res

# NORTHERN CALIFORNIA TRANSPORT (NCT) 1991
# 915 MHz WIND PROFILER/RAWINSONDE COMPARISON

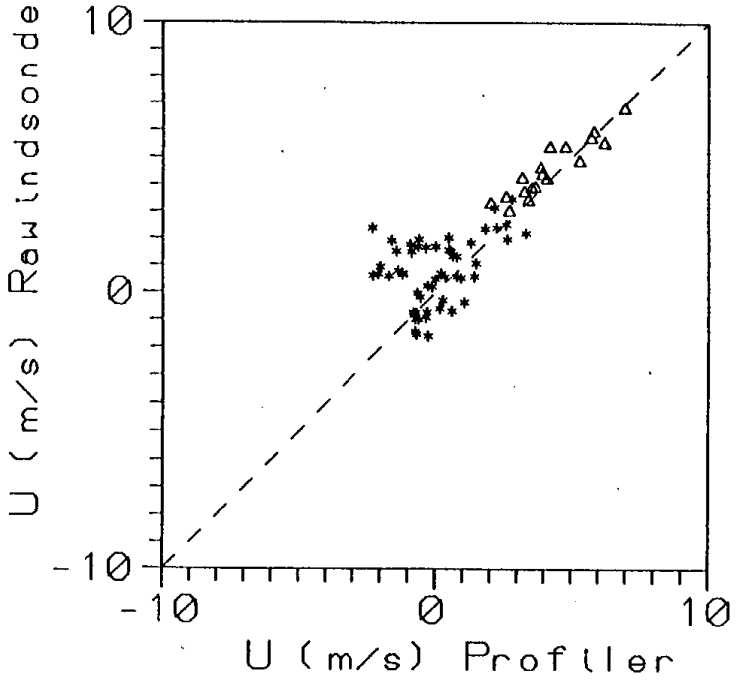


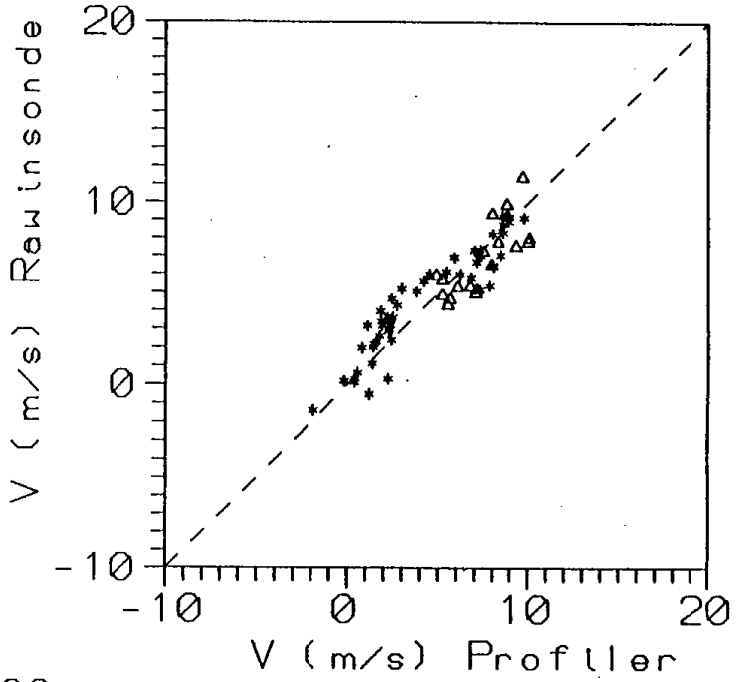


* * * * * 0-3000 m
△ △ △ △ △ > 3000 m

* RMSE for data <= 3000 m

| Var | n | min | max | Mean | SD | r | $r^2$ | SE | RMSE |
|---|---|---|---|---|---|---|---|---|---|
| RU | 74 | -2 | 7 | 1.8 | 2.1 | 0.84 | 0.71 | 1.13 | 1.6 |
| PU | 74 | -2 | 7 | 1.1 | 2.3 | 0.84 | 0.71 | 1.13 | 1.6 |
| RV | 74 | -1 | 11 | 5.1 | 2.9 | 0.93 | 0.86 | 1.08 | 1.1 |
| PV | 74 | -2 | 10 | 5.0 | 3.2 | 0.93 | 0.86 | 1.08 | 1.1 |

Rancho Seco (JD: 235-236)
Day: 0800 - 1900 PDT
No threshold/low res

# NORTHERN CALIFORNIA TRANSPORT (NCT) 1991
# 915 MHz WIND PROFILER/RAWINSONDE COMPARISON

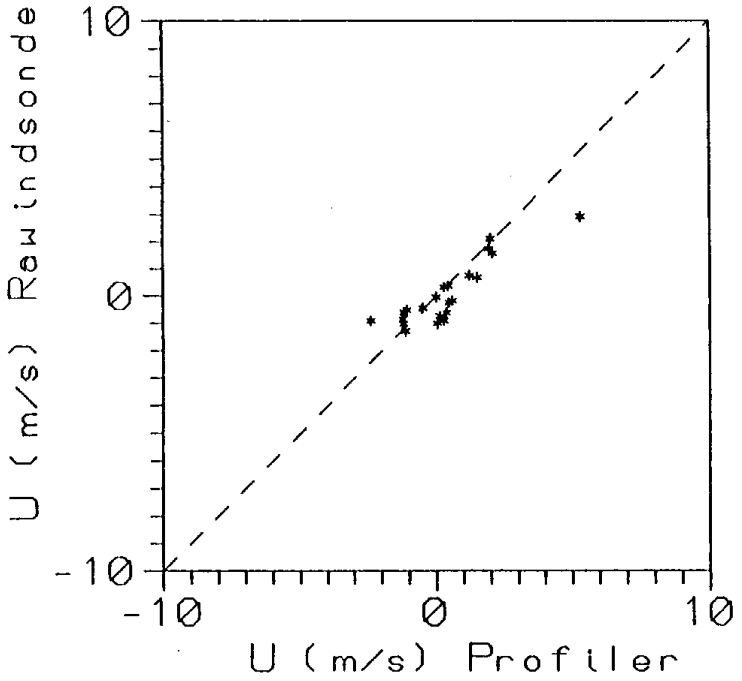


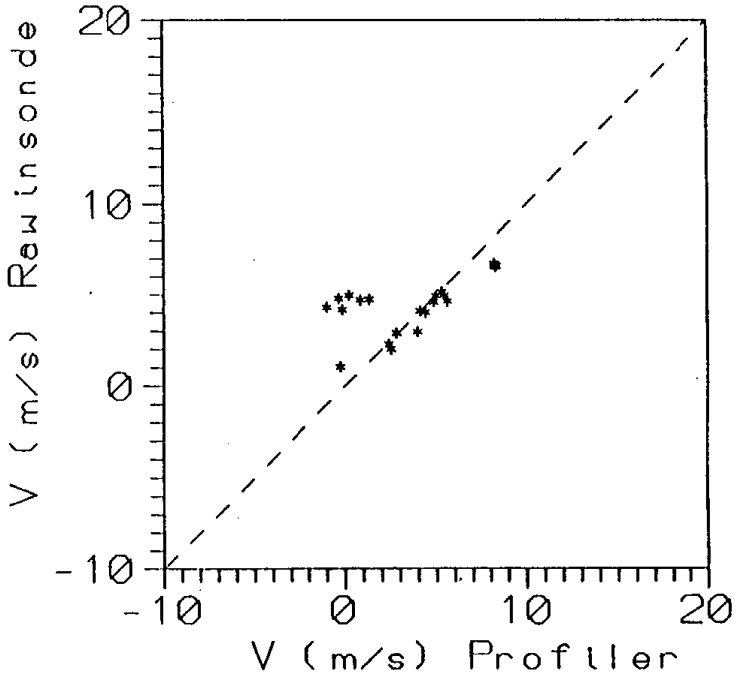


* * * * * 0-3000 m
△ △ △ △ △ > 3000 m

* RMSE for data <= 3000 m

| Var | n | min | max | Mean | SD | r | $r^2$ | SE | RMSE |
|---|---|---|---|---|---|---|---|---|---|
| RU | 22 | -1 | 3 | 0.0 | 1.1 | 0.89 | 0.79 | 0.54 | 0.8 |
| PU | 22 | -2 | 5 | 3.6 | 1.6 | 0.89 | 0.79 | 0.54 | 0.8 |
| RV | 22 | 1 | 7 | 4.4 | 1.5 | 0.62 | 0.38 | 1.21 | 2.5 |
| PV | 22 | -1 | 8 | 3.6 | 3.0 | 0.62 | 0.38 | 1.21 | 2.5 |

Rancho Seco (JD: 235-236)
Night: 1900 - 0800 PDT
Threshold/high res

# NORTHERN CALIFORNIA TRANSPORT (NCT) 1991
# 915 MHz WIND PROFILER/RAWINSONDE COMPARISON

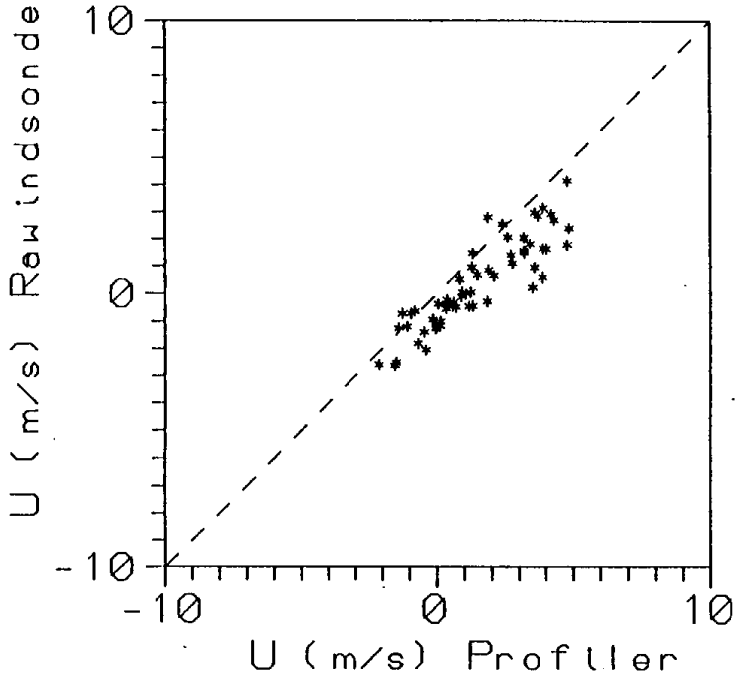


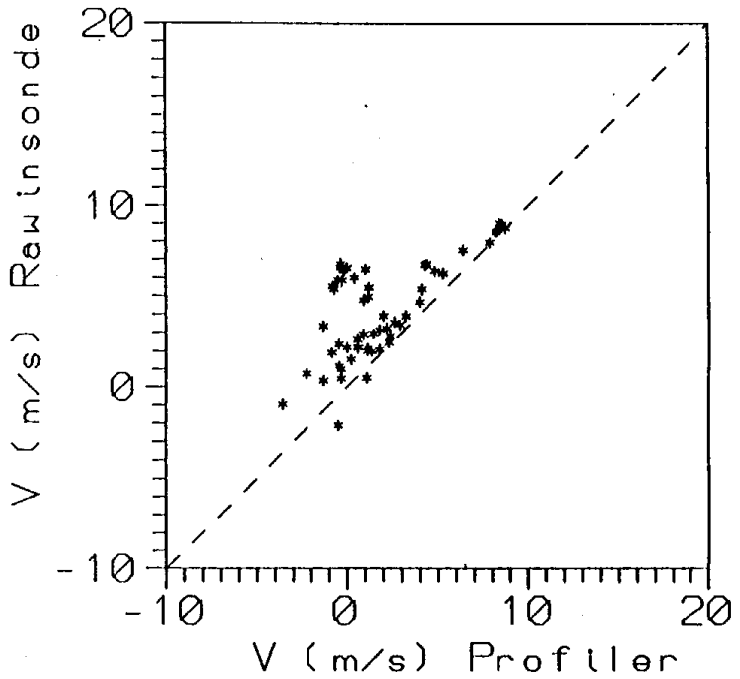


* * * * * 0-3000 m
△ △ △ △ △ > 3000 m

* RMSE for data <= 3000 m

| Var | n | min | max | Mean | SD | r | $r^2$ | SE | RMSE |
|---|---|---|---|---|---|---|---|---|---|
| RU | 58 | -3 | 4 | 0.4 | 1.6 | 0.89 | 0.79 | 0.74 | 1.4 |
| PU | 58 | -2 | 5 | 1.5 | 1.9 | 0.89 | 0.79 | 0.74 | 1.4 |
| RV | 58 | -2 | 9 | 4.2 | 2.7 | 0.68 | 0.47 | 1.97 | 3.2 |
| PV | 58 | -4 | 9 | 1.9 | 2.9 | 0.68 | 0.47 | 1.97 | 3.2 |

Rancho Seco (JD: 235-236)
Night: 1900 - 0800 PDT
No threshold/high res

# NORTHERN CALIFORNIA TRANSPORT (NCT) 1991
# 915 MHz WIND PROFILER/RAWINSONDE COMPARISON

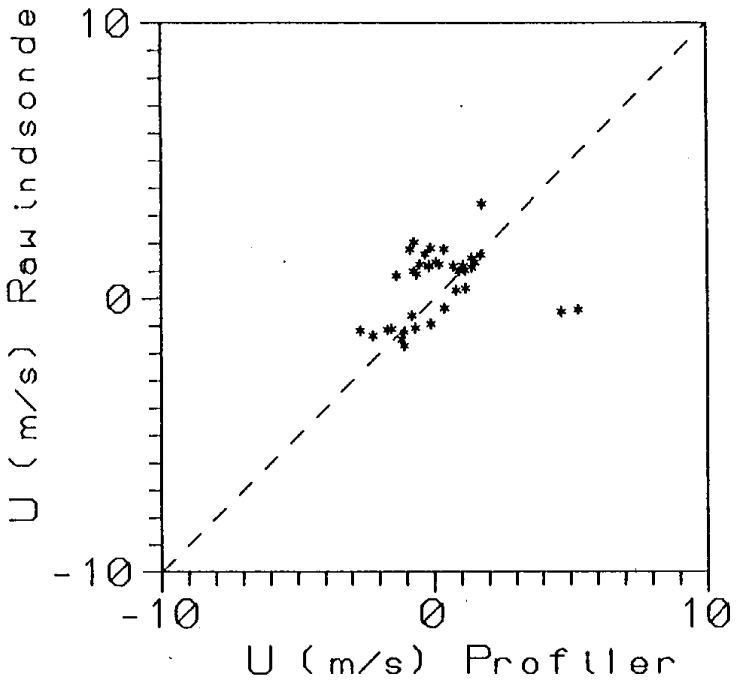


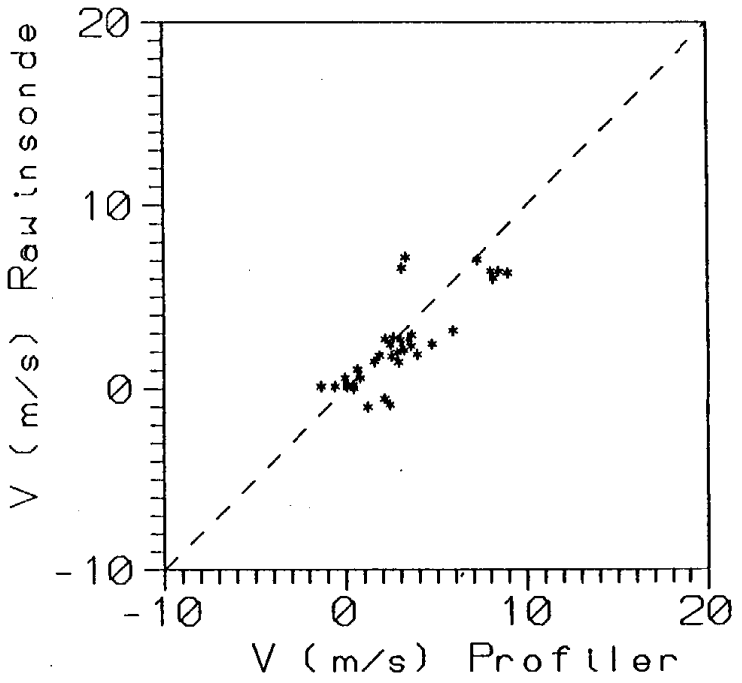


* * * * * 0-3000 m
Δ Δ Δ Δ Δ > 3000 m

* RMSE for data <= 3000 m

| Var | n | min | max | Mean | SD | r | $r^2$ | SE | RMSE |
|---|---|---|---|---|---|---|---|---|---|
| RU | 37 | -2 | 3 | 0.5 | 1.3 | 0.29 | 0.09 | 1.23 | 1.8 |
| PU | 37 | -3 | 5 | 0.1 | 1.6 | 0.29 | 0.09 | 1.23 | 1.8 |
| RV | 37 | -1 | 7 | 2.3 | 2.4 | 0.81 | 0.66 | 1.40 | 1.6 |
| PV | 37 | -1 | 9 | 2.9 | 2.6 | 0.81 | 0.66 | 1.40 | 1.6 |

Rancho Seco (JD: 235-236)
Day: 0800 - 1900 PDT
Threshold/high res

# NORTHERN CALIFORNIA TRANSPORT (NCT) 1991
# 915 MHz WIND PROFILER/RAWINSONDE COMPARISON

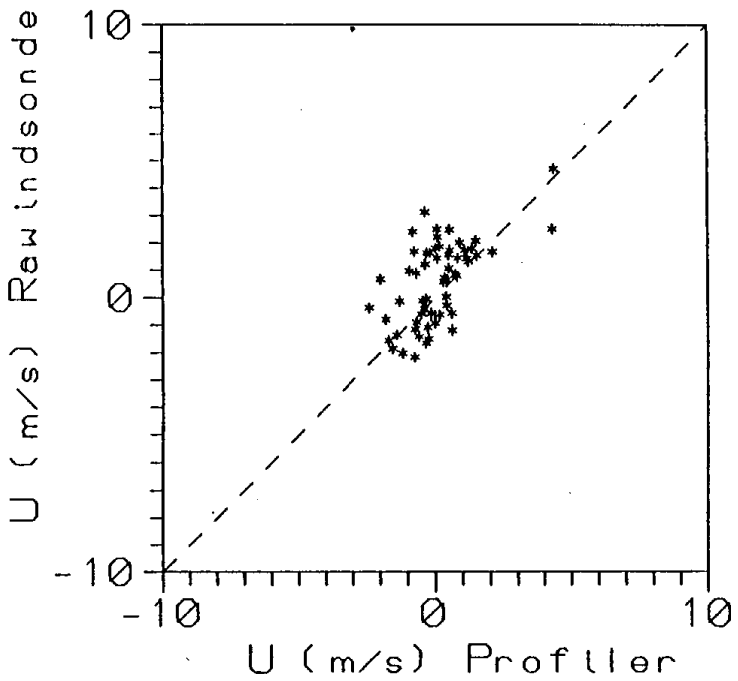


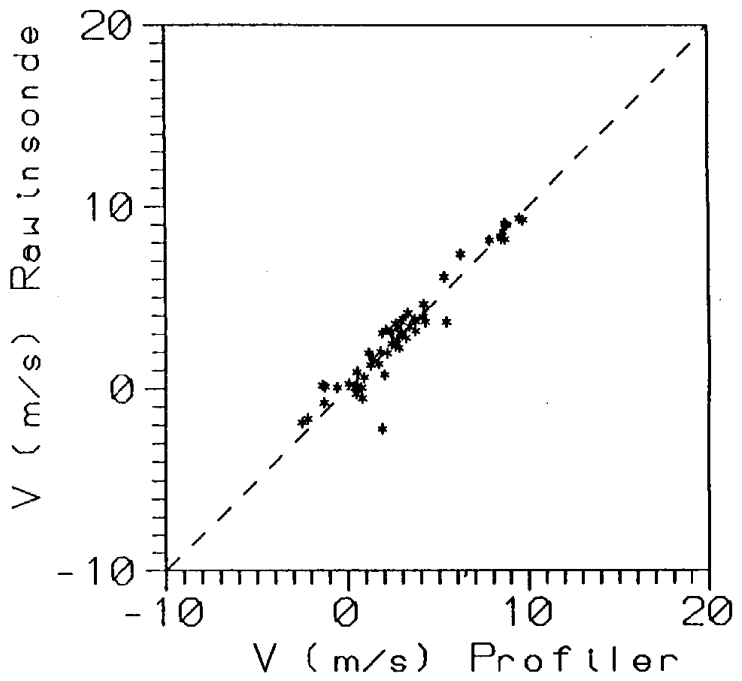


* * * * * 0-3000 m
△ △ △ △ △ > 3000 m

* RMSE for data <= 3000 m

| Var | n | min | max | Mean | SD | r | $r^2$ | SE | RMSE |
|---|---|---|---|---|---|---|---|---|---|
| RU | 61 | -2 | 5 | 0.6 | 1.5 | 0.59 | 0.35 | 1.20 | 1.3 |
| PU | 61 | -2 | 4 | 0.1 | 1.2 | 0.59 | 0.35 | 1.20 | 1.3 |
| RV | 61 | -2 | 9 | 3.0 | 3.0 | 0.96 | 0.92 | 0.85 | 0.8 |
| PV | 61 | -3 | 10 | 2.9 | 3.0 | 0.96 | 0.92 | 0.85 | 0.8 |

Rancho Seco (JD: 235-236)
Day: 0800 - 1900 PDT
No threshold/high res

# NORTHERN CALIFORNIA TRANSPORT (NCT) 1991
# 915 MHz WIND PROFILER/RAWINSONDE COMPARISON

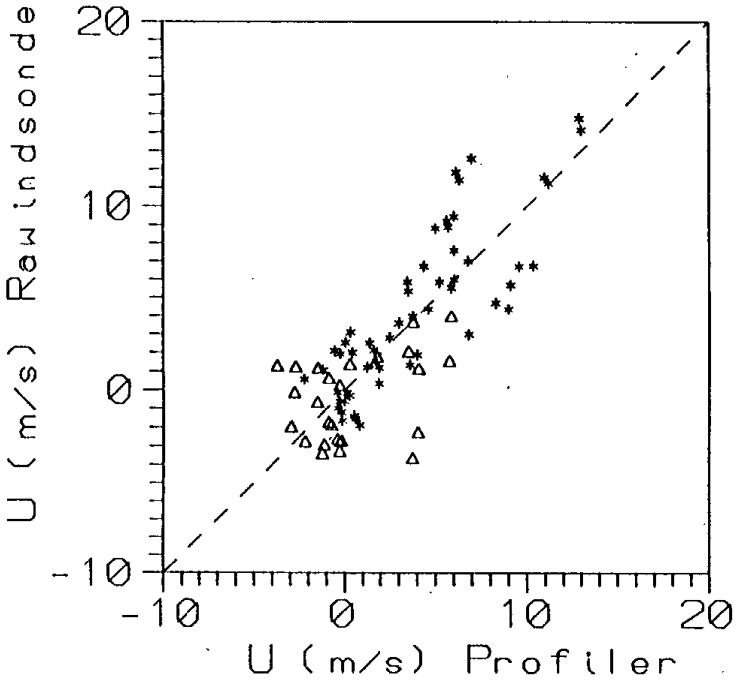


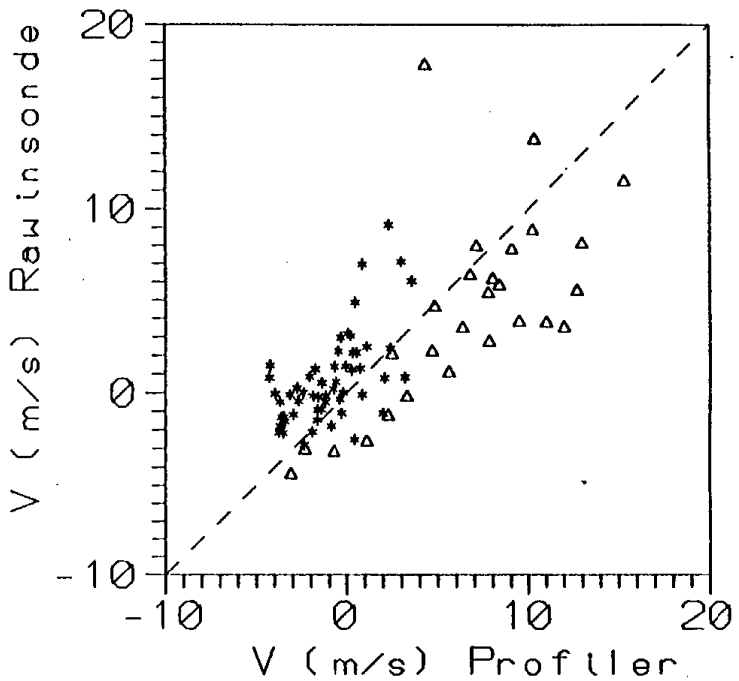


* * * * * 0-3000 m
△ △ △ △ △ > 3000 m

* RMSE for data <= 3000 m

| Var | n | min | max | Mean | SD | r | $r^2$ | SE | RMSE |
|---|---|---|---|---|---|---|---|---|---|
| RU | 83 | -4 | 15 | 2.7 | 4.4 | 0.81 | 0.66 | 2.58 | 2.4 |
| PU | 83 | -4 | 13 | 2.7 | 3.9 | 0.81 | 0.66 | 2.58 | 2.4 |
| RV | 83 | -4 | 18 | 1.9 | 4.0 | 0.72 | 0.51 | 2.79 | 2.6 |
| PV | 83 | -4 | 15 | 1.5 | 4.7 | 0.72 | 0.51 | 2.79 | 2.6 |

Travis North (JD: 226-227)
Day: 0800 - 1900 PDT
Threshold/low res

# NORTHERN CALIFORNIA TRANSPORT (NCT) 1991
# 915 MHz WIND PROFILER/RAWINSONDE COMPARISON

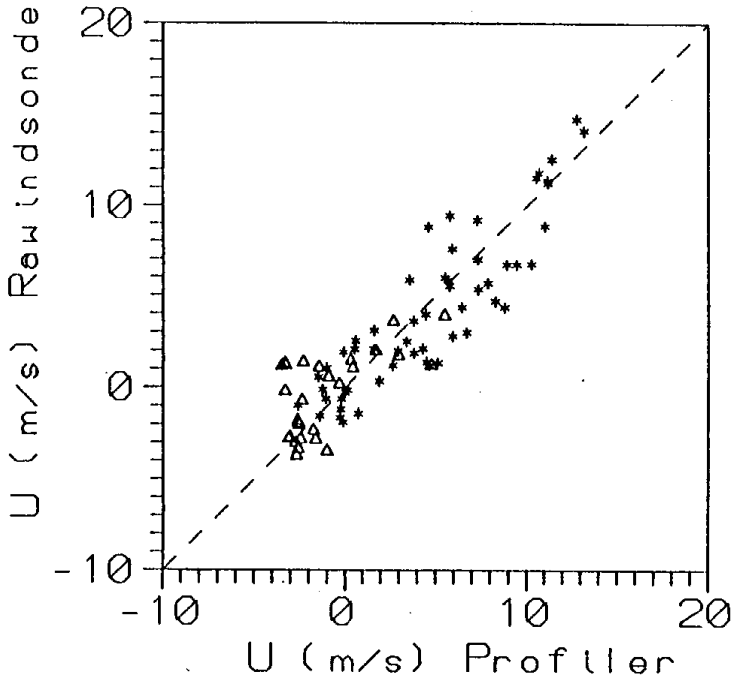


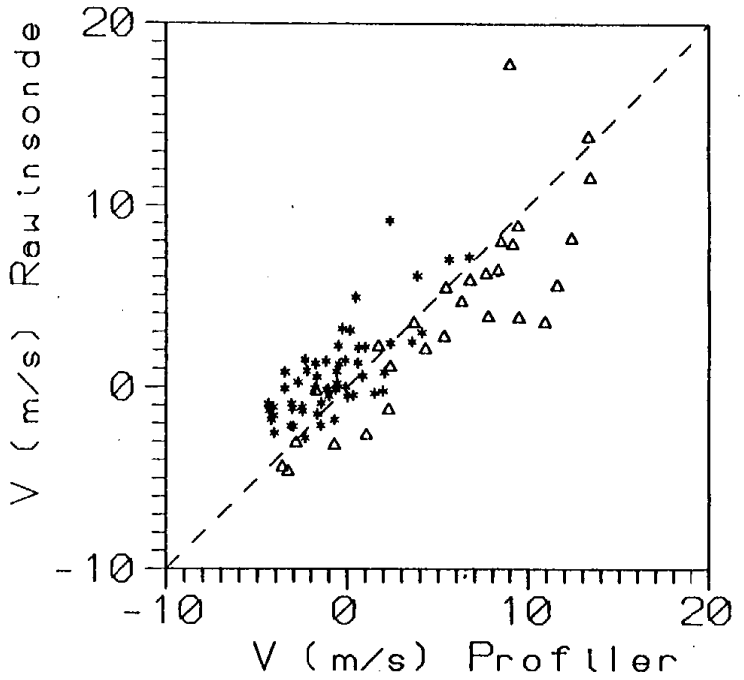


* * * * * 0-3000 m
△ △ △ △ △ > 3000 m

* RMSE for data <= 3000 m

| Var | n | min | max | Mean | SD | r | $r^2$ | SE | RMSE |
|---|---|---|---|---|---|---|---|---|---|
| RU | 84 | -4 | 15 | 2.7 | 4.4 | 0.89 | 0.80 | 1.98 | 2.1 |
| PU | 84 | -4 | 13 | 2.7 | 4.6 | 0.89 | 0.80 | 1.98 | 2.1 |
| RV | 84 | -5 | 18 | 1.8 | 4.0 | 0.83 | 0.69 | 2.24 | 2.2 |
| PV | 84 | -4 | 13 | 1.4 | 4.7 | 0.83 | 0.69 | 2.24 | 2.2 |

Travis North (JD: 226-227)
Day: 0800 - 1900 PDT
No threshold/low res

# NORTHERN CALIFORNIA TRANSPORT (NCT) 1991
## 915 MHz WIND PROFILER/RAWINSONDE COMPARISON

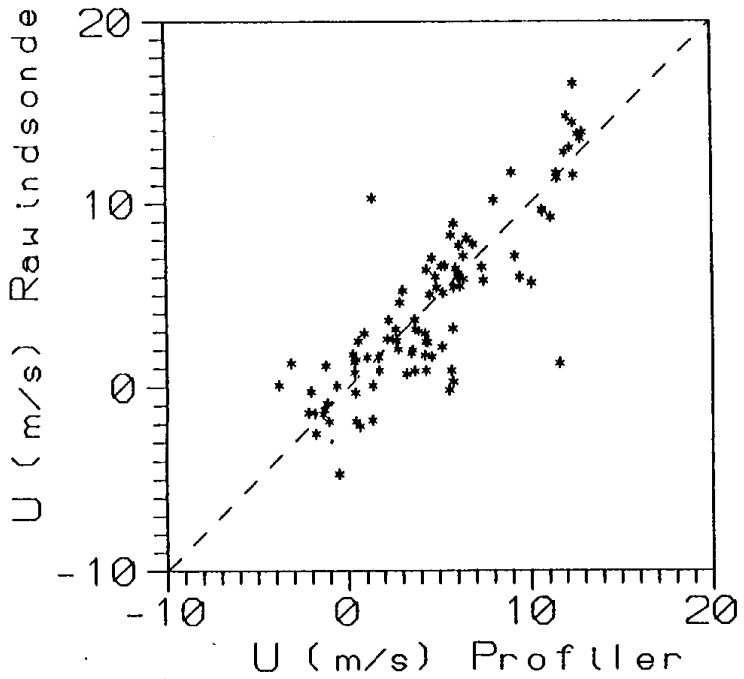


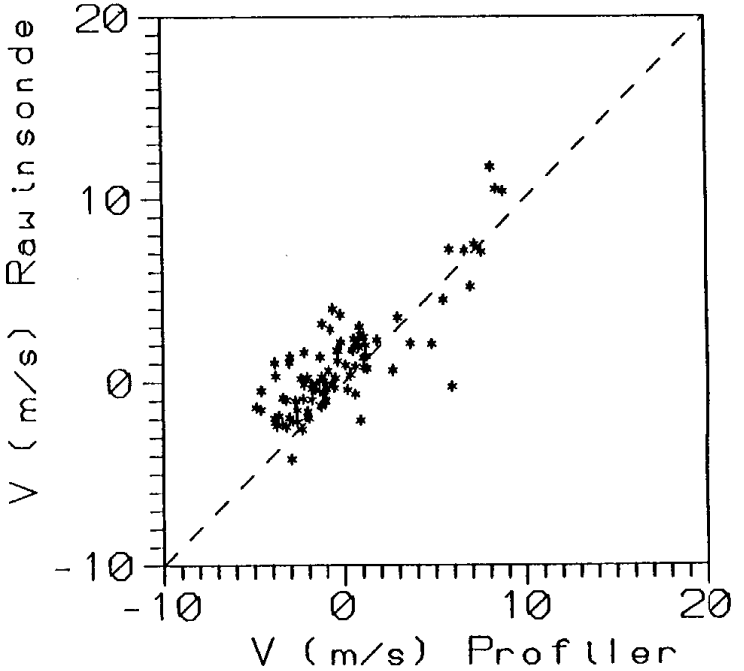


* * * * * 0-3000 m
∆ ∆ ∆ ∆ ∆ > 3000 m

* RMSE for data <= 3000 m

| Var | n | min | max | Mean | SD | r | $r^2$ | SE | RMSE |
|---|---|---|---|---|---|---|---|---|---|
| RU | 96 | -5 | 17 | 4.4 | 4.6 | 0.85 | 0.72 | 2.46 | 2.5 |
| PU | 96 | -4 | 13 | 4.6 | 4.3 | 0.85 | 0.72 | 2.46 | 2.5 |
| RV | 96 | -4 | 12 | 0.9 | 2.9 | 0.83 | 0.70 | 1.59 | 2.1 |
| PV | 96 | -5 | 9 | -0.2 | 3.1 | 0.83 | 0.70 | 1.59 | 2.1 |

Travis North (JD: 226-227)
Day: 0800 - 1900 PDT
Threshold/high res

# NORTHERN CALIFORNIA TRANSPORT (NCT) 1991
## 915 MHz WIND PROFILER/RAWINSONDE COMPARISON

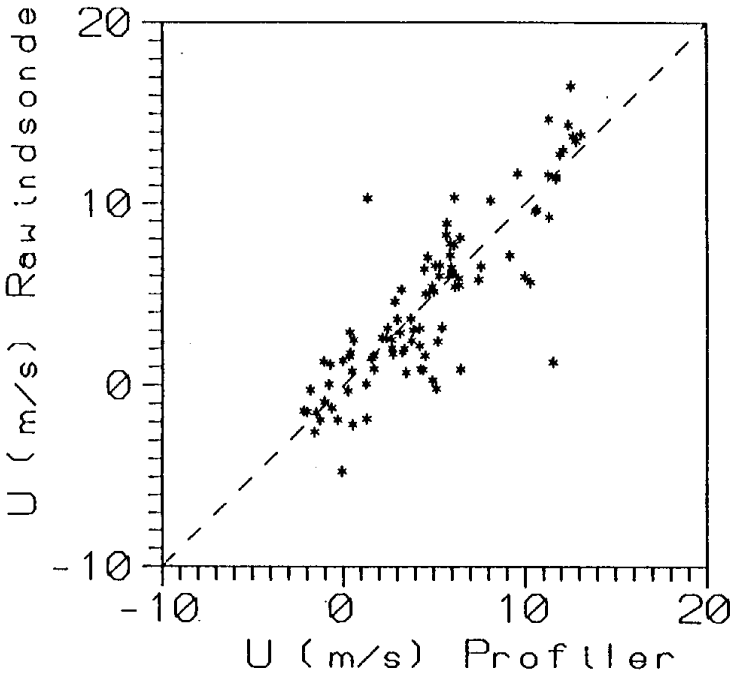


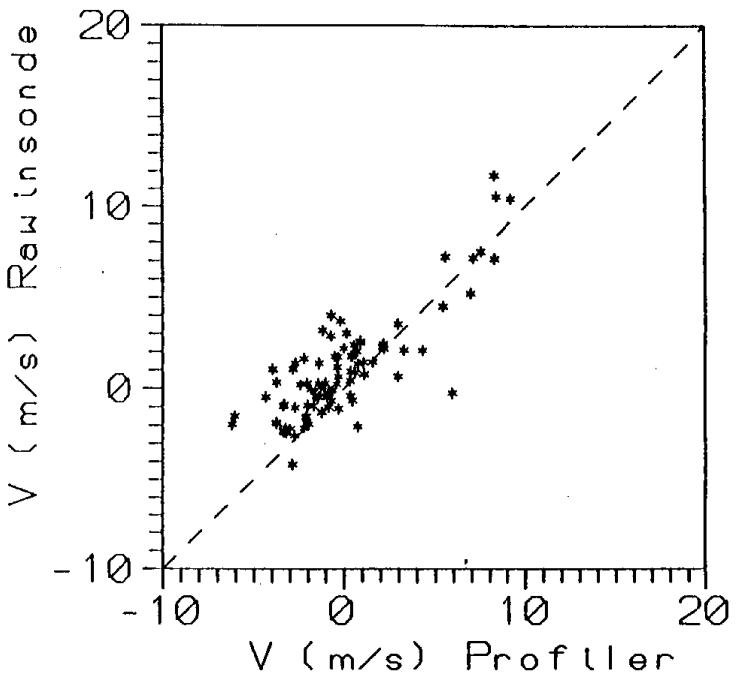


* * * * * 0-3000 m
△ △ △ △ △ > 3000 m

* RMSE for data <= 3000 m

| Var | n | min | max | Mean | SD | r | $r^2$ | SE | RMSE |
|---|---|---|---|---|---|---|---|---|---|
| RU | 96 | -5 | 17 | 4.6 | 4.7 | 0.85 | 0.73 | 2.45 | 2.4 |
| PU | 96 | -2 | 13 | 4.7 | 4.2 | 0.85 | 0.73 | 2.45 | 2.4 |
| RV | 96 | -4 | 12 | 0.9 | 2.9 | 0.83 | 0.69 | 1.60 | 2.1 |
| PV | 96 | -6 | 9 | -0.1 | 3.2 | 0.83 | 0.69 | 1.60 | 2.1 |

Travis North (JD: 226-227)
Day: 0800 - 1900 PDT

# NORTHERN CALIFORNIA TRANSPORT (NCT) 1991
# 915 MHz WIND PROFILER/RAWINSONDE COMPARISON

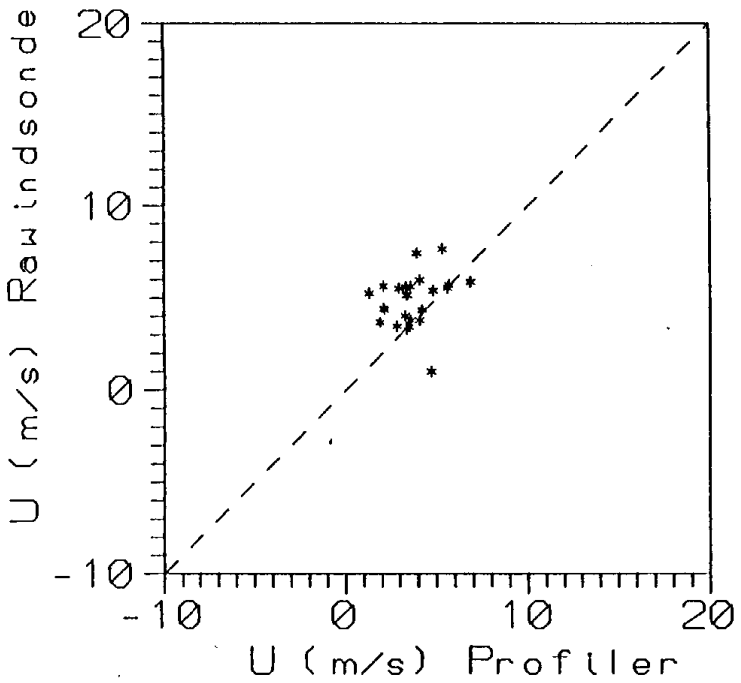


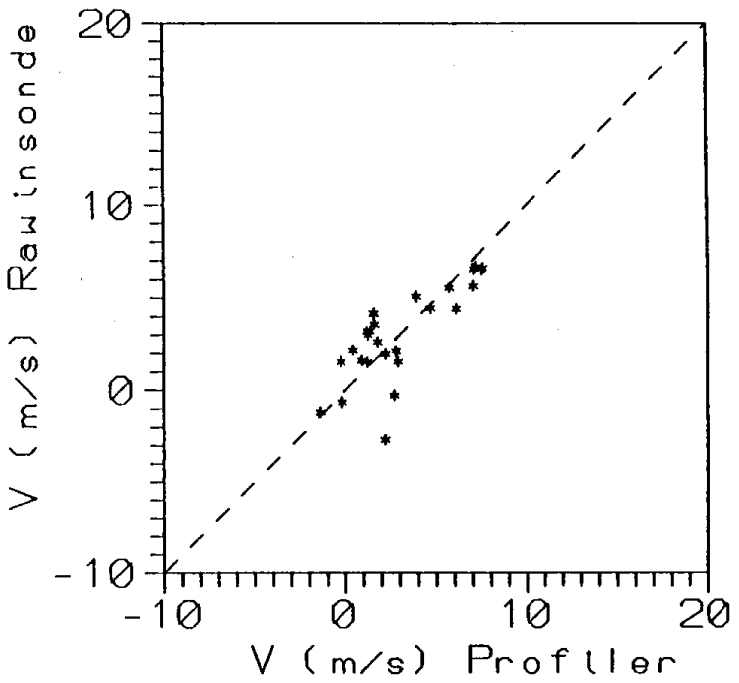


* * * * * 0-3000 m
∆ ∆ ∆ ∆ ∆ > 3000 m

* RMSE for data <= 3000 m

| Var | n | min | max | Mean | SD | r | $r^2$ | SE | RMSE |
|---|---|---|---|---|---|---|---|---|---|
| RU | 26 | 1 | 8 | 4.8 | 1.4 | 0.23 | 0.05 | 1.36 | 2.0 |
| PU | 26 | 1 | 7 | 3.7 | 1.3 | 0.23 | 0.05 | 1.36 | 2.0 |
| RV | 26 | -3 | 7 | 3.0 | 2.5 | 0.79 | 0.62 | 1.58 | 1.7 |
| PV | 26 | -1 | 8 | 3.0 | 2.7 | 0.79 | 0.62 | 1.58 | 1.7 |

Travis South (JD: 227-228)
Day: 0800 - 1900 PDT
Threshold/low pas

# NORTHERN CALIFORNIA TRANSPORT (NCT) 1991
# 915 MHz WIND PROFILER/RAWINSONDE COMPARISON

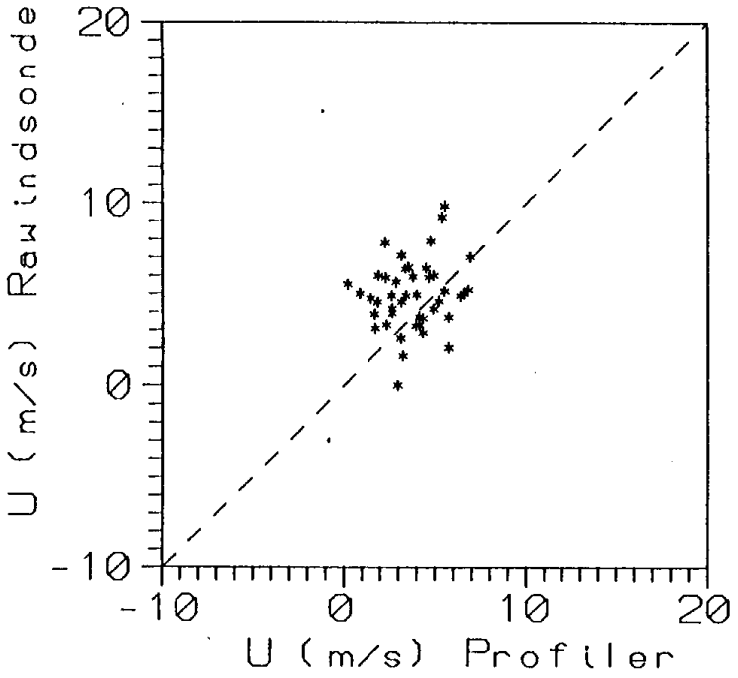


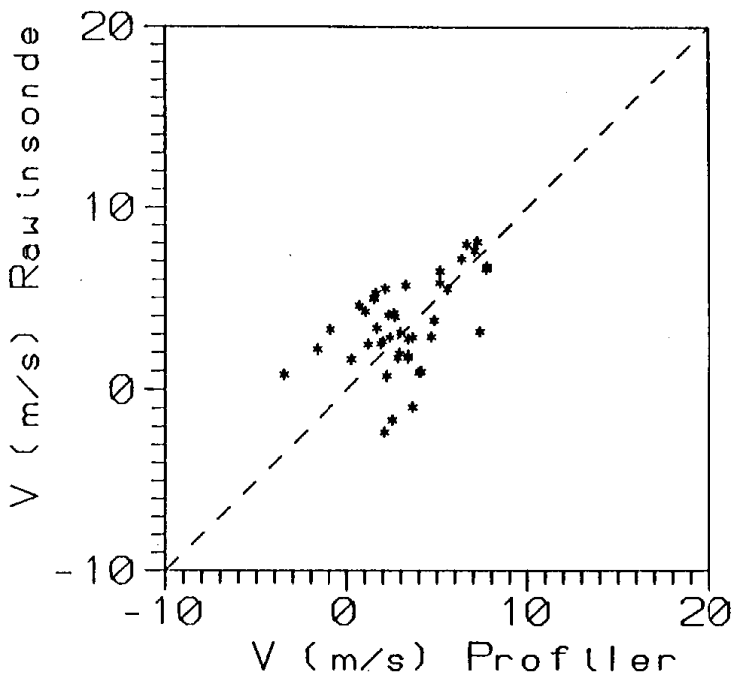


* * * * * 0-3000 m

∆ ∆ ∆ ∆ ∆ > 3000 m

* RMSE for data <= 3000 m

| Var | n | min | max | Mean | SD | r | $r^2$ | SE | RMSE |
|---|---|---|---|---|---|---|---|---|---|
| RU | 44 | 0 | 10 | 4.9 | 1.9 | 0.17 | 0.03 | 1.89 | 2.5 |
| PU | 44 | 0 | 7 | 3.7 | 1.6 | 0.17 | 0.03 | 1.89 | 2.5 |
| RV | 44 | -2 | 8 | 3.5 | 2.4 | 0.50 | 0.25 | 2.14 | 2.4 |
| PV | 44 | -4 | 8 | 3.1 | 2.5 | 0.50 | 0.25 | 2.14 | 2.4 |

Travis South (JD: 227-228)
Day: 0800 - 1900 PDT
Threshold/high res

# NORTHERN CALIFORNIA TRANSPORT (NCT) 1991
## 915 MHz WIND PROFILER/RAWINSONDE COMPARISON

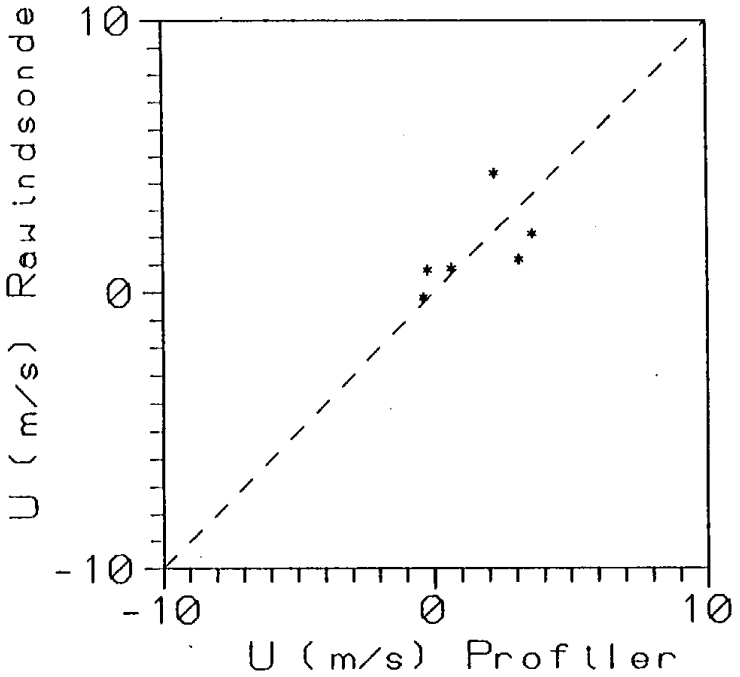


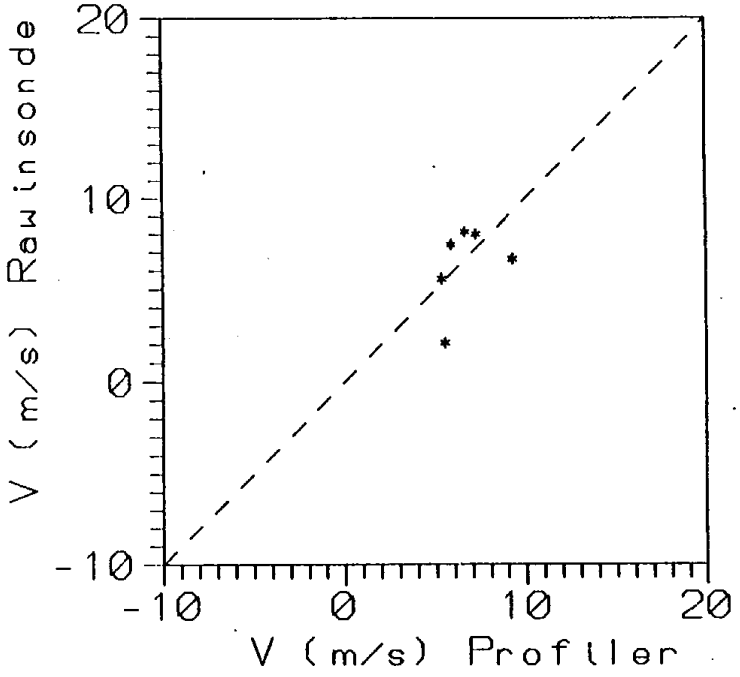


* * * * * 0-3000 m
Δ Δ Δ Δ Δ > 3000 m

* RMSE for data <= 3000 m

| Var | n | min | max | Mean | SD | r | $r^2$ | SE | RMSE |
|---|---|---|---|---|---|---|---|---|---|
| RU | 6 | 0 | 4 | 1.5 | 1.6 | 0.57 | 0.33 | 1.45 | 1.4 |
| PU | 6 | 0 | 4 | 1.5 | 1.7 | 0.57 | 0.33 | 1.45 | 1.4 |
| RV | 6 | 2 | 8 | 6.3 | 2.3 | 0.40 | 0.16 | 2.33 | 2.0 |
| PV | 6 | 5 | 9 | 6.6 | 1.5 | 0.40 | 0.16 | 2.33 | 2.0 |

U. C. Davis (JD: 225-225)
Night: 1900 - 0800 PDT
Threshold/low res

# NORTHERN CALIFORNIA TRANSPORT (NCT) 1991
# 915 MHz WIND PROFILER/RAWINSONDE COMPARISON

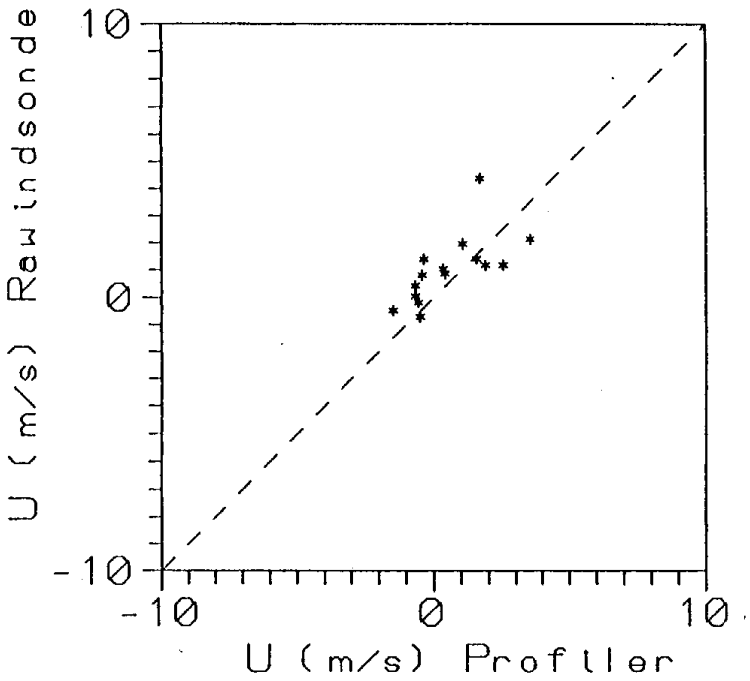


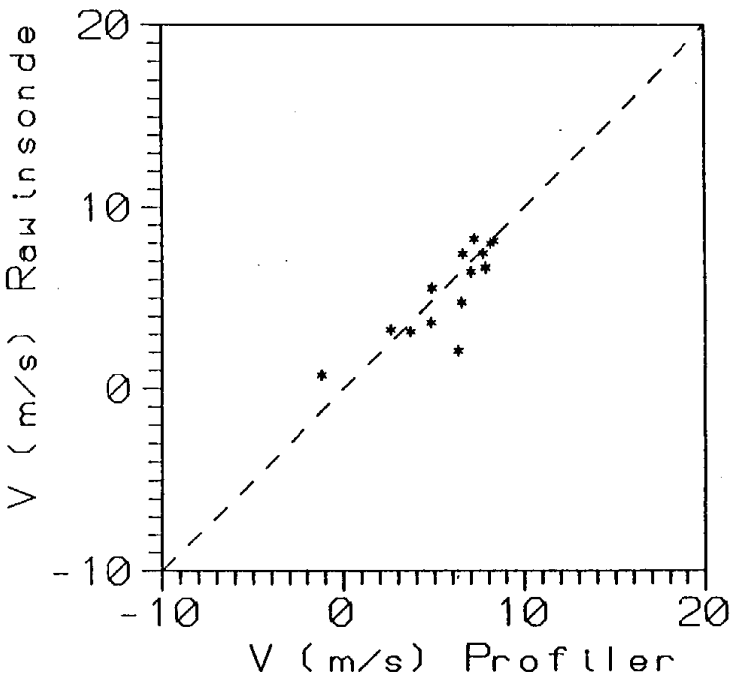


* * * * * 0-3000 m
^ ^ ^ ^ ^ > 3000 m

* RMSE for data <= 3000 m

| Var | n | min | max | Mean | SD | r | $r^2$ | SE | RMSE |
|---|---|---|---|---|---|---|---|---|---|
| RU | 15 | -1 | 4 | 1.0 | 1.2 | 0.66 | 0.44 | 0.97 | 1.2 |
| PU | 15 | -1 | 4 | 0.5 | 1.4 | 0.66 | 0.44 | 0.97 | 1.2 |
| RV | 15 | 1 | 8 | 5.5 | 2.4 | 0.83 | 0.69 | 1.38 | 1.5 |
| PV | 15 | -1 | 8 | 5.8 | 2.6 | 0.83 | 0.69 | 1.38 | 1.5 |

U. C. Davis (JD: 225-225)
Night: 1900 - 0800 PDT
No threshold/low res

NORTHERN CALIFORNIA TRANSPORT (NCT) 1991
915 MHz WIND PROFILER COMPARISON: Travis North/South

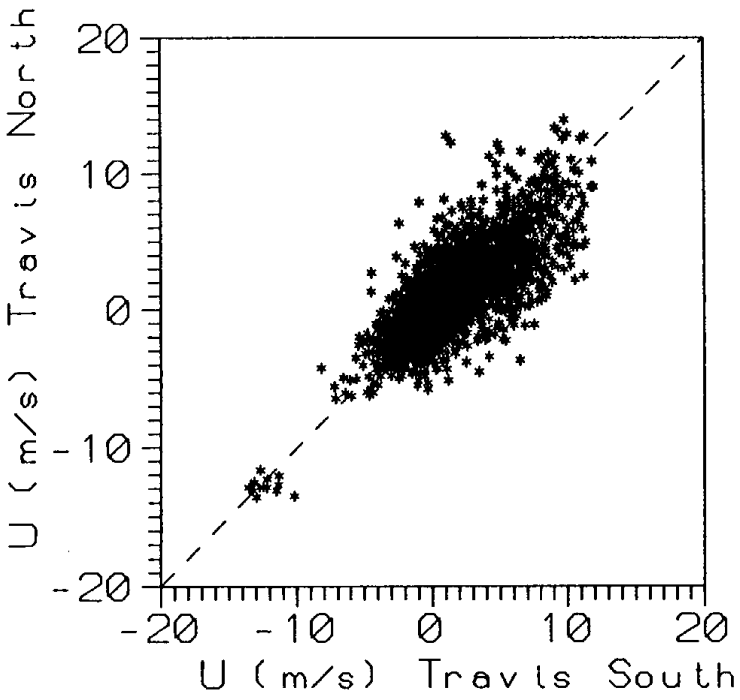


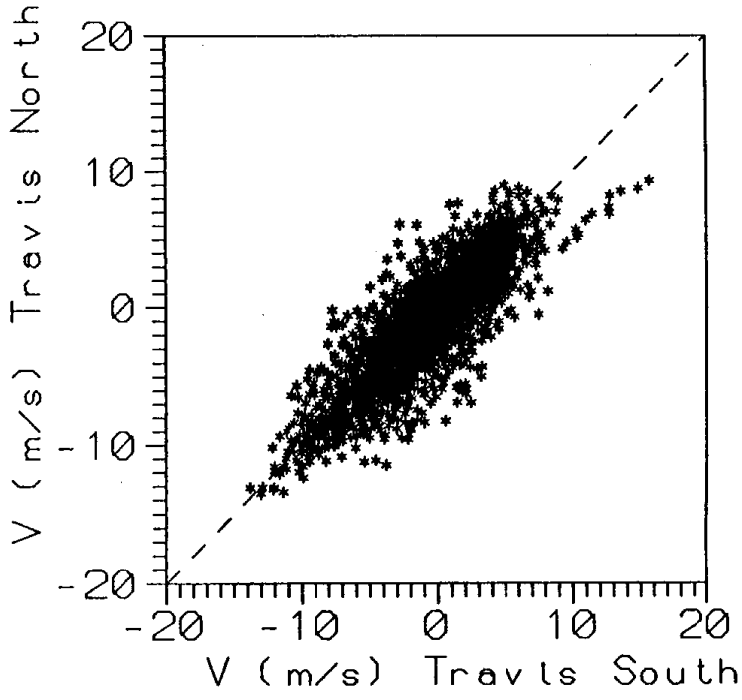


***** 0-3000 m

* RMSE for data <= 3000 m

| Var | n | min | max | Mean | SD | r | $r^2$ | SE | RMSE |
|---|---|---|---|---|---|---|---|---|---|
| SU | 4664 | -14 | 12 | 1.5 | 3.0 | 0.75 | 0.56 | 1.96 | 2.1 |
| NU | 4664 | -14 | 14 | 1.1 | 2.8 | | | | |
| SV | 4664 | -14 | 16 | -0.7 | 3.6 | 0.86 | 0.74 | 1.83 | 2.0 |
| NV | 4664 | -14 | 9 | -0.9 | 3.7 | | | | |

Travis North and South (JD: 179 - 238)
Morning-Day: 0100 - 1300 PDT
Threshold/high res

# NORTHERN CALIFORNIA TRANSPORT (NCT) 1991
# 915 MHz WIND PROFILER/RAWINSONDE COMPARISON

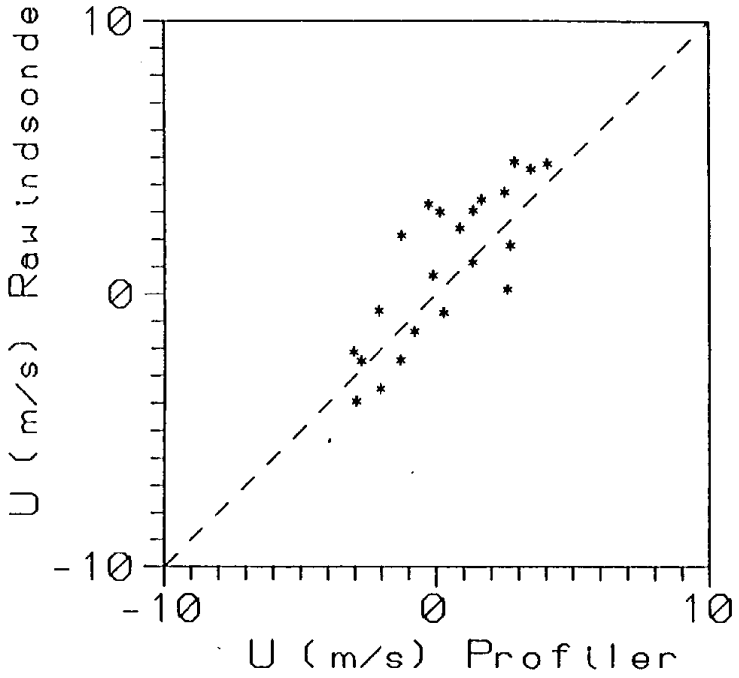


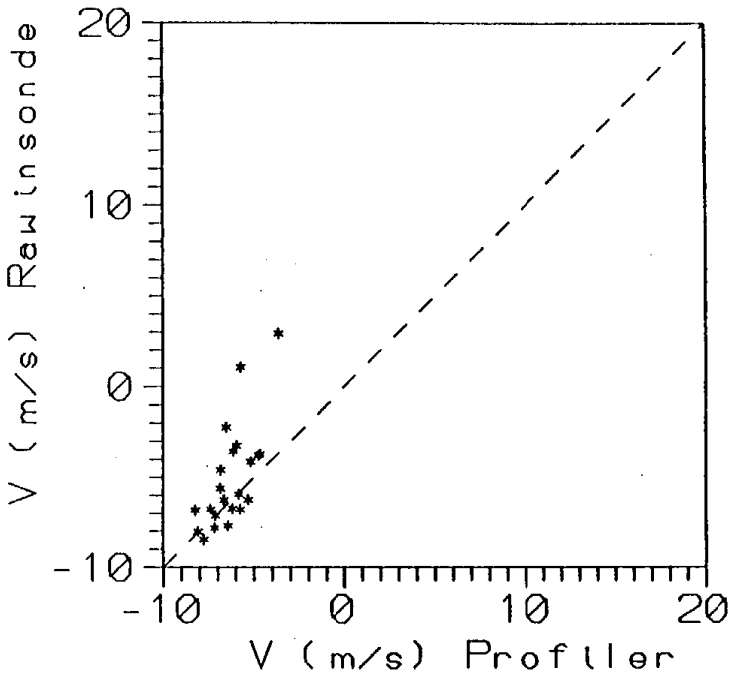


* * * * * 0-3000 m
Δ Δ Δ Δ Δ > 3000 m

* RMSE for data <= 3000 m

| Var | n | min | max | Mean | SD | r | $r^2$ | SE | RMSE |
|---|---|---|---|---|---|---|---|---|---|
| RU | 22 | -4 | 5 | 1.0 | 2.8 | 0.82 | 0.67 | 1.64 | 1.7 |
| PU | 22 | -3 | 4 | 0.3 | 2.2 | 0.82 | 0.67 | 1.64 | 1.7 |
| RV | 22 | -8 | 3 | -5.1 | 2.9 | 0.69 | 0.47 | 2.14 | 2.5 |
| PV | 22 | -8 | -4 | -6.3 | 1.1 | 0.69 | 0.47 | 2.14 | 2.5 |

U. C. Davis (JD: 225-225)
Day: 0800 - 1900 PDT
Threshold/low res

# NORTHERN CALIFORNIA TRANSPORT (NCT) 1991
## 915 MHz WIND PROFILER/RAWINSONDE COMPARISON

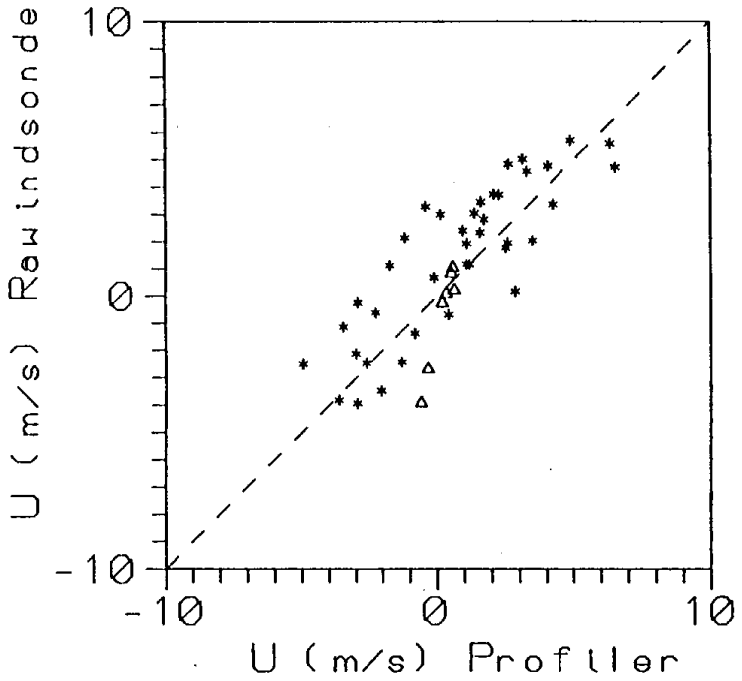


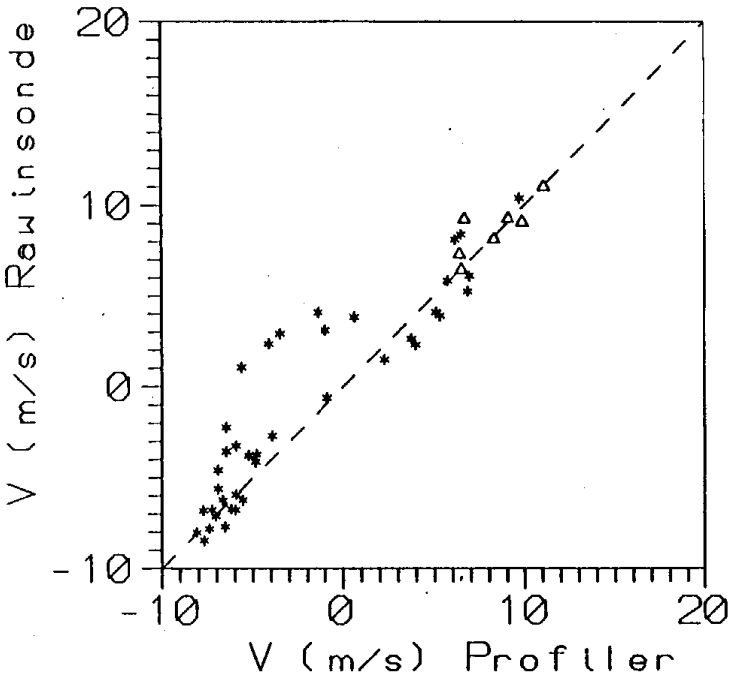


* * * * * 0-3000 m
△ △ △ △ △ > 3000 m

* RMSE for data <= 3000 m

| Var | n | min | max | Mean | SD | r | $r^2$ | SE | RMSE |
|---|---|---|---|---|---|---|---|---|---|
| RU | 46 | -4 | 6 | 1.1 | 2.7 | 0.82 | 0.67 | 1.59 | 1.7 |
| PU | 46 | -5 | 7 | 0.6 | 2.6 | 0.82 | 0.67 | 1.59 | 1.7 |
| RV | 46 | -8 | 11 | 0.4 | 6.2 | 0.94 | 0.88 | 2.14 | 2.6 |
| PV | 46 | -8 | 11 | -0.6 | 6.3 | 0.94 | 0.88 | 2.14 | 2.6 |

U. C. Davis (JD: 225-225)
Day: 0800 - 1900 PDT
No threshold/low res

# NORTHERN CALIFORNIA TRANSPORT (NCT) 1991
# 915 MHz WIND PROFILER/RAWINSONDE COMPARISON

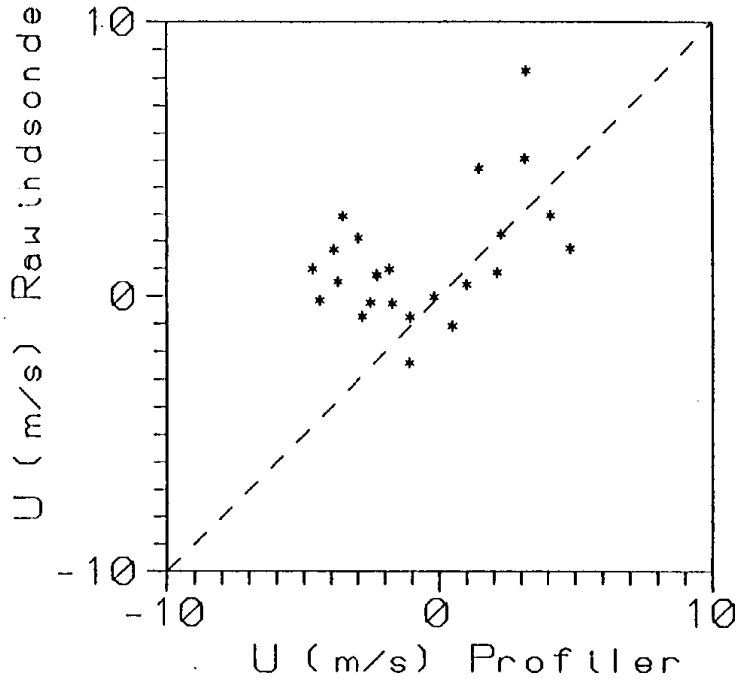


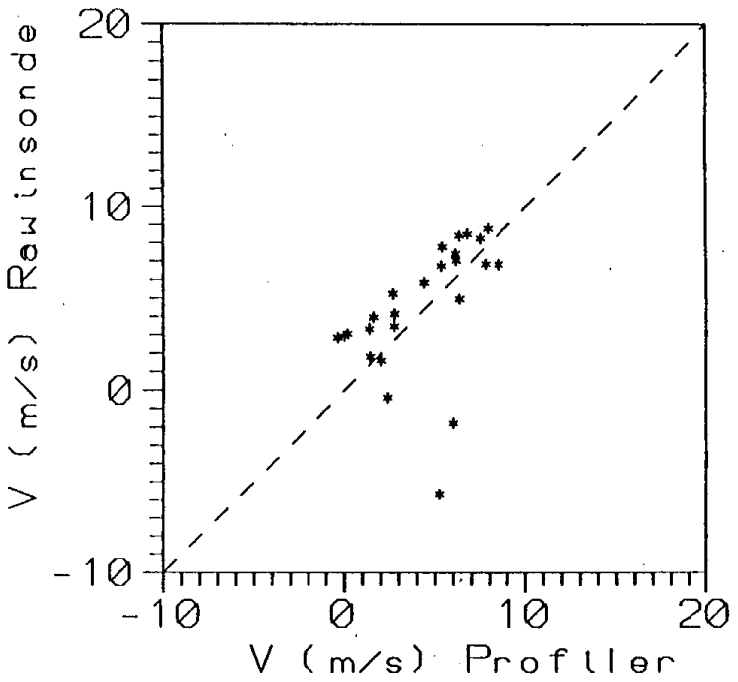


* * * * * 0-3000 m
△ △ △ △ △ > 3000 m

* RMSE for data <= 3000 m

| Var | n | min | max | Mean | SD | r | $r^2$ | SE | RMSE |
|---|---|---|---|---|---|---|---|---|---|
| RU | 25 | -2 | 8 | 1.3 | 2.2 | 0.45 | 0.20 | 2.05 | 3.4 |
| PU | 25 | -5 | 5 | -0.8 | 2.9 | 0.45 | 0.20 | 2.05 | 3.4 |
| RV | 25 | -6 | 9 | 4.5 | 3.5 | 0.47 | 0.23 | 3.18 | 3.2 |
| PV | 25 | 0 | 9 | 4.3 | 2.7 | 0.47 | 0.23 | 3.18 | 3.2 |

U. C. Davis (JD: 225-225)
Night: 1900 - 0800 PDT
Threshold/high res

# NORTHERN CALIFORNIA TRANSPORT (NCT) 1991
# 915 MHz WIND PROFILER/RAWINSONDE COMPARISON

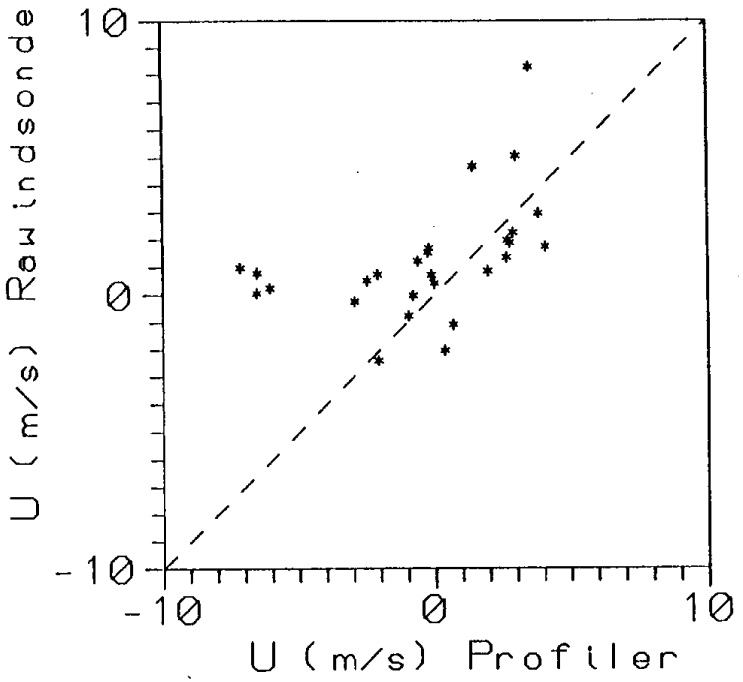


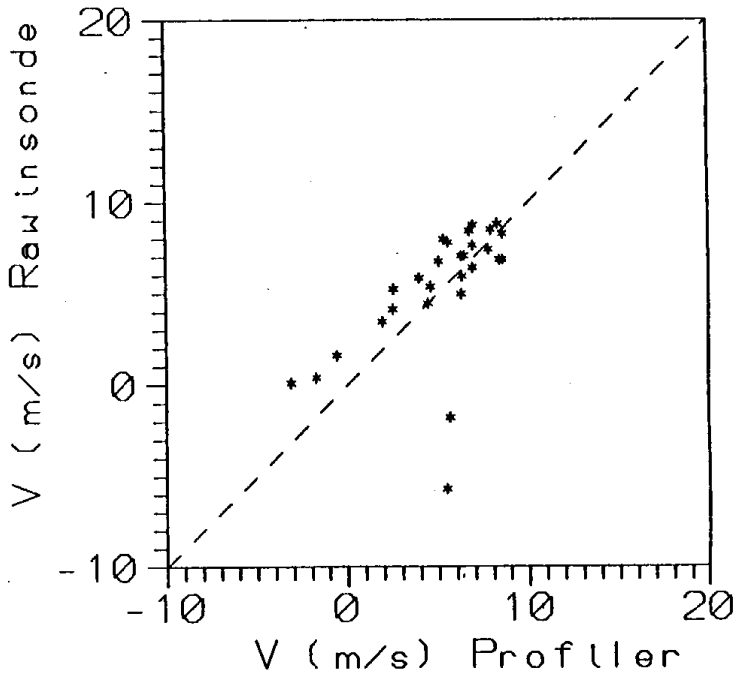


* * * * * 0-3000 m
△ △ △ △ △ > 3000 m

* RMSE for data <= 3000 m

| Var | n | min | max | Mean | SD | r | $r^2$ | SE | RMSE |
|---|---|---|---|---|---|---|---|---|---|
| RU | 28 | -2 | 8 | 1.2 | 2.2 | 0.49 | 0.24 | 1.92 | 3.3 |
| PU | 28 | -7 | 4 | -0.4 | 3.3 | 0.49 | 0.24 | 1.92 | 3.3 |
| RV | 28 | -6 | 9 | 5.3 | 3.5 | 0.59 | 0.34 | 2.89 | 3.0 |
| PV | 28 | -3 | 9 | 5.1 | 3.0 | 0.59 | 0.34 | 2.89 | 3.0 |

U. C. Davis (JD: 225-225)
Night: 1900 - 0800 PDT
No threshold/high res

# NORTHERN CALIFORNIA TRANSPORT (NCT) 1991
# 915 MHz WIND PROFILER/RAWINSONDE COMPARISON

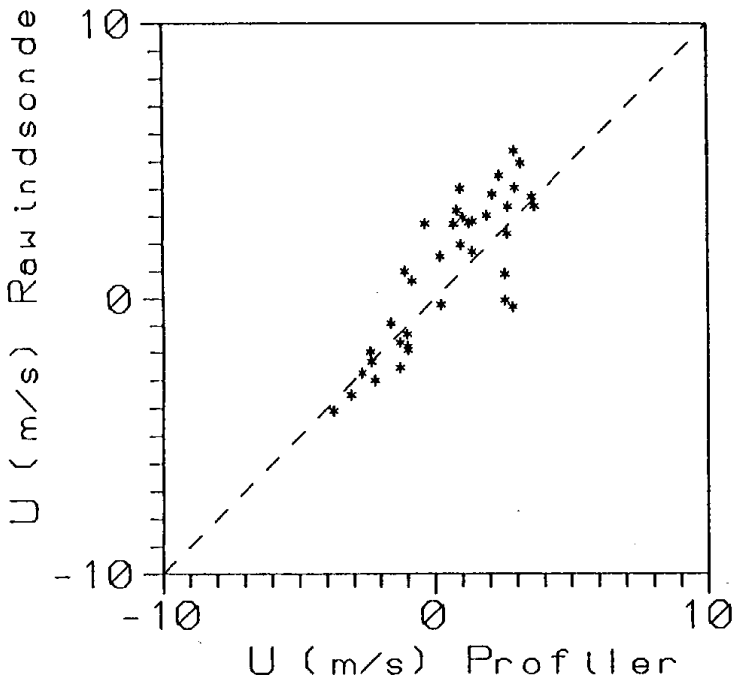


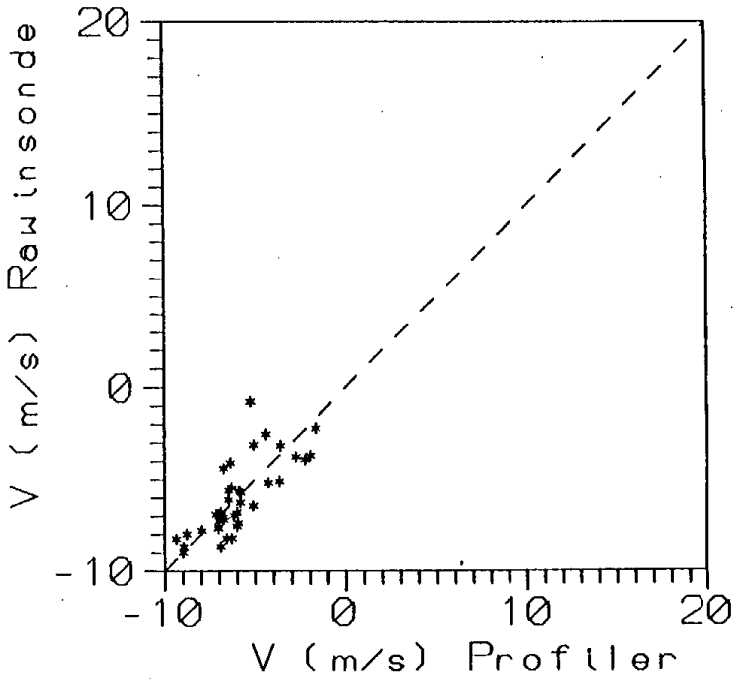


* * * * * 0-3000 m
△ △ △ △ △ > 3000 m

* RMSE for data <= 3000 m

| Var | n | min | max | Mean | SD | r | $r^2$ | SE | RMSE |
|---|---|---|---|---|---|---|---|---|---|
| RU | 38 | -4 | 5 | 1.0 | 2.7 | 0.84 | 0.70 | 1.48 | 1.5 |
| PU | 38 | -4 | 4 | 0.5 | 2.1 | 0.84 | 0.70 | 1.48 | 1.5 |
| RV | 38 | -9 | -1 | -6.0 | 2.0 | 0.76 | 0.57 | 1.36 | 1.4 |
| PV | 38 | -9 | -2 | -6.0 | 1.9 | 0.76 | 0.57 | 1.36 | 1.4 |

U. C. Davis (JD: 225-225)
Day: 0800 - 1900 PDT
Threshold/high res

# NORTHERN CALIFORNIA TRANSPORT (NCT) 1991
# 915 MHz WIND PROFILER/RAWINSONDE COMPARISON

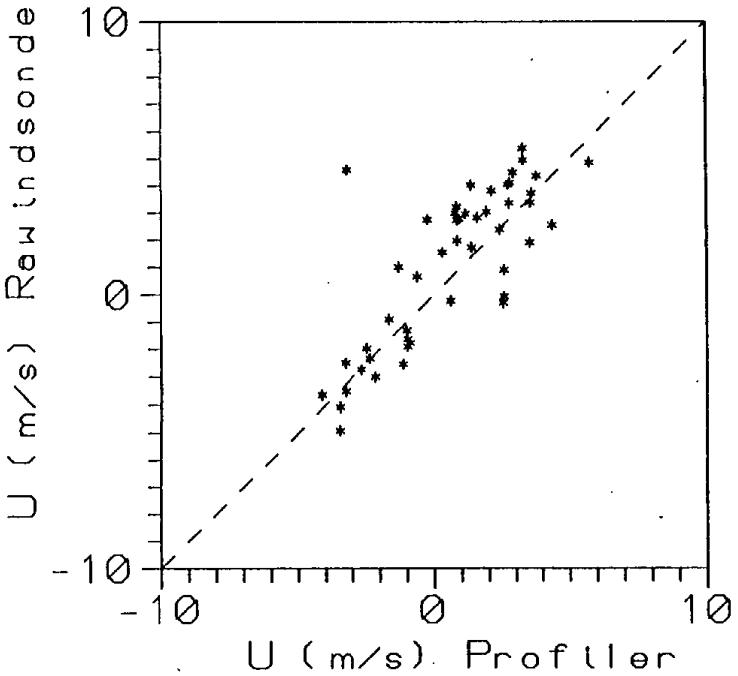


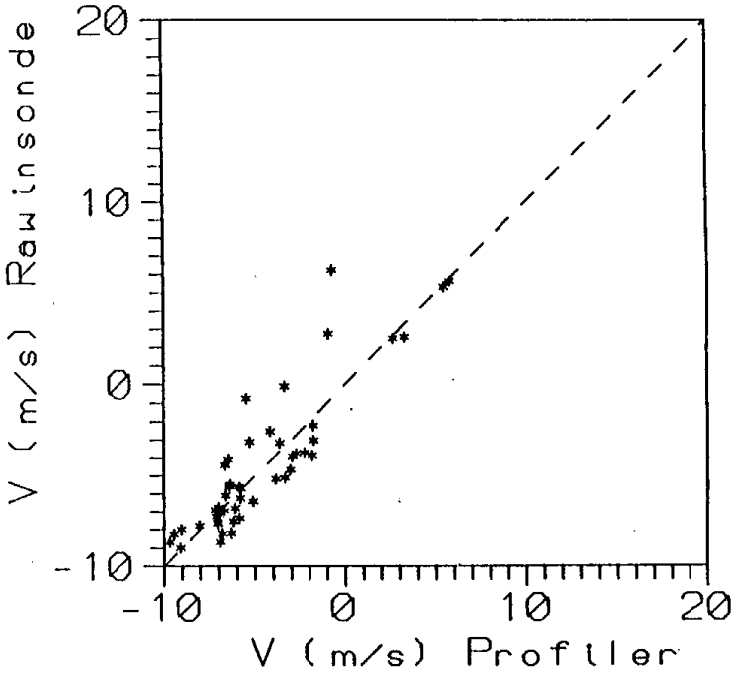


* * * * * 0-3000 m
△ △ △ △ △ > 3000 m

* RMSE for data <= 3000 m

| Var | n | min | max | Mean | SD | r | $r^2$ | SE | RMSE |
|---|---|---|---|---|---|---|---|---|---|
| RU | 48 | -5 | 5 | 1.1 | 2.9 | 0.79 | 0.63 | 1.78 | 1.8 |
| PU | 48 | -4 | 6 | 0.6 | 2.5 | 0.79 | 0.63 | 1.78 | 1.8 |
| RV | 48 | -9 | 6 | -4.5 | 3.9 | 0.89 | 0.79 | 1.81 | 1.8 |
| PV | 48 | -10 | 6 | -4.7 | 3.5 | 0.89 | 0.79 | 1.81 | 1.8 |

U. C. Davis (JD: 225-225)
Day: 0800 - 1900 PDT
No threshold/high res